



HOST UNIVERSITY: Ghent University

FACULTY: Faculty of Engineering

DEPARTMENT: Department of Flow, Heat and Combustion

Academic Year 2012-2013

**DETECTION OF CHANGES IN THE VENTILATION CONDITIONS OF A FIRE AND IMPLEMENTATION IN AN
INVERSE FIRE MODELLING FRAMEWORK**

Absar Ahmad

Promoters: Dr. Tarek Beji and Prof. Bart Merci

Master thesis submitted in the Erasmus Mundus Study Programme

International Master of Science in Fire Safety Engineering

DISCLAIMER

This thesis is submitted in partial fulfillment of the requirements for the degree of *The International Master of Science in Fire Safety Engineering (IMFSE)*. This thesis has never been submitted for any degree or examination to any other University/program. The author(s) declare(s) that this thesis is original work except where stated. This declaration constitutes an assertion that full and accurate references and citations have been included for all material, directly included and indirectly contributing to the thesis. The author(s) gives (give) permission to make this master thesis available for consultation and to copy parts of this master thesis for personal use. In the case of any other use, the limitations of the copyright have to be respected, in particular with regard to the obligation to state expressly the source when quoting results from this master thesis. The thesis supervisor must be informed when data or results are used.

29th April, 2013

A handwritten signature in blue ink, consisting of the letters 'AA' followed by the name 'Absar Ahmad' in a cursive script.

Absar Ahmad

Abstract

A study is carried out to develop an Inverse Fire Modelling framework, which allows an estimation of fire growth along with changes in the ventilation conditions in a single room. In the first stage, the results of three forward models are compared in terms of smoke layer height and upper layer temperature. These three forward models are: (1) a Computational Fluid Dynamics Code (CFD), namely the Fire Dynamics Simulator (FDS), (2) a two-zone model, the Consolidated Model of Fire Growth and Smoke Transport (CFAST), and (3) a simplified two-zone model referred to as analytical model in this dissertation. This comparison reveals maximum deviations of 40% in both smoke layer height and temperature. In the second stage, the inverse fire model is developed using the same conservation correlations as in the analytical model. The upper layer temperature, T_u , and smoke layer height, h , obtained from CFAST are assimilated into the inverse model over a given period of time (called assimilation window) in order to estimate the fire growth together with any change in the ventilation conditions of the compartment. The results show that the HRR has a scatter of up to 40%, whereas the ventilation factor can be estimated with 50-150% deviations from the 'actual' value.

Keywords Single room fires, ISO 9705, Inverse modeling, Fire forecasting

خلاصہ

اس تحقیق میں ایک انورس فائبر ماڈلنگ کے طریقہ کار پر کام کیا گیا ہے جو ایک کمرے میں وینٹیلیشن کے حالات کے ساتھ ساتھ آگ کی بڑھوتی کا بھی اندازہ کر سکتا ہے۔ پہلے مرحلے میں تین فارورڈ ماڈلوں سے حاصل کردہ ہوا کی تہہ اور اوپری لیئر کے درجہ حرارت کے نتائج کا موازنہ لگایا گیا ہے۔ یہ تین فارورڈ ماڈل، ایف ڈی ایس، سی فاسٹ اور اینالٹییکل ماڈل ہیں۔ اس موازنے سے دونوں ہوا کی تہہ اور اوپری لیئر کے درجہ حرارت کے نتائج سے ۴۰ فیصد انحراف ملتا ہے۔ دوسرے مرحلے میں انہی کنزرویشن کے اصولوں کو استعمال کرتے ہوئے انورس ماڈل تیار کیا گیا ہے۔ جو سی فاسٹ سے حاصل کردہ ہوا کی تہہ اور اوپری لیئر کے درجہ حرارت کو استعمال کرتے ہوئے آگ کی بڑھوتی کے ساتھ ساتھ وینٹیلیشن میں تبدیلی کا اندازہ لگاتا ہے۔ نتائج سے وینٹیلیشن فیکٹر میں ۱۵۰-۵۰ فیصد جبکہ آگ کی بڑھوتی میں ۴۰ فیصد انحراف ظاہر ہوتا ہے۔

Contents

Abstract	ii
Notations	vi
List of Figures.....	viii
List of Tables.....	x
1 Introduction.....	1
1.1 Literature review	2
1.2 Objective.....	3
1.3 Methodology	3
2 Geometrical configuration and list of test cases.....	4
2.1 Room Geometry	4
2.2 Fire Source.....	5
2.3 Ventilation factor	6
2.4 List of cases.....	8
3 Presentation of the fire models	11
3.1 CFD	11
3.2 Zone Models.....	11
3.3 Analytical model.....	13
4 Forward modeling results	16
4.1 FDS simulations	16
4.1.1 Grid size	16
4.1.2 Domain effect.....	18
4.1.3 FDS Turbulence resolution	19
4.1.4 Positions of sensors.....	21
4.1.5 Representation in Smokeview.....	21
4.2 CFAST simulations	24
4.2.1 Vertical location of window.....	27
4.3 Analytical model.....	30
4.4 Comparison of results	33
4.4.1 Between FDS and the Analytical model	33
4.4.2 Between CFAST and the Analytical model	36
4.4.3 Between FDS and CFAST.....	38

5 Inverse Modeling..... 40

5.1 Description of the procedure 40

5.2 Results and Discussions..... 42

6 Conclusion 47

7 Acknowledgement..... 48

References..... 49

Appendix A1 51

Appendix A2 53

Appendix A3 55

Appendix A4 57

Appendix A5 59

Appendix A6 61

Appendix B1 64

Appendix B2 68

Appendix B3 71

Notations

A	floor surface area of the compartment (m^2)
A_o	area of the opening in the compartment (m^2)
c_p	specific heat of air (kJ/kg.K)
C_d	flow discharge coefficient (dimensionless)
D^*	characteristic fire diameter (dimensionless)
g	gravitational acceleration (m/s^2)
h	smoke layer height (m)
\dot{h}_L	rate of addition of enthalpy into lower layer (J/s)
\dot{h}_U	rate of addition of enthalpy into upper layer (J/s)
H	room height (m)
H_D	height of the door (m)
H_o	height of the opening (m)
$\dot{m}_{in,u}$	mass flow rate of air into upper layer (kg/s)
$\dot{m}_{out,u}$	mass flow rate out of the compartment (kg/s)
\dot{m}_p	mass flow rate of the plume (kg/s)
P	pressure (Pa)
\dot{Q}_f	total heat release rate (kW)
$\dot{Q}_{f,c}$	convective heat release rate (kW)
r	radial distance from the fire (m)
t	time (s)
T_a	ambient temperature of air (K)
T_L	temperature of cold lower layer (K)
T_U	temperature of hot upper layer (K)
T_u	temperature of hot upper layer ($^{\circ}C$)

V	volume of the compartment (m^3)
V_f	ventilation factor ($\text{m}^{5/2}$)
V_L	volume of lower layer in the compartment (m^3)
V_U	volume of upper layer in the compartment (m^3)
X_N	neutral layer height (m)
z_f	height of fire source from floor level (m)
z_0	height of virtual origin of fire source (m)
γ	ratio of c_p/c_v (dimensionless)
λ_c	heat loss factor (dimensionless)
ρ_a	ambient density (kg/m^3)
ρ_u	hot upper layer density (kg/m^3)

List of Figures

Figure 2-1 Dimensions of the room and burner location.....	4
Figure 2-2 Dimensions of door	4
Figure 2-3 Linear HRR case	5
Figure 2-4 Positioning of windows	7
Figure 4-1 Effect of grid size on temperature	17
Figure 4-2 Effect of grid size on smoke layer height	17
Figure 4-3 Effect of domain size on temperature	18
Figure 4-4 Effect of domain size on smoke layer height	18
Figure 4-5 Turbulence resolution for 1_Case_1.....	19
Figure 4-6 Turbulence resolution for 1_Case_8.....	20
Figure 4-7 Turbulence resolution for 5_Case_4.....	20
Figure 4-8 Location of devices for measuring upper layer temperature and height.....	21
Figure 4-9 Top view of geometry in FDS	21
Figure 4-10 Flame and smoke before the opening of windows.....	22
Figure 4-11 Flame and smoke after the opening of windows.....	22
Figure 4-12 Temperature profile at the beginning of simulation	23
Figure 4-13 Temperature profile after the opening of windows	23
Figure 4-14 Temperature profile at the end of simulation	23
Figure 4-15 Basic geometry setup in CFAST	24
Figure 4-16 Upper layer temperature and height at the beginning of simulation	25
Figure 4-17 Upper layer temperature and height at 60s	25
Figure 4-18 Upper layer temperature and height at 61s	26
Figure 4-19 Upper layer temperature and height at the end of simulation	26
Figure 4-20 Variation in upper layer temperature because of vertical location of vent	27
Figure 4-21 Variation in smoke layer height because of vertical location of vent.....	28
Figure 4-22 Upper layer temperature and height for 3_Case_4 at 120s	28
Figure 4-23 Upper layer temperature and height for 3_Case_4_low at 120s	29
Figure 4-24 Upper layer temperature and height for 3_Case_4_high at 120s	29
Figure 4-25 Step profile of HRR used for Analytical Model.....	32
Figure 4-26 Hot layer temperature estimated by FDS and Analytical model for constant HRR	34
Figure 4-27 Smoke layer height estimated by FDS and Analytical model for constant HRR	34
Figure 4-28 Hot layer temperature estimated by FDS and Analytical model for linearly increasing HRR..	35
Figure 4-29 Smoke layer height estimated by FDS and Analytical model for linearly increasing HRR	35
Figure 4-30 Hot layer temperature estimated by CFAST and Analytical model for constant HRR	36
Figure 4-31 Smoke layer height estimated by CFAST and Analytical model for constant HRR.....	36
Figure 4-32 Hot layer temperature estimated by CFAST and Analytical model for linearly increasing HRR	37
Figure 4-33 Smoke layer height estimated by CFAST and Analytical model for linearly increasing HRR ...	37
Figure 4-34 Hot layer temperature estimated by FDS and CFAST for constant HRR	38
Figure 4-35 Hot layer temperature estimated by FDS and CFAST for linearly increasing HRR.....	38
Figure 4-36 Smoke layer height estimated by FDS and CFAST for constant HRR	39

Figure 4-37 Smoke layer height estimated by FDS and CFAST for linearly increasing HRR	39
Figure 5-1 Inverse model estimation of HRR for constant HRR scenarios using McCaffrey's correlations	42
Figure 5-2 Inverse model estimation of ventilation factor for constant HRR scenarios using McCaffrey's correlations	43
Figure 5-3 Inverse model estimation of ventilation factor for constant HRR scenarios using only continuous flame region	43
Figure 5-4 Inverse model estimation of HRR for constant HRR scenarios using only continuous flame region	44
Figure 5-5 Inverse model estimation of HRR for linear HRR scenarios using McCaffrey's correlations	44
Figure 5-6 Inverse model estimation of ventilation factor for linear HRR scenarios using McCaffrey's correlations	45
Figure 5-7 Ventilation factor estimation for 3_Case_linear.....	45
Figure 5-8 HRR estimation for 3_Case_linear	46

List of Tables

Table 2-1 Constant HRR cases	5
Table 2-2 Different approaches for ventilation factor	6
Table 2-3 Opening dimensions and effective ventilation factor	7
Table 2-4 List of cases for constant HRR	10
Table 2-5 List of cases for linear HRR	10
Table 3-1 Recommended compartment dimension limits for zone models.....	12
Table 4-1 Correct implementation of McCaffrey's correlation for 1_Case_1-8.....	30
Table 4-2 Correct implementation of McCaffrey's correlation for 4_Case_1-8.....	31
Table 4-3 Comparison between using door or effective opening height for 4_Case_1-8	31
Table 4-4 Upper layer temperature and height using Analytical model for 1_Case_linear.....	32
Table 4-5 Upper layer temperature and height using Analytical model for 4_Case_linear.....	33

1 Introduction

Fire dynamics involves a strong interaction and coupling between several parameters and aspects such as chemistry, turbulence and radiation. Modelling advances along with the increase in computational resources has allowed the visualizing and studying of fire dynamics in a manner which closely imitates reality. In fire safety design calculations, in addition to the geometrical configuration, the Heat Release Rate (HRR) must be specified in advance. But in reality this information is not always known due to the complexity of the burning materials and other factors affecting the fire development.

Real-time knowledge of the fire growth and conditions inside the compartment can greatly help firefighters and rescue personnel. Currently, firefighting strategies are mainly based upon intuition and experience gained from previous accidents without solid scientific and technological grounds. It would be of great added value if these strategies can be based on the forecast of the fire development depending on parameters like temperature and smoke concentration inside the compartment. This would also help to save the lives of firefighters and rescue service personnel.

Thus, the first step is to develop a framework using a mathematical methodology that allows the display of a forecast of the fire development based on the physical data collected from a fire monitoring system. Despite the substantial advances in the field of fire dynamics and computational power in the previous decade, the development of numerical modeling for forecasting remains limited. The effectiveness of the forecasting model mainly depends on whether it is quick enough to provide results with a sufficient positive lead time. That is to say that the forecasting should be faster than the fire evolution itself.

The Computational Fluid Dynamics (CFD) based fire models, which are used to study the fire dynamics, are computationally very expensive. The computation time required for such simulations can be hours and even days, which is far greater than the simulated time. If conventional fire models are to be used for the purpose of forecasting, the computational time has to be decreased considerably so that the estimation of the development of the fire can be made available with positive lead time.

The fire models which are based on the CFD solve the conservation equations at the smallest possible level by dividing the domain into small cells. This gives satisfactory results but increases the computational effort many folds, even with the current computational capacity. To decrease the computational time, one approach may be to use a coarser mesh. However, the results are not precise, even for the simplest cases.

An alternative approach is to use zone models. Although zone models solve the fire dynamics by using similar energy and mass conservation correlations, the computational time is reduced by dividing the domain into 2 zones (in case of 2-zone models). This is a crude approximation, which however provides reasonable results with positive lead times in the early stages of the fire.

1.1 Literature review

For most of the studies on the development of a forecasting methodology, real-time sensor data is used in terms of temperature, smoke and heat detector, mass flow rate out of the compartment or even flow velocities. In a study by Cowlard et al. [1], one such approach is suggested where sensor data in real time is coupled with high performance computers which run multiple simulations. The closest match provides the forecast. Jahn et al. [2,3] developed a forecasting methodology which uses a tangent linear model for optimization. This methodology is tested with a simple two-zone model as well as with CFD using a coarse grid. Both models provide a positive lead time. The two-zone model approach is able to reasonably estimate the temperature and hot layer height, whereas for the CFD approach, more details are required.

In addition to an estimation of HRR, Davis and Forney [4] developed a model at NIST which also gives an approximation of the location of fire. This sensor-driven inverse fire model (SDIFM) uses sensor signals in terms of temperature and smoke concentration from heat and smoke detectors to estimate HRR. Since it is linked with CFAST, the estimation is instantaneous. In a similar manner, Richards et al. [5] developed a model to estimate HRR and the location of fire in large compartments using the transient temperature data from sensors on the ceiling. This prediction is based on the difference between times of activation of the actual sensor and the activation time provided by the zone model. The inverse HRR had an error of 300% - 500%.

Neviackas [6] established a genetic algorithm (GA) to estimate the HRR along with other parameters using only the upper layer temperature measurement from the reference BRI zone model simulations. The GA runs numerous possible solutions to find the one whose upper layer temperature is close to the previous BRI reference temperature. Although the model performs well, the simulation time is of the order of several hours. In addition, Overholt and Ezekoye [7] developed an inverse model for estimating transient HRR which satisfies the measured transient temperature. The model provides HRR solution with relatively small error between 0.04 and 0.24 within a few seconds.

Since most of the sensor-driven forecasting rely on the fact that these sensors should be present inside the building before the forecasting to provide the data, another approach to this problem can be the use of video feedback. The advancement in video and imaging technologies has made it possible to correctly estimate the temperature and other parameters inside the compartment. In such an approach, Beji et al. [8,9] presented a forecasting model which estimates the natural smoke filling of a large atrium using feed from video. The assimilated data from the video allows a prediction of the HRR development, which is then used as an input to a two-zone forecasting model to estimate temperature and smoke layer height. Because of the use of a zone model, positive lead time is obtained. In another article, Beji et al. [10] developed a forecasting methodology which estimates the fire growth factor and heat loss factor based on assimilation of temperature from thermocouples and video data. The model provides positive lead time when analyzed with experimental data of furniture fires in an ISO room.

1.2 Objective

The goal of this study is to develop an inverse zone modeling framework, which allows providing estimates of the heat release rate (HRR) inside the compartment and tracking changes in the ventilation conditions (which may result from window breakage for example). Such framework could be integrated in a fire forecasting system that provides real-time predictions of the fire development. By using the upper layer temperature and smoke layer height inside the compartment as an input, an estimate can be made of the heat release rate and the ventilation factor. This input data in terms of smoke layer temperature and height can be gathered through the sensors, thermal imaging or by using the output of forward fire models. This assimilated data then can be coupled with the inverse model to determine the development of fire along with any change in the ventilation conditions of the compartment.

In case of a typical forward fire model, geometrical configurations and fire characteristics are used as an input to estimate the temperature, smoke and gas species concentrations, whereas in the inverse modeling, the fire characteristics in terms of heat release rate (HRR) and location are estimated using data from sensors or by other means. Typical inputs for the inverse modeling can be the temperature and smoke concentration inside the compartment. Inverse fire modeling is important since it can provide the estimation of the fire load, which can be helpful to the firefighters to be able to understand the situation and efficiently design a strategy.

1.3 Methodology

An ISO room is considered for the study. Instead of performing physical experiments which require resources and time, the scenarios are studied using computational models. Since most of the fire models have been validated by comparing the results with experimental data, it is safe to assume that for this study similar outcomes can be expected in case of using experimental data. The geometrical configuration of the ISO room is discussed in Chapter 2.

Two fire models are used, one based on computational fluid dynamics i.e. FDS v5.5.3 and another based on simple zone modeling i.e. CFAST v6.02.0291. The results of these models are then compared with an analytical forward model which will be used for forecasting. At the second stage, an inverse zone model is developed which takes the input information on the upper layer temperature and smoke layer height and predicts the appropriate heat release rate and ventilation factor.

For the analytical forward model and the inverse model, simple energy and mass conservation correlations are used. For the numerical solution, MATLAB v 7.9.0.529 (R2209b) is used.

2 Geometrical configuration and list of test cases

2.1 Room Geometry

For consistency, an ISO 9705 [11] standard full-size room is considered with the dimensions of 3.6m long, 2.4m wide and 2.4m high. The door is 2m high and 0.8m wide. Figures 2-1 and 2-2 below show the dimensions of the compartment and the location of the fire source. For simplicity, the thermal properties and losses are not considered, which gives an adiabatic case.

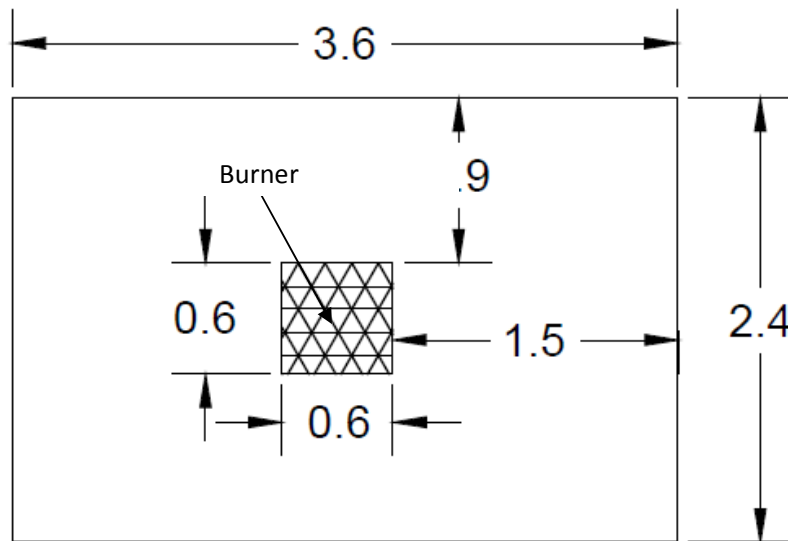


Figure 2-1 Dimensions of the room and burner location

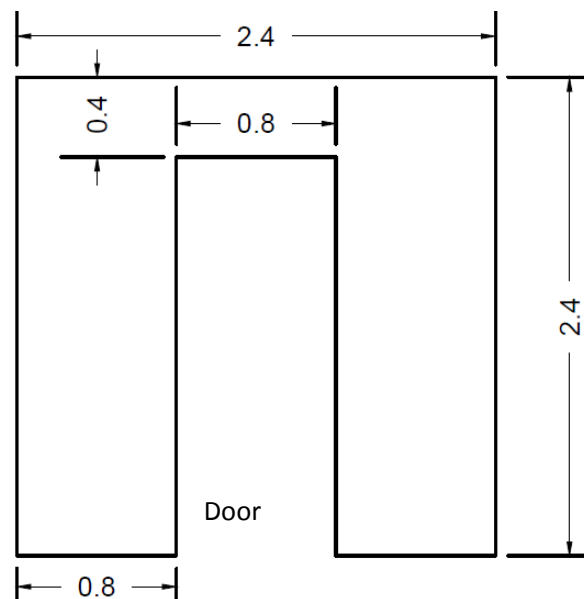


Figure 2-2 Dimensions of door

2.2 Fire Source

The fire source is placed in the middle of the room with a surface area of 0.36m^2 ($0.6\text{m} \times 0.6\text{m}$). Propane with 50000 kJ/kg heat of combustion is used as fuel. Two configurations are tested, one with constant HRR and another with linear increase over a specified interval.

For a constant HRR configuration, cases are simulated for a set of different HRR from 300 to 1000kW with an increment of 100kW to check the dependence of the model on change in HRR. For the linearly increasing HRR configuration, a linear HRR curve from 0 to 1000 kW over an interval of 300 seconds is used.

Scenarios	Heat release rate (kW)	Simulation time (s)
Case_1	300	120
Case_2	400	120
Case_3	500	120
Case_4	600	120
Case_5	700	120
Case_6	800	120
Case_7	900	120
Case_8	1000	120

Table 2-1 Constant HRR cases

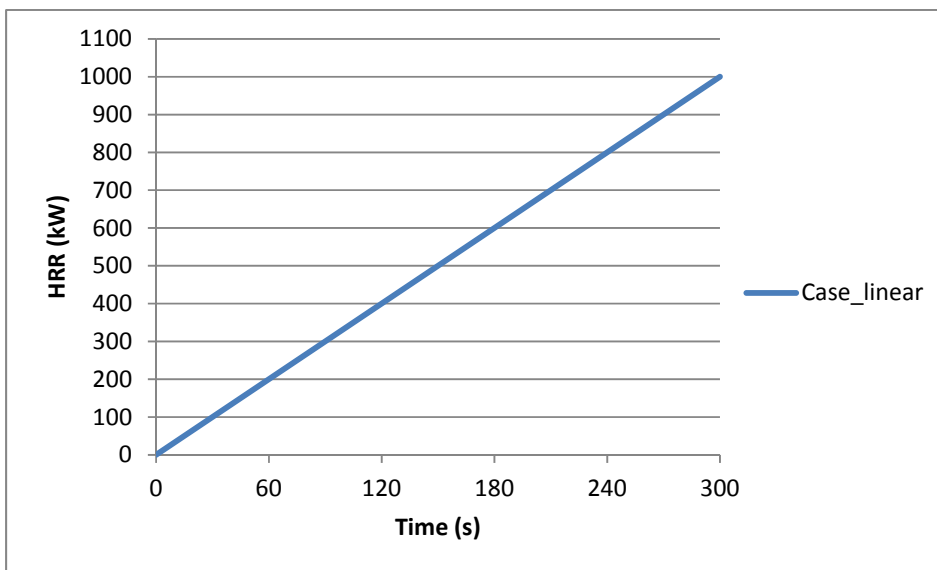


Figure 2-3 Linear HRR case

2.3 Ventilation factor

As discussed earlier, different ventilation factors V_f are simulated by changing the window size and numbers. In total, 6 different configurations are used ranging from 2 to 10.5. For a constant HRR configuration, simulations are run for 120 seconds and the window(s) opens after 60 seconds changing the ventilation factor. For the linear HRR case, the simulations are run for 300 seconds and the window(s) opens at 150 seconds.

For a simple case with only one opening, the ventilation factor can be calculated by the product of the opening area and square root of the opening height. In case of multiple openings, the ventilation factor can be calculated using the effective area and height of the openings. There are 2 approaches for this, and both are described and compared. In Enclosure Fire Dynamics, the effective ventilation factor is calculated using the weighted average of the opening height [12].

$$V_f = A_o \sqrt{H_o} \tag{2-1}$$

where,

$$A_o = A_1 + A_2 + \dots + A_N \tag{2-2}$$

$$H_o = A_1 H_1 + A_2 H_2 + \dots + A_N H_N \tag{2-3}$$

In contrast, according to the other approach, the ventilation factor can be calculated using the relation below [13].

$$H_o = \left(\frac{A_1 \sqrt{H_1} + A_2 \sqrt{H_2} + \dots + A_N \sqrt{H_N}}{A_o} \right)^2 \tag{2-4}$$

The difference between the two approaches is shown below in the Table 2-2. For the further use, the results from the second relation are used in calculations.

Case	H_o^1	V_f^1	H_o^2	V_f^2
1	2	2.2627	2	2.2627
2	1.66	2.88	1.60	2.84
3	1.67	4.60	1.65	4.60
4	1.53	6.20	1.52	6.16
5	1.87	8.55	1.85	8.50
6	1.84	10.27	1.83	10.24
				1 using equation 2-3 2 using equation 2-4

Table 2-2 Different approaches for ventilation factor

The dimensions of the window(s) and the respective ventilation factor are described in Table 2-3, and the positioning is shown in Figure 2-4.

Case	Door	Window 1	Window 2	Ventilation Factor V_f
1_CASE	0.8m x 2m	-	-	2.2627
2_CASE	0.8m x 2m	0.8m x 0.8m	-	2.84
3_CASE	0.8m x 2m	1.4m x 1.4m	-	4.60
4_CASE	0.8m x 2m	1.4m x 1.4m	1.2m x 1.2m	6.16
5_CASE	0.8m x 2m	0.8m x 0.8m	2m x 2m	8.50
6_CASE	0.8m x 2m	1.4m x 1.4m	2m x 2m	10.24

Table 2-3 Opening dimensions and effective ventilation factor

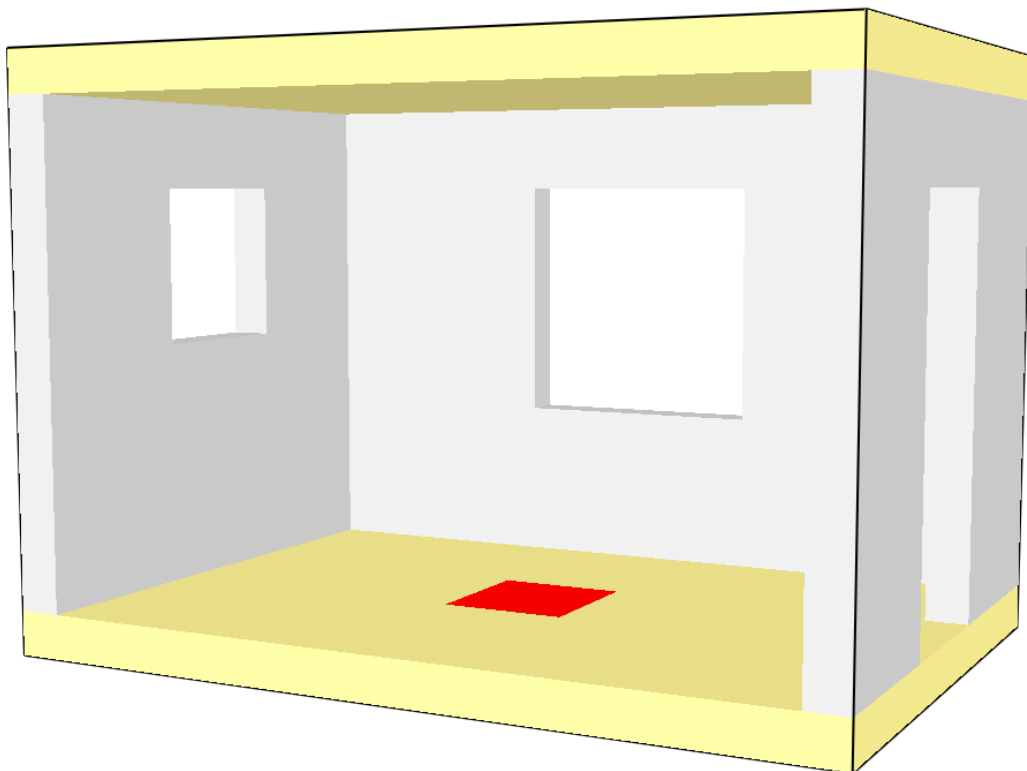


Figure 2-4 Positioning of windows

2.4 List of cases

Since the combination of different ventilation factors and the HRR gives a lot of scenarios, a periodic approach is used for naming the scenarios. For the scenarios with a constant HRR, the naming is done in form of 'X_Case_Y'. The prefix 'X' represents the ventilation factor, and the suffix 'B' represents the HRR. For example, 2_Case_4 means that the ventilation factor is 2.84 while the HRR is 600 kW. The list of all the scenarios is represented in Table 2-4 along with an indication of which fire model is used for calculation purposes.

Case	Ventilation factor	HRR (kW)	Dimensions of vents (m)			Fire model used
			Door	Window 1	Window 2	
1_Case_1	2.2627	300	0.8 x 2.0	-	-	CFAST, Analytical model
1_Case_2	2.2627	400	0.8 x 2.0	-	-	CFAST, Analytical model
1_Case_3	2.2627	500	0.8 x 2.0	-	-	CFAST, Analytical model
1_Case_4	2.2627	600	0.8 x 2.0	-	-	FDS, CFAST, Analytical model
1_Case_5	2.2627	700	0.8 x 2.0	-	-	CFAST, Analytical model
1_Case_6	2.2627	800	0.8 x 2.0	-	-	CFAST, Analytical model
1_Case_7	2.2627	900	0.8 x 2.0	-	-	CFAST, Analytical model
1_Case_8	2.2627	1000	0.8 x 2.0	-	-	CFAST, Analytical model
2_Case_1	2.84	300	0.8 x 2.0	0.8 x 0.8	-	FDS, CFAST, Analytical model
2_Case_2	2.84	400	0.8 x 2.0	0.8 x 0.8	-	FDS, CFAST, Analytical model
2_Case_3	2.84	500	0.8 x 2.0	0.8 x 0.8	-	FDS, CFAST, Analytical model
2_Case_4	2.84	600	0.8 x 2.0	0.8 x 0.8	-	FDS, CFAST, Analytical model
2_Case_5	2.84	700	0.8 x 2.0	0.8 x 0.8	-	FDS, CFAST, Analytical model
2_Case_6	2.84	800	0.8 x 2.0	0.8 x 0.8	-	FDS, CFAST, Analytical model
2_Case_7	2.84	900	0.8 x 2.0	0.8 x 0.8	-	FDS, CFAST, Analytical model
2_Case_8	2.84	1000	0.8 x 2.0	0.8 x 0.8	-	FDS, CFAST, Analytical model
3_Case_1	4.60	300	0.8 x 2.0	1.4 x 1.4	-	CFAST, Analytical model
3_Case_2	4.60	400	0.8 x 2.0	1.4 x 1.4	-	CFAST, Analytical model

3_Case_3	4.60	500	0.8 x 2.0	1.4 x 1.4	-	CFAST, Analytical model
3_Case_4	4.60	600	0.8 x 2.0	1.4 x 1.4	-	FDS, CFAST, Analytical model
3_Case_5	4.60	700	0.8 x 2.0	1.4 x 1.4	-	CFAST, Analytical model
3_Case_6	4.60	800	0.8 x 2.0	1.4 x 1.4	-	CFAST, Analytical model
3_Case_7	4.60	900	0.8 x 2.0	1.4 x 1.4	-	CFAST, Analytical model
3_Case_8	4.60	1000	0.8 x 2.0	1.4 x 1.4	-	CFAST, Analytical model
4_Case_1	6.16	300	0.8 x 2.0	1.4 x 1.4	1.2 x 1.2	CFAST, Analytical model
4_Case_2	6.16	400	0.8 x 2.0	1.4 x 1.4	1.2 x 1.2	CFAST, Analytical model
4_Case_3	6.16	500	0.8 x 2.0	1.4 x 1.4	1.2 x 1.2	CFAST, Analytical model
4_Case_4	6.16	600	0.8 x 2.0	1.4 x 1.4	1.2 x 1.2	FDS, CFAST, Analytical model
4_Case_5	6.16	700	0.8 x 2.0	1.4 x 1.4	1.2 x 1.2	CFAST, Analytical model
4_Case_6	6.16	800	0.8 x 2.0	1.4 x 1.4	1.2 x 1.2	CFAST, Analytical model
4_Case_7	6.16	900	0.8 x 2.0	1.4 x 1.4	1.2 x 1.2	CFAST, Analytical model
4_Case_8	6.16	1000	0.8 x 2.0	1.4 x 1.4	1.2 x 1.2	CFAST, Analytical model
5_Case_1	8.50	300	0.8 x 2.0	0.8 x 0.8	2.0 x 2.0	FDS, CFAST, Analytical model
5_Case_2	8.50	400	0.8 x 2.0	0.8 x 0.8	2.0 x 2.0	FDS, CFAST, Analytical model
5_Case_3	8.50	500	0.8 x 2.0	0.8 x 0.8	2.0 x 2.0	FDS, CFAST, Analytical model
5_Case_4	8.50	600	0.8 x 2.0	0.8 x 0.8	2.0 x 2.0	FDS, CFAST, Analytical model
5_Case_5	8.50	700	0.8 x 2.0	0.8 x 0.8	2.0 x 2.0	FDS, CFAST, Analytical model
5_Case_6	8.50	800	0.8 x 2.0	0.8 x 0.8	2.0 x 2.0	FDS, CFAST, Analytical model
5_Case_7	8.50	900	0.8 x 2.0	0.8 x 0.8	2.0 x 2.0	FDS, CFAST, Analytical model
5_Case_8	8.50	1000	0.8 x 2.0	0.8 x 0.8	2.0 x 2.0	FDS, CFAST, Analytical model
6_Case_1	10.24	300	0.8 x 2.0	1.4 x 1.4	2.0 x 2.0	CFAST, Analytical model
6_Case_2	10.24	400	0.8 x 2.0	1.4 x 1.4	2.0 x 2.0	CFAST, Analytical model
6_Case_3	10.24	500	0.8 x 2.0	1.4 x 1.4	2.0 x 2.0	CFAST, Analytical model

6_Case_4	10.24	600	0.8 x 2.0	1.4 x 1.4	2.0 x 2.0	FDS, CFAST, Analytical model
6_Case_5	10.24	700	0.8 x 2.0	1.4 x 1.4	2.0 x 2.0	CFAST, Analytical model
6_Case_6	10.24	800	0.8 x 2.0	1.4 x 1.4	2.0 x 2.0	CFAST, Analytical model
6_Case_7	10.24	900	0.8 x 2.0	1.4 x 1.4	2.0 x 2.0	CFAST, Analytical model
6_Case_8	10.24	1000	0.8 x 2.0	1.4 x 1.4	2.0 x 2.0	CFAST, Analytical model

Table 2-4 List of cases for constant HRR

For the scenarios where the HRR is linearly increased from 0 kW to 100 kW, the naming is done in the form of 'X_Case_linear' where 'X' represents the ventilation factor, similar to the constant HRR cases. The list of all 6 scenarios is provided in Table 2-5. For all of these scenarios, FDS, CFAST and the analytical model are used for calculations.

Case	Ventilation factor	HRR (kW)	Dimensions of vents (m)			Fire model used
			Door	Window 1	Window 2	
1_Case_linear	2.2627	0-1000	0.8 x 2.0	-	-	FDS, CFAST, Analytical model
2_Case_linear	2.84	0-1000	0.8 x 2.0	0.8 x 0.8	-	FDS, CFAST, Analytical model
3_Case_linear	4.60	0-1000	0.8 x 2.0	1.4 x 1.4	-	FDS, CFAST, Analytical model
4_Case_linear	6.16	0-1000	0.8 x 2.0	1.4 x 1.4	1.2 x 1.2	FDS, CFAST, Analytical model
5_Case_linear	8.50	0-1000	0.8 x 2.0	0.8 x 0.8	2.0 x 2.0	FDS, CFAST, Analytical model
6_Case_linear	10.24	0-1000	0.8 x 2.0	1.4 x 1.4	2.0 x 2.0	FDS, CFAST, Analytical model

Table 2-5 List of cases for linear HRR

3 Presentation of the fire models

Most of the fire models require geometric configuration and HRR. Using these parameters and solving the basic mass, momentum and energy conservation, temperature, density and smoke layer height are calculated.

3.1 CFD

Different CFD packages are available which incorporate the fire dynamics and smoke movement. Among these packages FDS (Fire Dynamics Simulator) developed by NIST is most widely used. FDS solves a form of the Navier-Stokes equation adequate for low-speed thermally driven flows. It is based on LES (Large Eddies Simulations) [14]. Large eddies are solved directly while the turbulences at the subgrid level are modeled using Smagorinsky's approach [15]. The basic idea behind the LES technique is that the eddies that account for most of the mixing are large enough to be calculated with reasonable accuracy from the equations of fluid dynamics.

In FDS the computational domain is divided into several small individual control volumes equivalent to the grid cell. As a result mass, momentum and energy conservation is solved for each cell. Although resolving these phenomenon and conservation at the individual cell level gives better results but it computational expensive and time consuming.

3.2 Zone Models

Zone models solve basic correlations. For zone models, the basic assumption is that the compartment is divided into control volumes where each control volume has one temperature and smoke density. Different models divide the compartment into a different number of volumes or zones.

Most of the models use only 2 control volumes. Fire induces plume in the compartment, which gives a smoke filled hot upper layer and a clear clod lower layer. Therefore, it is assumed that the density is uniform in both control volumes; as a consequence, the temperature is also considered as uniform. However, the temperature and density are not uniform in reality, and the compartment cannot be divided into 2 zones. But the difference within the layers is small, and thus for simplification it can be assumed as 2 distinctive zones.

CFAST [16] is a 2-zone model which solves the equation for conservation of mass and energy the ideal gas law. The momentum equation is not solved explicitly, except for the flow velocity at the vents, for which the Bernoulli equation is used [17]. CFAST solves the following set of equations for layer temperature, layer volume and pressure.

$$\frac{dP}{dt} = \frac{\gamma-1}{V} (\dot{h}_L + \dot{h}_U) \quad (3-1)$$

$$\frac{dV_U}{dt} = \frac{1}{P\gamma} \left((\gamma - 1)\dot{h}_i - V_U \frac{dP}{dt} \right) \quad (3-2)$$

$$\frac{dT_U}{dt} = \frac{1}{c_{pr} h_{oi} V_U} \left((\dot{h}_U - c_p \dot{m}_U T_U) + V_U \frac{dP}{dt} \right) \quad (3-3a)$$

$$\frac{dT_L}{dt} = \frac{1}{c_p r h_{oi} V_L} \left((\dot{h}_L - c_p \dot{m}_L T_L) + V_L \frac{dP}{dt} \right) \quad (3-3b)$$

The concept of zone models is best suited for enclosures in which the width and the length are not too different. In CFAST, the results and assumptions are valid only if the geometrical ratios are within the acceptable range. This is shown in Table 3-1.

Group	Acceptable	Special consideration required	Corridor flow algorithm
$(L/W)_{\max}$	$L/W < 3$	$3 < L/W < 5$	$L/W < 5$
$(L/H)_{\max}$	$L/H < 3$	$3 < L/H < 6$	$L/H > 6$
$(W/H)_{\max}$	$W/H > 0.4$	$0.2 < W/H < 0.4$	$W/H < 0.2$

Table 3-1 Recommended compartment dimension limits for zone models

Burning creates plume which acts as a pump transferring mass and enthalpy from the lower layer into the upper layer. The amount of mass and enthalpy that is transferred can be calculated using empirical correlations which also take into account air entrainment from the surroundings.

CFAST uses the correlations provided by McCaffrey [18] and Heskestad [19], and both give similar results. McCaffrey divides the plume into 3 regions depending on the flame length, and provides 3 separate equations.

$$\dot{m}_p = 0.011 \dot{Q}_f \left(\frac{h-z_f}{\dot{Q}_f^{2/5}} \right)^{0.566}, \quad 0 < \frac{h-z_f}{\dot{Q}_f^{2/5}} < 0.08 \quad (3-4a)$$

$$\dot{m}_p = 0.026 \dot{Q}_f \left(\frac{h-z_f}{\dot{Q}_f^{2/5}} \right)^{0.909}, \quad 0.08 < \frac{h-z_f}{\dot{Q}_f^{2/5}} < 0.2 \quad (3-4b)$$

$$\dot{m}_p = 0.124 \dot{Q}_f \left(\frac{h-z_f}{\dot{Q}_f^{2/5}} \right)^{1.895}, \quad 0.20 < \frac{h-z_f}{\dot{Q}_f^{2/5}} \quad (3-4c)$$

where z_f is the height of the fire source from the floor level.

On the other hand, Heskestad provides a single correlation for the plume which depends on the convective heat release rate $\dot{Q}_{f,c}$ and virtual origin z_0 .

$$\dot{m}_p = 0.071 \dot{Q}_{f,c}^{1/3} (h - z_0)^{5/3} (1 + 0.026 \dot{Q}_{f,c}^{2/3} (h - z_0)^{-5/3}) \quad (3-5)$$

where,

$$z_0 = -1.02D + 0.083 \dot{Q}_f^{2/5}$$

The benefit of the McCaffrey model over Heskestad is that it requires only 2 parameters compared to 3 parameters for Heskestad. In addition to the fire load (HRR) and smoke layer height, the Heskestad correlation requires the diameter of the fire, thus making it more complicated.

3.3 Analytical model

For the analytical model, using the basic mass and energy conservation equation, a relationship can be achieved to calculate the upper layer temperature and smoke layer height. The idea is to formulate a set of equations which give similar results for upper layer height and temperature to the forward modeling packages. If the results are comparable, the same model can be used for developing the correlations for inverse modeling.

The following basic energy conservation and mass conservation equations can be used for this purpose as presented by Beji et al. [10]

Energy conservation:

$$\frac{d}{dt} [\rho_u c_p (T_u - T_a) A (H - h)] = (1 - \lambda_c) \dot{Q}_f - \dot{m}_{out,u} c_p (T_u - T_a) \quad (3-6)$$

Mass conservation:

$$\frac{d}{dt} [\rho_u A (H - h)] = \dot{m}_p + \dot{m}_{in,u} - \dot{m}_{out,u} \quad (3-7)$$

where t is the time, ρ_u is the upper layer density, c_p represents the specific heat of air, T_u is upper layer temperature, T_a is ambient temperature, A is the surface area of the room with height H . λ_c represents the fraction of HRR \dot{Q}_f lost to the surrounding and room boundary. $\dot{m}_{out,u}$ is the mass flow rate out of the room through openings. $\dot{m}_{in,u}$ represents the mass flow into the compartment in the form of air entrainment, while \dot{m}_p is the plume mass flow rate.

According to the basic assumptions, only adiabatic configuration is studied meaning there are no losses to the boundary and surroundings except to the hot upper layer. This results in λ_c being equal to zero. Secondly, the transient terms in both energy and mass conservation equations are neglected. For constant HRR cases, these terms can be neglected since the change with time is minute. For simplification in case of the linearly increasing HRR, the linear curve is transformed into a step curve where the HRR remains constant during the interval. Thus, the transient term can be neglected again in case of linear HRR. On the basis of above assumptions, the conservation equations can be simplified as follows.

Energy conservation:

$$\dot{Q}_f = \dot{m}_{out} c_p (T_u - T_a) \quad (3-8)$$

Mass conservation:

$$\dot{m}_{out} = \dot{m}_p \quad (3-9)$$

where \dot{m}_p is given from McCaffrey's plume correlation as discussed in section 3.2.

$$\dot{m}_p = a \dot{Q}_f \left(\frac{h}{\dot{Q}_f^{2/5}} \right)^n \quad (3-4)$$

and for \dot{m}_{out} [13] following correlation can be used

$$\dot{m}_{out} = \frac{2}{3} C_d A_o \sqrt{H_o} \rho_a \sqrt{2g \frac{T_a}{T_u} \left(1 - \frac{T_a}{T_u}\right)} \left(1 - \frac{X_N}{H_D}\right)^{3/2} \quad (3-10)$$

where X_N is the neutral layer height and can be calculated using the relation below.

$$\sqrt{\rho_a(X_N - h)} \left(X_N + \frac{h}{2}\right) = \sqrt{\rho_a(H_D - X_N)}^{3/2} \quad (3-11)$$

The neutral layer height X_N and smoke layer height h are comparable for small HRR but the difference increases for higher HRR. The implementation of neutral layer height will result in more complexity and increased computation. Thus, for simplification of the model, X_N is assumed to be equivalent to the smoke layer height h . **Equation 3-10** is transformed as below.

$$\dot{m}_{out} = \frac{2}{3} C_d A_o \sqrt{H_o} \rho_a \sqrt{2g \frac{T_a}{T_u} \left(1 - \frac{T_a}{T_u}\right)} \left(1 - \frac{h}{H_D}\right)^{3/2} \quad (3-12)$$

using \dot{m}_p in **Equation 3-8** since $\dot{m}_{out} = \dot{m}_p$

$$\dot{Q}_f = a \dot{Q}_f \left(\frac{h}{\dot{Q}_f^{2/5}} \right)^n c_p (T_u - T_a)$$

$$\dot{Q}_f = \left(a \dot{Q}_f^{1-\frac{2n}{5}} h^n \right) c_p (T_u - T_a)$$

$$T_u = \frac{\left(\frac{\dot{Q}_f^{2n/5}}{a} \right)}{h^n c_p} + T_a$$

using this value of T_u from the above correlation in the mass conservation equation gives the following

$$\frac{2}{3} C_d A_o \sqrt{H_o} \rho_a \sqrt{2g \frac{T_a}{T_u} \left(1 - \frac{T_a}{T_u}\right)} \left(1 - \frac{h}{H_D}\right)^{3/2} = a \dot{Q}_f \left(\frac{h}{\dot{Q}_f^{2/5}} \right)^n$$

$$\left(\frac{2}{3} C_d A_o \sqrt{H_o} \rho_a\right) \sqrt{2g \frac{T_a}{\left(\frac{\dot{Q}_f^{2n}}{a}\right) + T_a} \left(1 - \frac{T_a}{\left(\frac{\dot{Q}_f^{2n}}{a}\right) + T_a}\right) \left(1 - \frac{h}{H_D}\right)^{3/2}} = a \dot{Q}_f^{1-\frac{2n}{5}} h^n$$

this can be simplified as

$$C_1 \sqrt{2g \frac{T_a}{\frac{c_2}{h^n c_p} + T_a} \left(1 - \frac{T_a}{\frac{c_2}{h^n c_p} + T_a}\right) \left(1 - \frac{h}{H_D}\right)^{3/2}} = C_3 h^n \quad (3-13)$$

$$T_u = \frac{T_a}{\frac{c_2}{h^n c_p} + T_a} \quad (3-14)$$

where,

$$C_1 = \left(\frac{2}{3} C_d A_o \sqrt{H_o} \rho_a\right)$$

$$C_2 = \left(\frac{\dot{Q}_f^{2n}}{a}\right)$$

$$C_3 = a \dot{Q}_f^{1-\frac{2n}{5}}$$

Equation 3-13 has only one unknown 'h' and can be solved iteratively to get the value. Using this value of h, T_u can be calculated using **Equation 3-14**.

4 Forward modeling results

As discussed in the methodology, the aim of this study is to develop an inverse model which detects the changes in HRR and ventilation factor using upper layer temperature and height as input parameters. Most of the fire models available today use HRR and the ventilation factor to predict the temperature and layer height.

In this chapter, the results are examined in terms of smoke layer height h and the upper layer temperature T_u . These results from the forward fire models like FDS and CFAST are compared with the analytical model developed in section 3.3. The idea is to see how comparable the results are, since these models are using the same basic energy and mass conservation principle. If the results are in good agreement, the analytical model can be implemented in such a way to get the inverse modeling.

4.1 FDS simulations

For FDS simulation, the same properties and configurations are used for all cases. To achieve the adiabatic conditions, the default surface is defined as adiabatic. To minimize the influence of inflowing air, sufficient space is provided around the compartment. The amount of space and its effect are discussed below. Open boundary conditions are used at the exterior of the compartment to avoid any accumulation of the smoke.

Radiation is allowed with a default radiation fraction of 0.33 and 300 radiation angles. All other parameters are kept at default values. A representative script file for one of the cases is presented in the **Appendix B1**. Since CFD is complex and the validity of the results depend on the user, a sensitivity study is done on different parameters which include the grid size and effect of extra domain.

4.1.1 Grid size

Grid size is an important factor which can influence the results greatly. Grid size should be reasonable so as to give good convergence. Most of the time, decreasing cell size results in improved results but at the expense of increased computation. Decreasing a cell size by half will result in an 8 times increase in computation. Grid size of 10cm and 5cm are chosen, and a comparison of upper layer temperature is done. Figure 4-1 shows a close approximation of temperature values between the two grid sizes especially for the steady state.

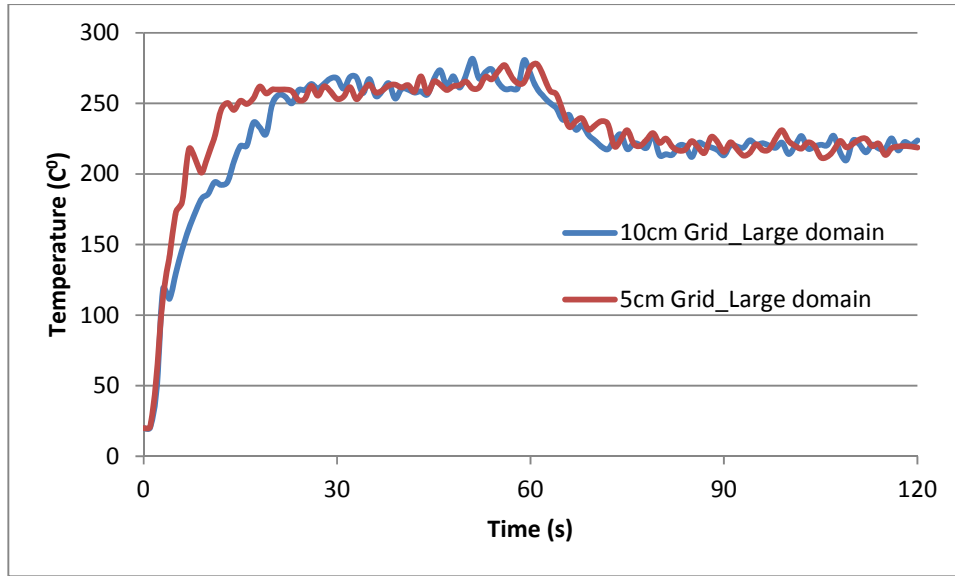


Figure 4-1 Effect of grid size on temperature

The grid size of 5cm gives slightly higher smoke layer height values as compared to the 10cm grid size but the difference is quite minute in this case. Similarly, the smoke layer height is also compared, and a similar negligible difference is observed.

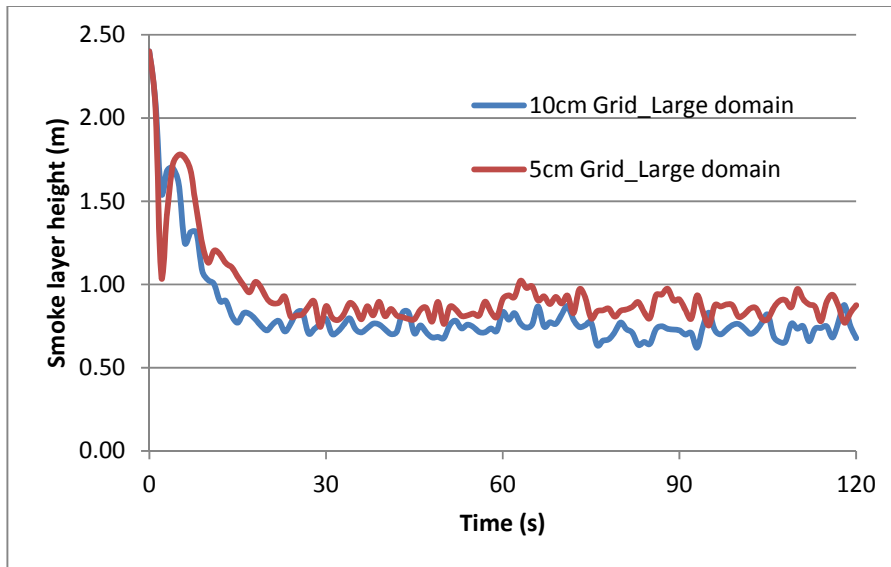


Figure 4-2 Effect of grid size on smoke layer height

From these results, the cell size is taken as 10cm since it will also reduce the computation time. For a better resolution, the ratio between D^* and the grid size should be at least 5 to 10. The relationship for D^* is given below. For 10cm grid size, the ratio is between 6 and 10 for HRR of 300kW to 1000kW.

$$D^* = \left(\frac{\dot{Q}}{\rho_{\infty} C_p T_{\infty} \sqrt{g}} \right)^{2/5} \quad (4-1)$$

4.1.2 Domain effect

Extra space is provided outside of the room to accommodate smoke and also to have a stable inflow of air. Two different domain size are compared to check for the influence on the upper layer temperature and on the smoke layer height. The larger domain is 0.5 times the dimension, while the smaller domain is 0.33 times the room dimension.

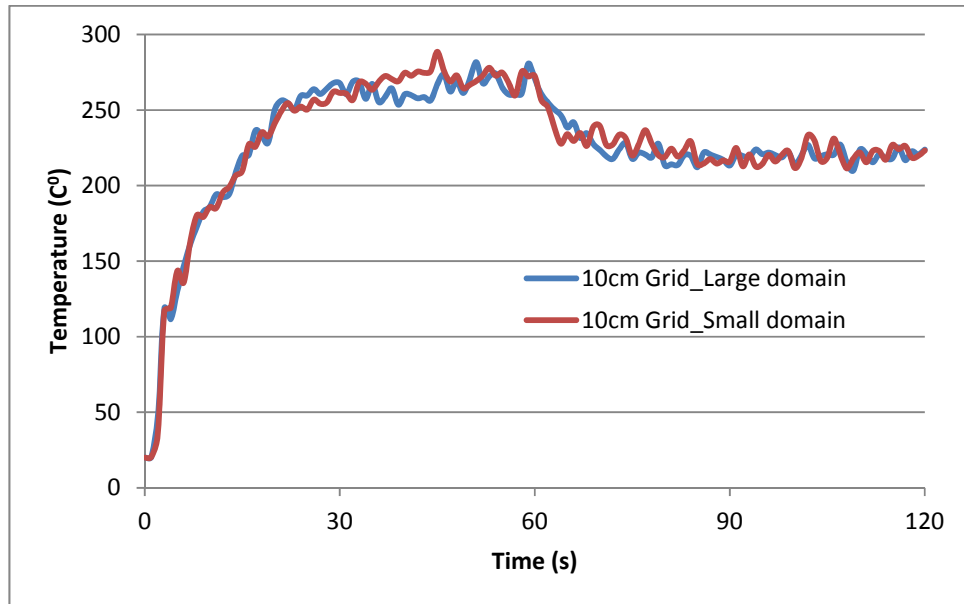


Figure 4-3 Effect of domain size on temperature

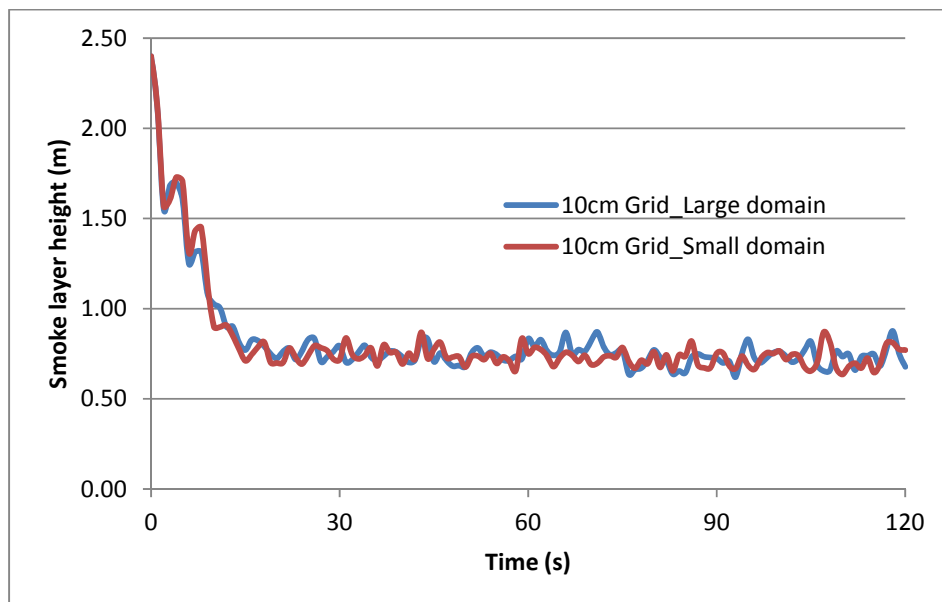


Figure 4-4 Effect of domain size on smoke layer height

As is clear from the Figure 4-3 and Figure 4-4, the domain size does not have any major effect on the output.

4.1.3 FDS Turbulence resolution

FDS is based on LES in which the kinetic energy of only the large eddies is resolved, which is usually 80% of the total according to the criteria provide by Pope [15]. The remaining 20% is resolved using sub-models. FDS provides a way to check the turbulence resolution by using the MTR (measure of turbulence resolution) as a plane. The result is provided in a color scale ranging from 0 to 1, with 0 indicating a perfect resolution and 1 indicating a poor resolution [14].

To check the effect of HRR and the ventilation factor on the turbulence resolution, results from 3 cases with the grid size of 10cm are presented below. Figure 4-5 represents MTR for scenario 1_Case_1, where the ventilation factor is 2.2627 and HRR is 100 kW. The turbulence is resolved effectively and is within a decent range as described above. Similarly, Figure 4-6 shows the MTR for scenario 1_Case_8 for which the HRR is increased to 1000 kW, and Figure 4-7 describes the case with ventilation factor 8.16 and HRR 600 kW. There are some unresolved turbulences with the increase in HRR and ventilation factor because more energy is produced and due to increased outflow of the hot gases through vents, but overall it is still within the acceptable range.

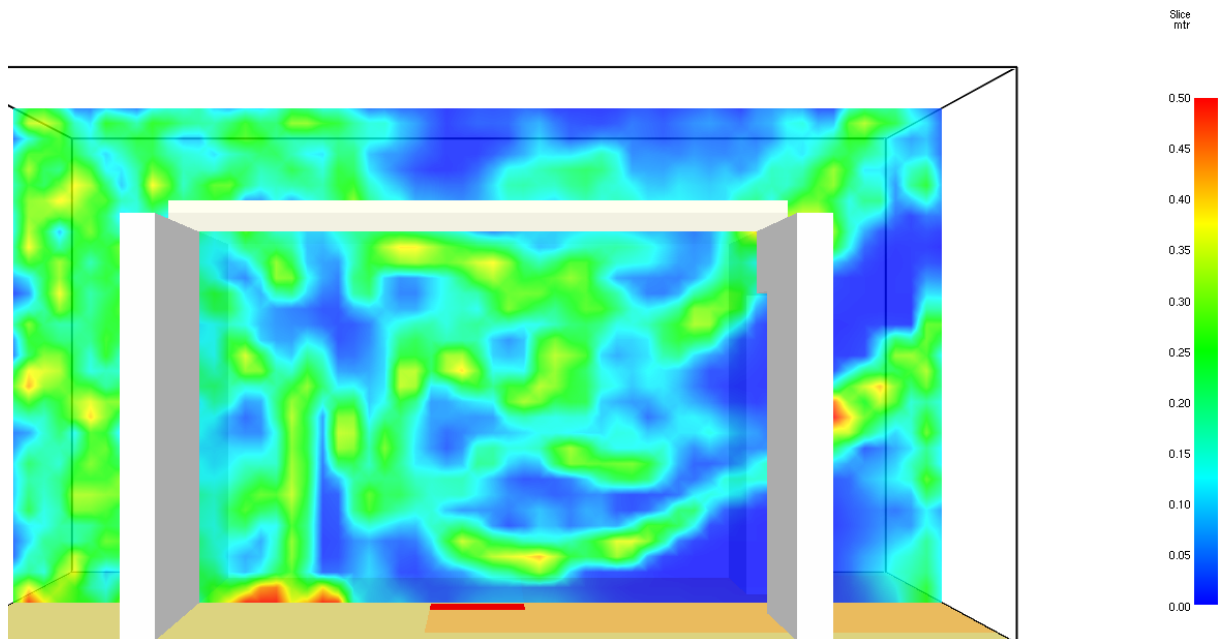


Figure 4-5 Turbulence resolution for 1_Case_1

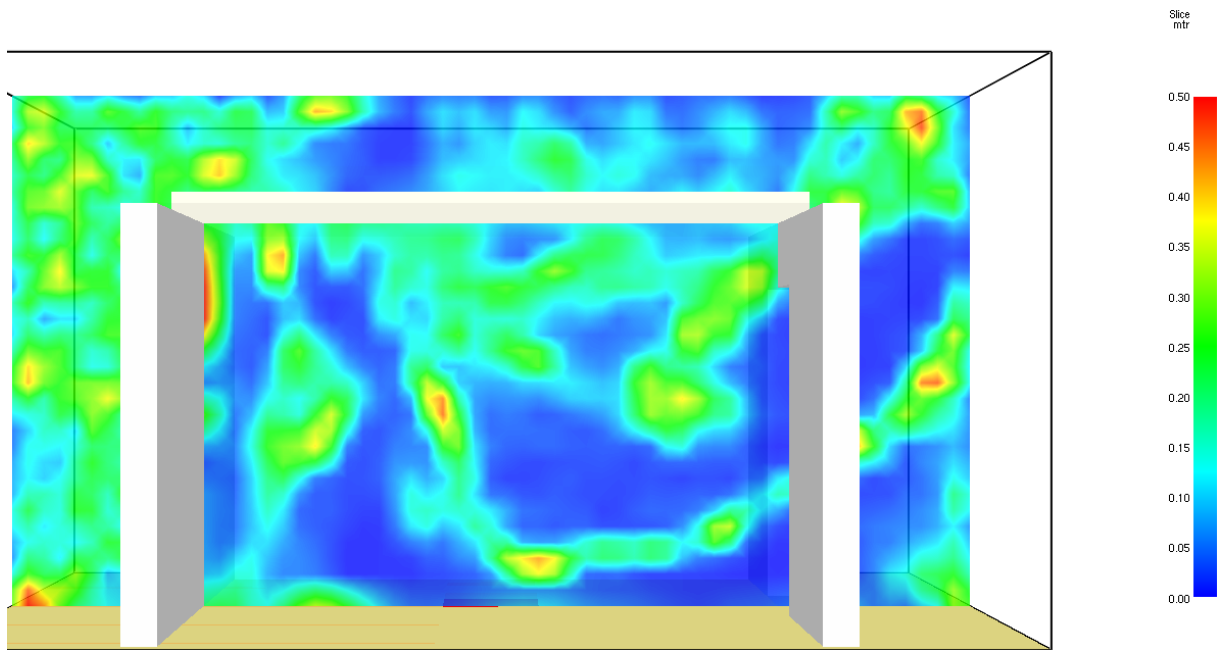


Figure 4-6 Turbulence resolution for 1_Case_8

10

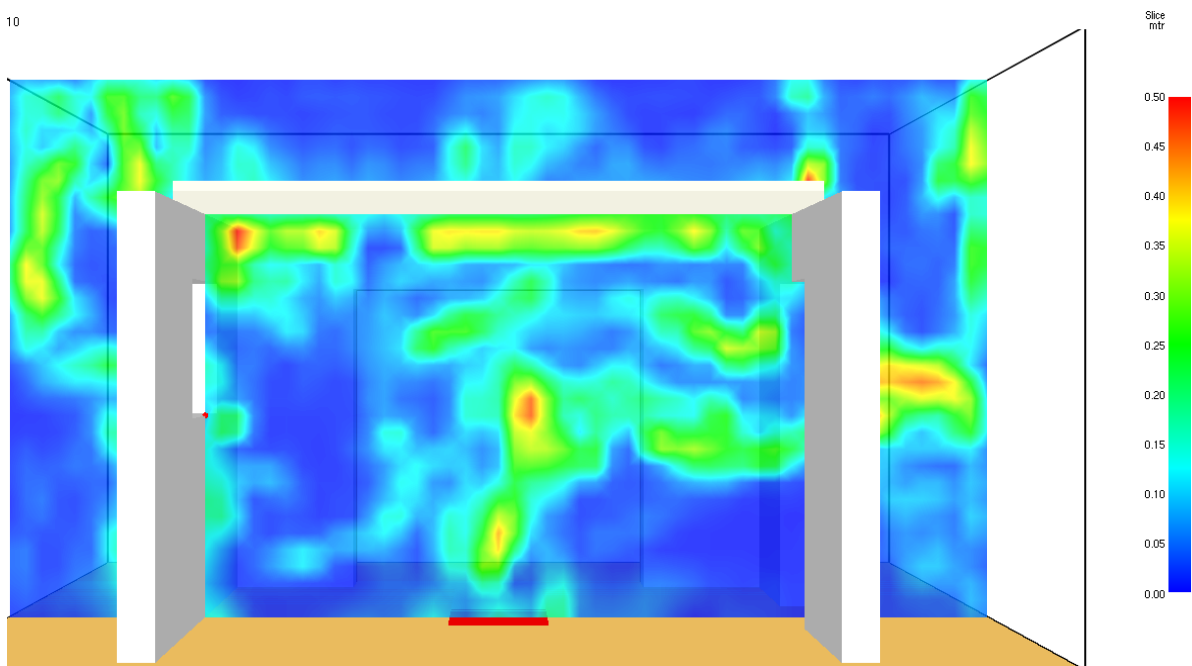


Figure 4-7 Turbulence resolution for 5_Case_4

4.1.4 Positions of sensors

FDS allows the measurement of the smoke layer height and upper hot zone temperature by using a device with the quantity 'UPPER TEMPERATURE' and 'LAYER HEIGHT'. The device is defined as a line, and measures the corresponding quantity along the length. To get a better approximation, the devices are distributed in the compartment so as to reduce the influence of direct flame. The distribution is shown in Figure 4-8.

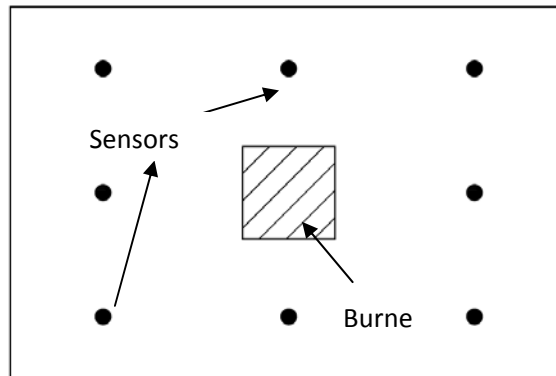


Figure 4-8 Location of devices for measuring upper layer temperature and height

4.1.5 Representation in Smokeview

For simplification, only one representative case is presented here, since most of the phenomena are similar. The window(s) opening is activated after 60s in case of constant HRR or 150s for linear HRR scenarios. Figure 4-9 presents the top view of one of the scenarios, showing the location of the fire source and the devices to measure the upper layer height and temperature. Extra domain is provided along all the openings as to minimize the effect of inflow air.

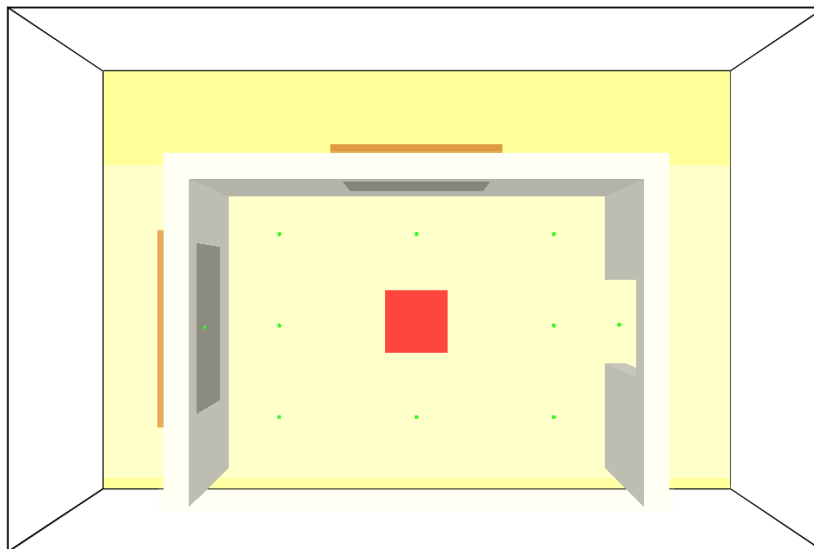


Figure 4-9 Top view of geometry in FDS

Figure 4-10 represents the smoke filling in the compartment before the activation of the opening when the outflow is only through the door which is open from the beginning. In addition, Figure 4-11 shows the situation when the openings are activated and the smoke is allowed to escape. Due to mass flow out of the compartment, air also enters through the lower portion of the openings. After some time, a balance is achieved in case of constant HRR scenarios.

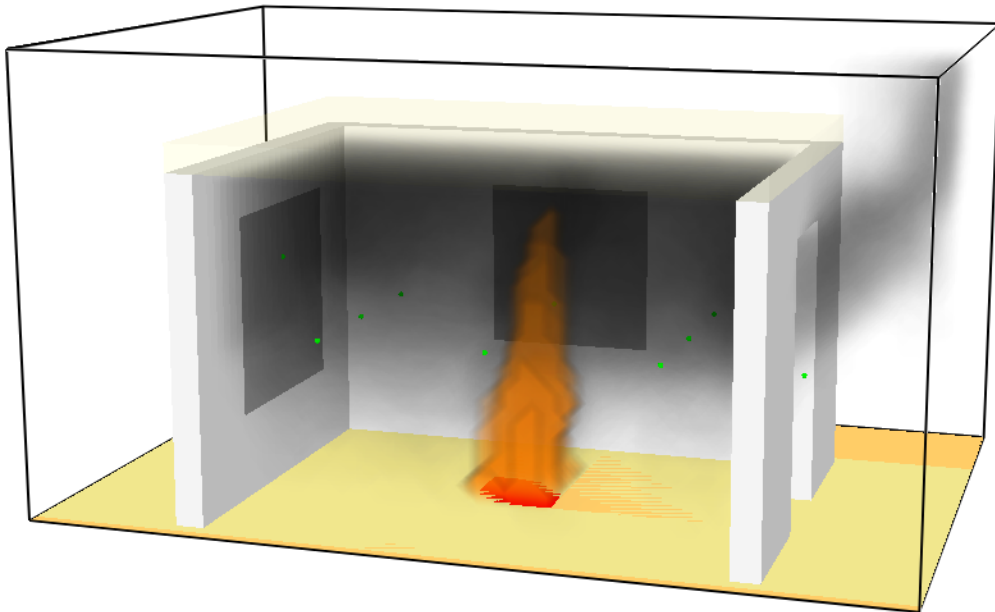


Figure 4-10 Flame and smoke before the opening of windows

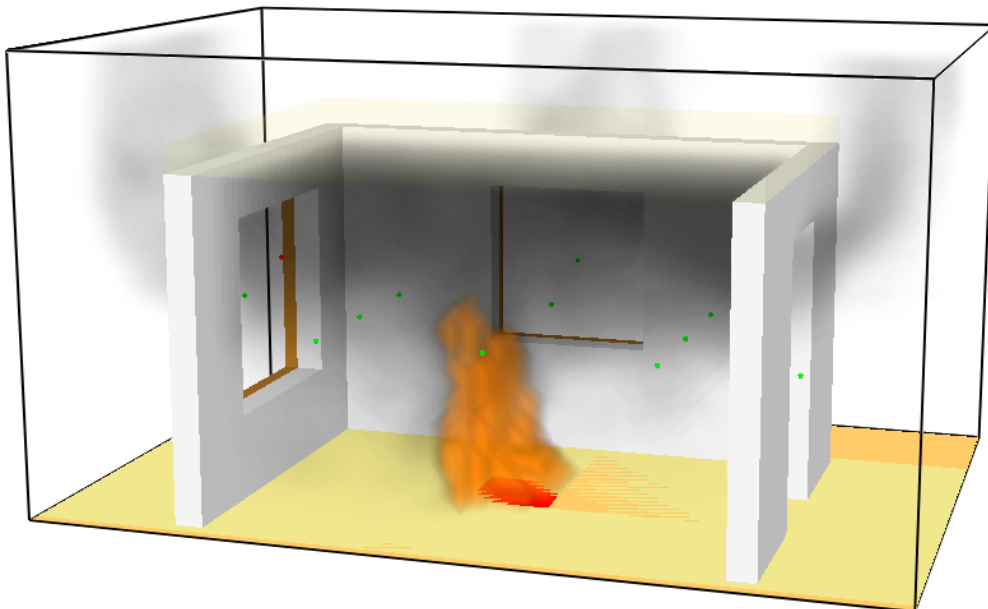


Figure 4-11 Flame and smoke after the opening of windows

Figure 4-12 to Figure 4-14 demonstrate the variation in the temperature profile with time for the scenario 4_Case_4. The temperature in the compartment increases until the point when the windows are activated, resulting in the inflow of ambient air and outflow of hot gases. This reduces the temperature due to mixing caused by fresh air and less radiation feedback from accumulated smoke.

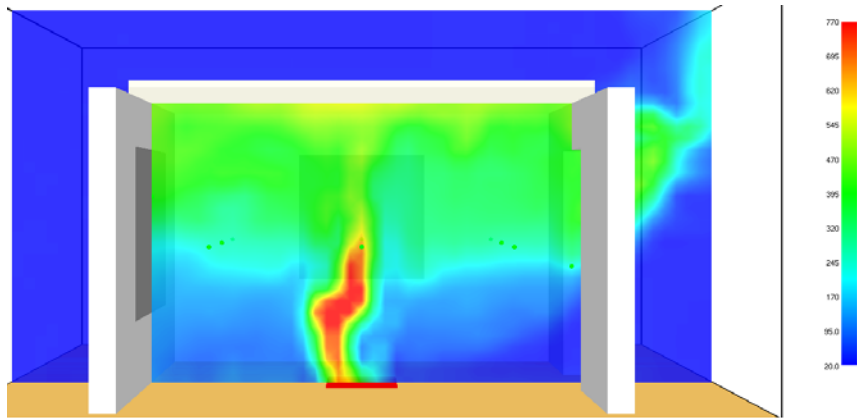


Figure 4-12 Temperature profile at the beginning of simulation

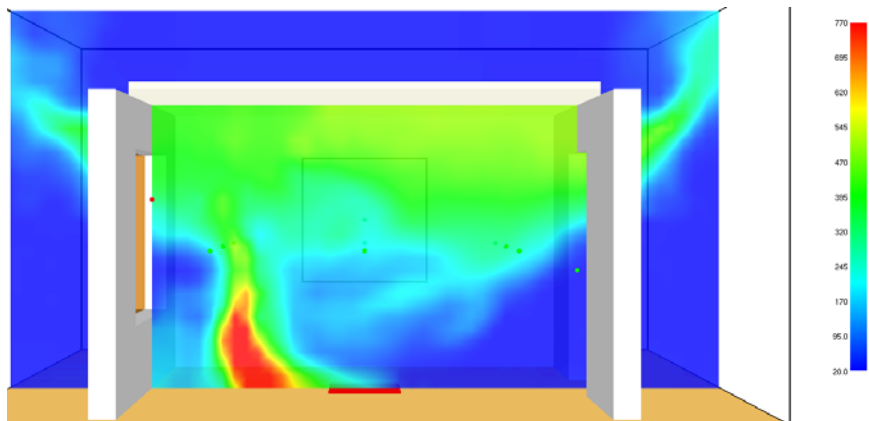


Figure 4-13 Temperature profile after the opening of windows

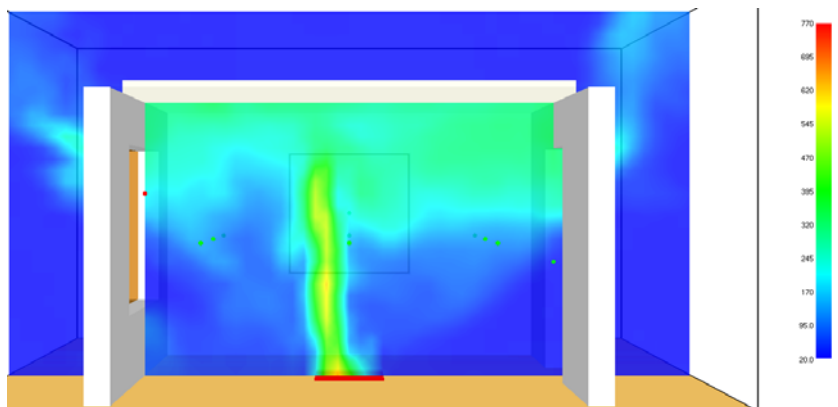


Figure 4-14 Temperature profile at the end of simulation

4.2 CFAST simulations

Similarly for CFAST simulations, all the ambient properties and other configurations are kept constant for all the scenarios. To achieve the adiabatic conditions, in compartment geometry the material properties are kept off. For Flow Characteristics, Normal Standard two-zone model is selected. Geometric configurations are described similar to FDS.

Since CFAST is based on simple empirical correlations, there is no concept of providing access space to minimize the effect of air inflow. CFAST offers two plume correlations, McCaffrey and Heskestad as discussed earlier. For comparability with the analytical model, McCaffrey's plume correlation is selected in CFAST as well. All the other parameter are kept with default values.

Figure 4-15 shows the basic geometry configuration used for all the scenarios. The location and size of window(s) depends on the scenario. The fire source is placed in the middle of the room with an area of 0.36 m^2 .

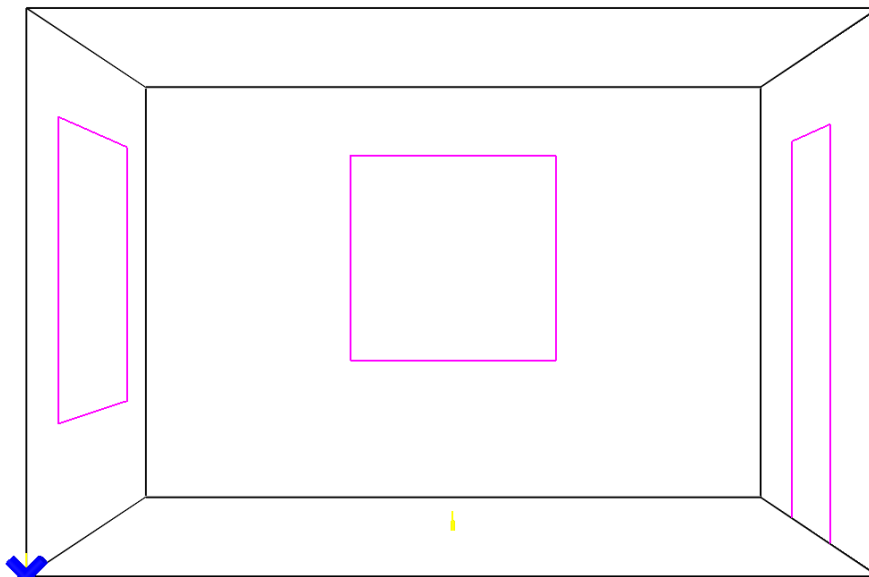


Figure 4-15 Basic geometry setup in CFAST

Figure 4-16 to 4-19 display the development of upper layer temperature and height profile with time. In the beginning, the layer descends and temperature increases as shown in Figure 4-16. But after a few seconds, the layer temperature and height stabilizes. This phenomenon continues up to the point when the windows are activated.

After the activation of the windows, hot smoke flows out and cold ambient air enters the compartment. The flow at the vents can be observed in Figure 4-18. The outflow is over the upper part of the vents while air at ambient temperature flows into the compartment through the lower part of the vents. This inflow of ambient air mixes with the hot air, and in addition the removal of smoke from the compartment reduces the overall temperature and smoke layer height as shown in Figure 4-19.

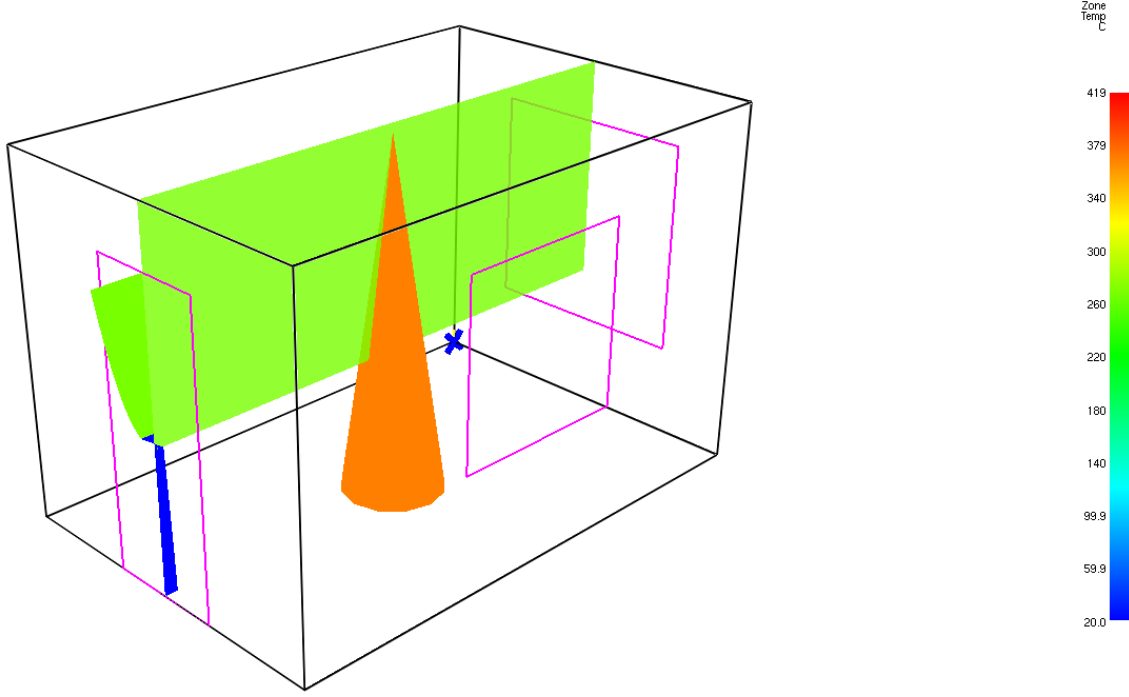


Figure 4-16 Upper layer temperature and height at the beginning of simulation

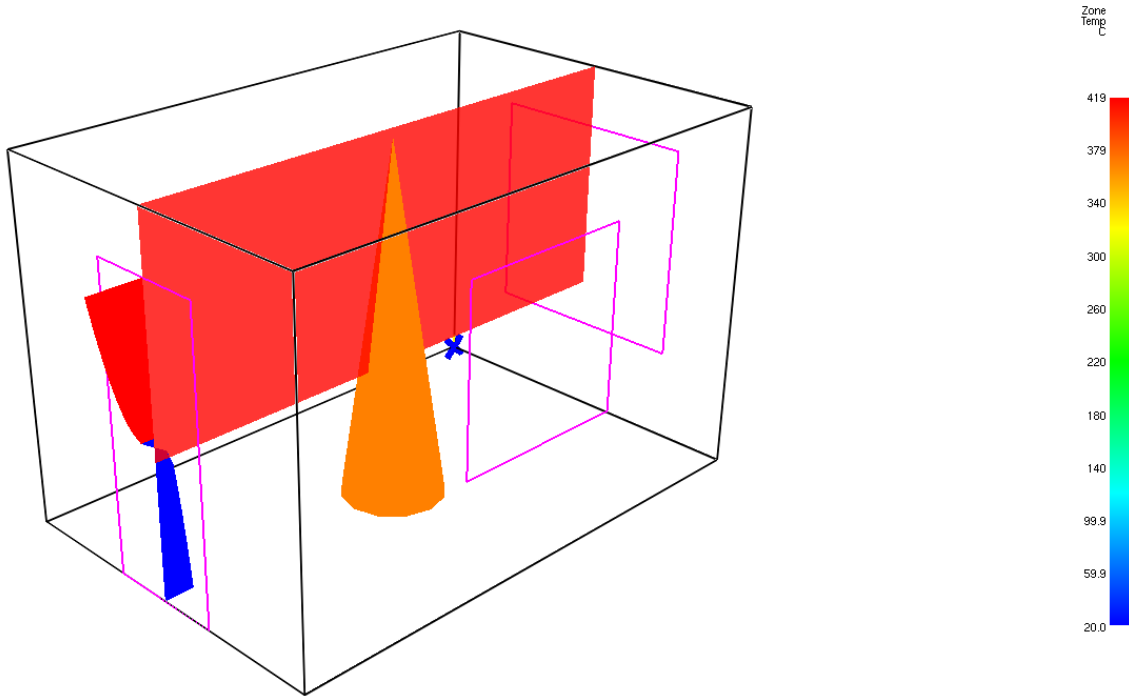


Figure 4-17 Upper layer temperature and height at 60s

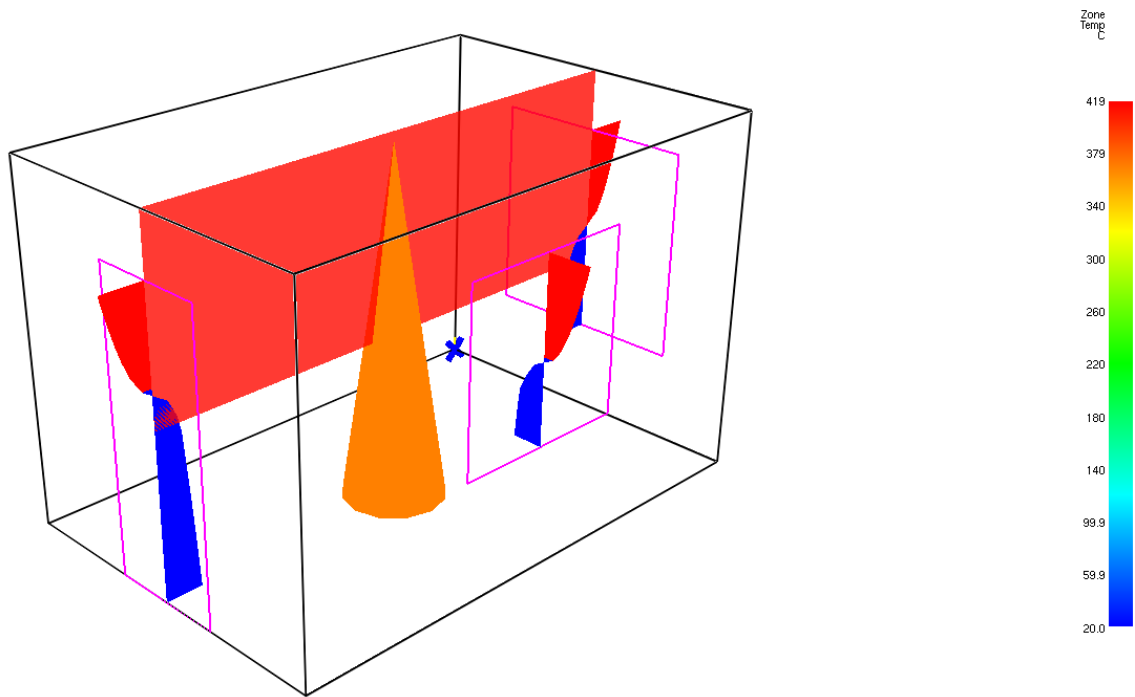


Figure 4-18 Upper layer temperature and height at 61s

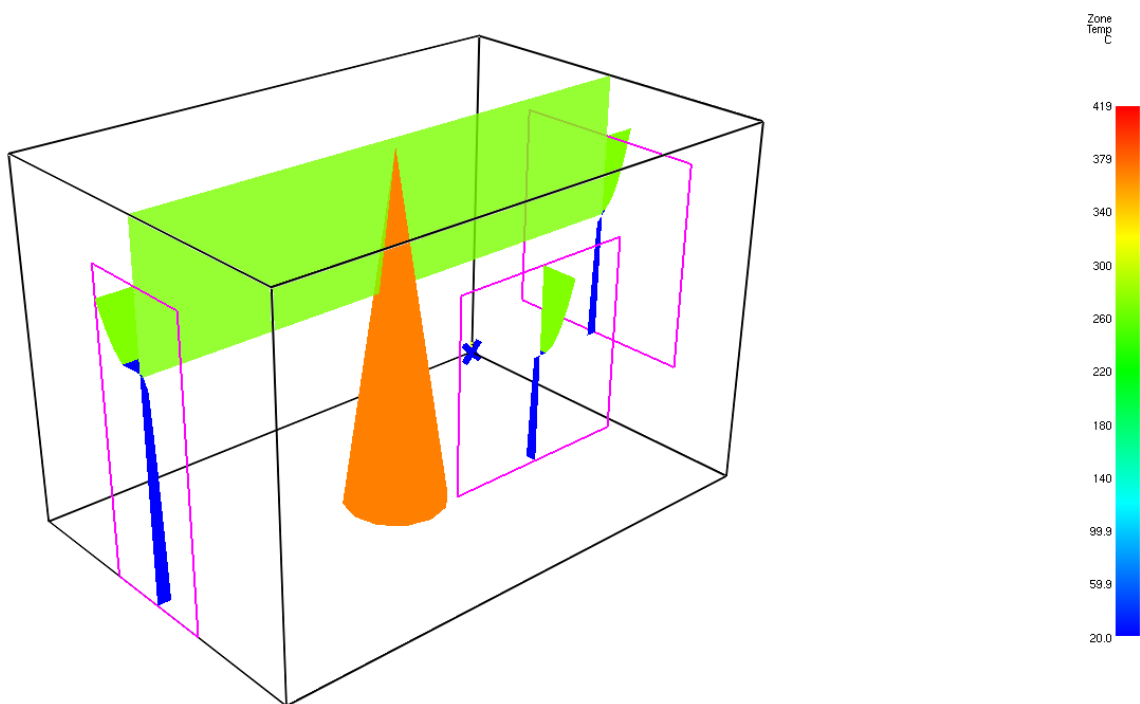


Figure 4-19 Upper layer temperature and height at the end of simulation

4.2.1 Vertical location of window

It is observed that by changing the vertical position of an opening the hot zone layer height and temperature changes even though the ventilation factor is constant. To check this, a sensitivity study is done on scenario 3_Case_4 by changing the position of the window.

Two more configurations are compared with the original configuration where the window height is kept at the same level as the door i.e. 2m. For configuration 2, i.e. 3_Case_4_low, the window is lowered to the ground level with height 1.4m. While for the configuration 3, i.e. 3_Case_4_high, the window is raised to maximum height of the room i.e. 2.4m, the lower end of the window being at 1.0m.

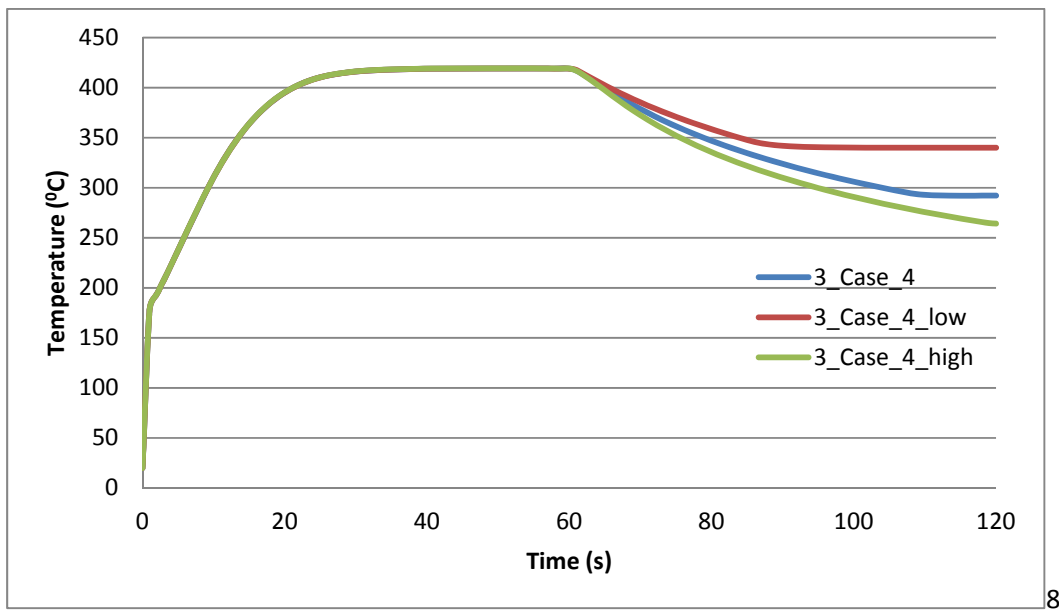


Figure 4-20 Variation in upper layer temperature because of vertical location of vent

The phenomenon is easily understandable. By observing the upper layer temperature in Figure 4-20, it can be deduced that the overall temperature in the compartment is higher for scenario 3_Case_4_low compared to 3_Case_4_high. The simple explanation is that since the soffit of the window is lower in case of 3_Case_4_low, more smoke is accumulated which results in increased radiation and less outflow, thus increasing the overall upper layer temperature.

In contrast to scenario 3_Case_4_high, the vent height is at maximum. Thus, when the vent is activated after 60s the accumulated smoke easily escapes and more air at ambient temperature enters the compartment resulting in cooling down.

Similarly, from Figure 4-21 it can be concluded that the lower the vertical height of the vent, the lower the smoke layer height is, thus increasing smoke layer thickness.

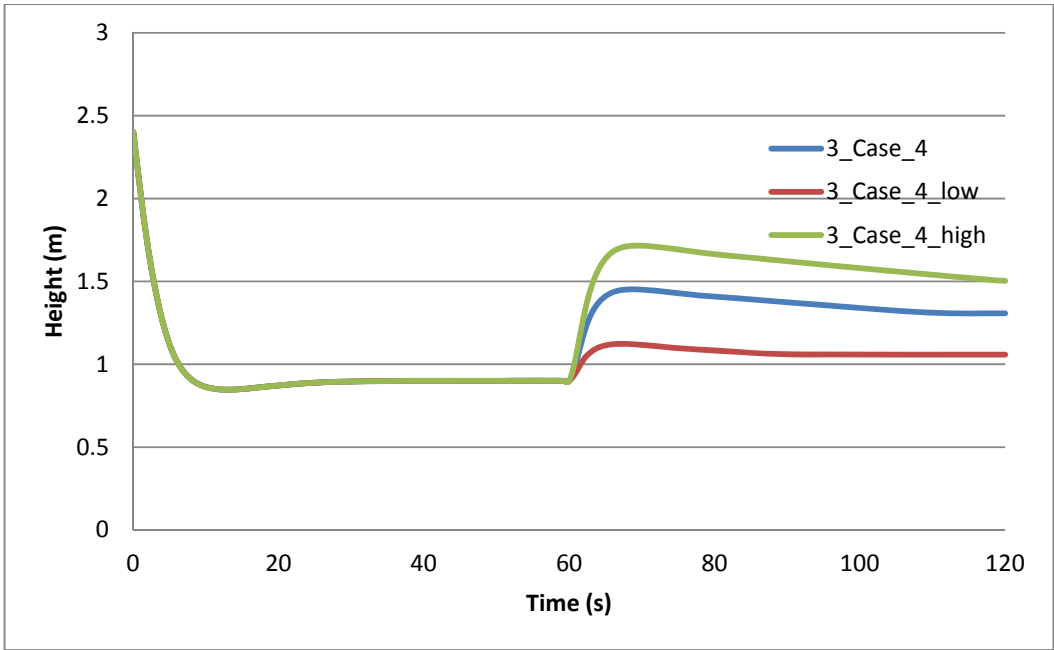


Figure 4-21 Variation in smoke layer height because of vertical location of vent

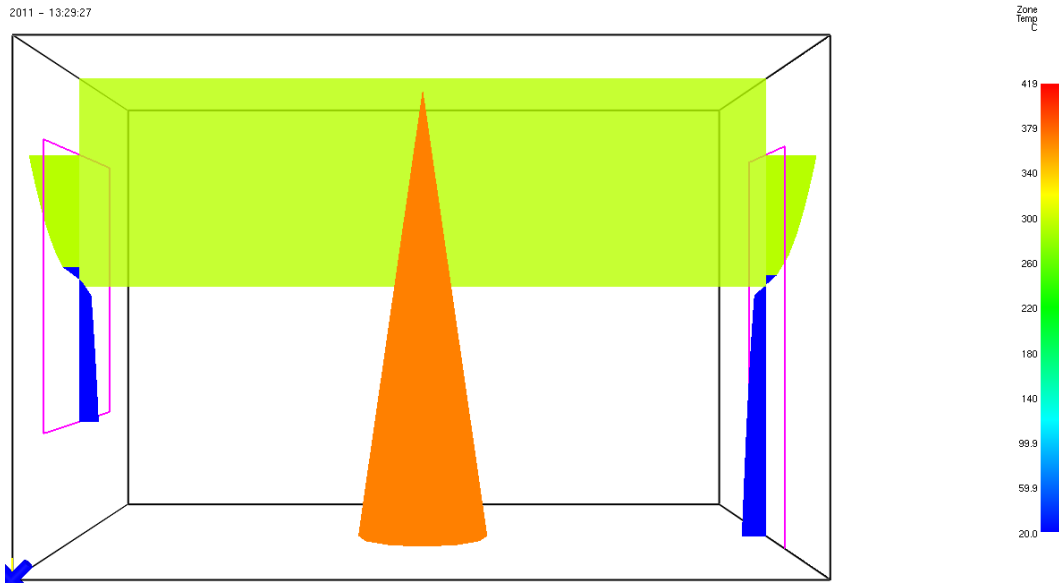


Figure 4-22 Upper layer temperature and height for 3_Case_4 at 120s

2011 - 13:29:27

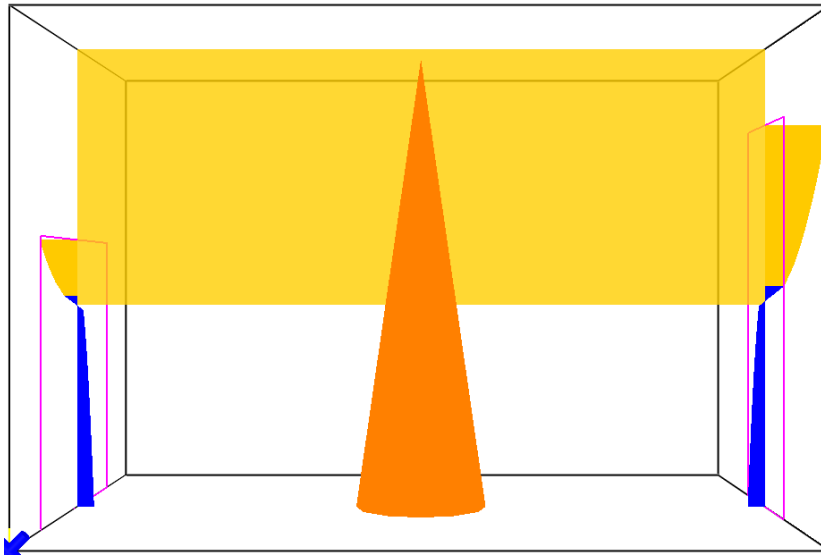


Figure 4-23 Upper layer temperature and height for 3_Case_4_low at 120s

2011 - 13:29:27

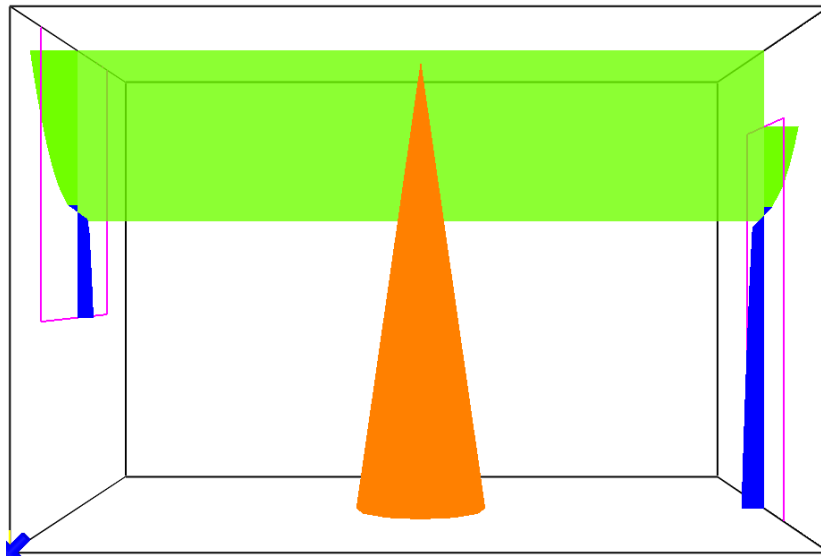


Figure 4-24 Upper layer temperature and height for 3_Case_4_high at 120s

4.3 Analytical model

For implementation of the analytical model developed in section 3.3, MATLAB is used. The advantage of using MATLAB is that GUI can be developed easily. Secondly, reading and writing CSV (coma separated values) and excel files is easy in MATLAB compared to other programming packages. Most importantly, MATLAB is designed for efficiently solving systems of equations.

Ventilation factor, HRR and door height are given as an input. The input data is stored in an excel file, which is then read by MATLAB, and calculations are carried out. Upper layer temperature and layer height are saved as outputs in an excel file. The MATLAB script for the forward analytical model is presented in **Appendix B2**.

As described earlier, the mass flow rate of plume is given by the McCaffrey's plume correlation, which gives 3 separate equations depending on the location in the flame/plume region. The criterion to determine which region and correlation can be applied is given by the ratio $\frac{h}{\dot{Q}_f^{2/5}}$. For every scenario or step (in case of linear HRR), the condition is checked, and the appropriate McCaffrey's correlation is applied to calculate the upper layer temperature and height.

Implementation of the conditioning and the appropriate McCaffrey's correlation are shown below in Table 4-1 and Table 4-2 for 2 configurations. Results for all of the scenarios are described in details in **Appendix A1**. The color indexing represents the usage of that particular McCaffrey's relation.

V _f	Q	Continuous Flame region		Intermittent Flame region		Plume region		Correct result	
		T _u (°C)	h (m)	T _u (°C)	h (m)	T _u (°C)	h (m)	T _u (°C)	h (m)
2.26	300.00	342.56	1.05	323.78	1.01	449.36	1.20	323.78	1.01
2.26	400.00	386.64	0.94	383.25	0.93	580.17	1.17	383.25	0.93
2.26	500.00	428.64	0.84	440.81	0.86	713.36	1.15	428.64	0.84
2.26	600.00	469.56	0.77	496.81	0.81	848.73	1.12	469.56	0.77
2.26	700.00	509.85	0.70	552.46	0.76	988.77	1.10	509.85	0.70
2.26	800.00	549.71	0.64	608.47	0.72	1131.92	1.08	549.71	0.64
2.26	900.00	590.03	0.59	664.35	0.68	1277.46	1.06	590.03	0.59
2.26	1000.00	631.09	0.55	720.30	0.65	1429.59	1.04	631.09	0.55

Table 4-1 Correct implementation of McCaffrey's correlation for 1_Case_1-8

From the results it can be concluded that with increasing HRR, the flame length increases along with the decreasing smoke layer height, thus resulting in the continuous flame region. On the other hand, increasing the ventilation factor allows more smoke outflow from the compartment resulting in an decreased smoke layer thickness. Thus, this combination gives a ratio which corresponds to the intermittent region. For small HRR and ventilation factor, the smoke layer height is within the intermittent flame region, which shifts to the continuous flame region with the increasing HRR. For all scenarios, the smoke layer height is never in the plume region since the compartment height is not too large compared with the HRR.

V _f	Q	Continuous Flame region		Intermittent Flame region		Plume region		Correct result	
		T _u (°C)	h (m)	T _u (°C)	h (m)	T _u (°C)	h (m)	T _u (°C)	h (m)
6.16	300.00	288.29	1.45	248.18	1.38	310.95	1.48	248.18	1.38
6.16	400.00	315.22	1.37	283.59	1.32	390.36	1.46	283.59	1.32
6.16	500.00	339.04	1.31	316.07	1.27	469.06	1.44	316.07	1.27
6.16	600.00	360.98	1.25	346.41	1.23	546.64	1.42	346.41	1.23
6.16	700.00	381.51	1.20	375.22	1.19	623.92	1.41	375.22	1.19
6.16	800.00	400.95	1.15	403.14	1.16	701.01	1.40	400.95	1.15
6.16	900.00	419.55	1.11	429.91	1.13	777.93	1.38	419.55	1.11
6.16	1000.00	437.78	1.07	456.15	1.10	855.78	1.37	437.78	1.07

Table 4-2 Correct implementation of McCaffrey's correlation for 4_Case_1-8

One other factor which can influence the results greatly is the height of the opening represented as H in **Equation 3-13**. In case of only a door, the opening height is equivalent to the door height. But for configurations in which there are more openings, the effective opening height is required, which can be calculated using **Equation 2-4**.

However, for inverse modeling the effective opening height cannot be known prior since the vent(s) configuration is unknown. Therefore, for simplification the opening height is assumed to be the door height. Although this assumption will introduce error in the inverse modeling, it makes the model much simpler. In Table 4-3, the effect of the choice of opening height on upper layer temperature and height is shown for scenario 4_Case_1-8.

Since the effective opening height is smaller than the door height for all scenarios as mentioned in Table 2-2, the smoke layer height is lower when effective opening height is used. This is due to the fact that the effective opening height is lower resulting in more accumulation of smoke and thus the smoke layer descends. The temperature increase is also due to excess of hot gases in upper layer. Results for all of the scenarios are described in details in **Appendix A2**.

V _f	Q	Using door height		Using effective opening height	
		T _u (°C)	h (m)	T _u (°C)	h (m)
6.16	300.00	248.18	1.38	298.53	1.11
6.16	400.00	283.59	1.32	340.56	1.07
6.16	500.00	316.07	1.27	378.68	1.03
6.16	600.00	346.41	1.23	408.20	0.99
6.16	700.00	375.22	1.19	430.72	0.96
6.16	800.00	400.95	1.15	452.08	0.92
6.16	900.00	419.55	1.11	472.42	0.89
6.16	1000.00	437.78	1.07	492.09	0.86

Table 4-3 Comparison between using door or effective opening height for 4_Case_1-8

In case of scenarios with linear HRR, the same analytical model is used. As discussed earlier, the transient terms in the conservation equations are neglected. The linear curve is transformed into a step function, and the HRR and conditions are assumed to remain the same during this interval. This transformation still provides the trend of the curve as shown in Figure 4-25. The interval is taken as 30s, and the values of the HRR, temperature and layer height are averaged.

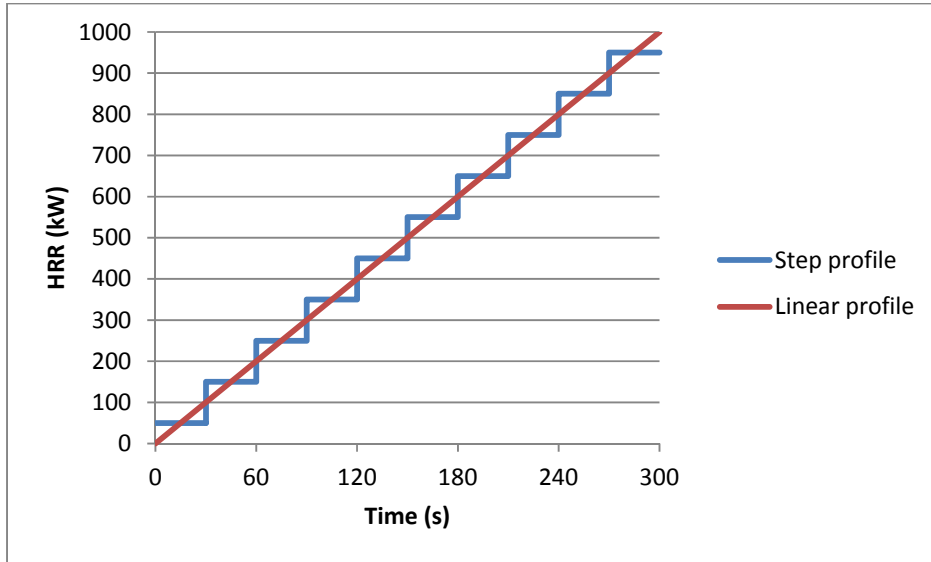


Figure 4-25 Step profile of HRR used for Analytical Model

In Table 4-4, the results of 1_Case_linear are shown. For this scenario, the ventilation factor is constant throughout the simulations since the only vent is the door. It is clear that for a constant ventilation factor with increasing HRR the upper layer temperature rises and the layer height descends. This is simply because with increasing HRR more fuel is burnt and thus more hot gases are produced which accumulate in the compartment. This increased amount of hot smoke will result in an increasing of the upper layer temperature.

Time	HRR	V _f	Analytical model	
			T _u (°C)	h (m)
15.00	50.00	2.26	116.71	1.29
45.00	150.00	2.26	224.92	1.18
75.00	250.00	2.26	292.76	1.06
105.00	350.00	2.26	353.97	0.97
135.00	450.00	2.26	407.94	0.89
165.00	550.00	2.26	449.19	0.80
195.00	650.00	2.26	489.68	0.73
225.00	750.00	2.26	529.60	0.67
255.00	850.00	2.26	570.21	0.62
285.00	950.00	2.26	610.70	0.57

Table 4-4 Upper layer temperature and height using Analytical model for 1_Case_linear

For a scenario like 4_Case_linear in which vents other than the door are activated after some time a different phenomenon occurs. Up to the point where the vents are activated, similar behavior is observed as discussed earlier. With increasing HRR, temperature increases and the smoke layer descends. But when the vents are activated, hot smoke is allowed to leave the compartment and ambient air enters causing a cooling effect. Due to outflow of the smoke, the smoke layer ascends considerably in the beginning depending on the ventilation factor. After some time, the smoke layer stabilizes and starts to descends again resulting in increased upper layer temperature.

Time	HRR	V _f	Analytical model	
			T _u (°C)	h (m)
15.00	50.00	2.26	116.71	1.29
45.00	150.00	2.26	224.92	1.18
75.00	250.00	2.26	292.76	1.06
105.00	350.00	2.26	353.97	0.97
135.00	450.00	2.26	407.94	0.89
165.00	550.00	6.16	331.41	1.25
195.00	650.00	6.16	361.10	1.21
225.00	750.00	6.16	389.32	1.17
255.00	850.00	6.16	410.45	1.13
285.00	950.00	6.16	428.65	1.09

Table 4-5 Upper layer temperature and height using Analytical model for 4_Case_linear

The results from the forward analytical model agree with other fire models in theory. Similar phenomenon and trend is observed because of the similar basis i.e. conservation equations. Detailed comparison of the results between the fire models and the developed analytical model is done in the next section.

4.4 Comparison of results

The aim of comparing the results is to check the agreement between the fire models and the analytical model. Since these model have been validated with experimental data, if the results of the analytical model are a good match, this model can be used to develop the inverse model.

The smoke layer height and the hot layer temperature acquired by using the analytical forward model are compared with FDS and CFAST, and are discussed below in the sub-sections. Detailed results are presented in the **Appendix A3** for scenarios with constant HRR and in **Appendix A4** for scenarios with linearly increasing HRR . For constant HRR scenarios, the data is averaged when the conditions are steady, whereas for the scenarios with linear HRR, the data is averaged over a period of 30 seconds.

4.4.1 Between FDS and the Analytical model

Since CFD is more detailed and requires more computational time, only selected scenarios as per the Table 2-4 and Table 2-5 are simulated in FDS. The hot layer temperature predicted by FDS follows the same trend but overall it is 40% underpredicted. Temperature increases with the increasing HRR while

for smoke layer height, the change in the layer height is not that obvious in FDS. FDS solves the smoke and flow movement in a more complex manner.

The smoke movement is also affected by the turbulence. Compared to the simple analytical model, FDS also takes into account the air entrainment. The accumulation of the smoke in the compartment is high from the beginning since the air entrainment increases the mass flow.

In case of a constant HRR, the difference in temperature prediction between FDS and the analytical model is less, especially for higher HRR as show in Figure 4-26. Similarly, for higher HRR the smoke layer height results have also less divergence.

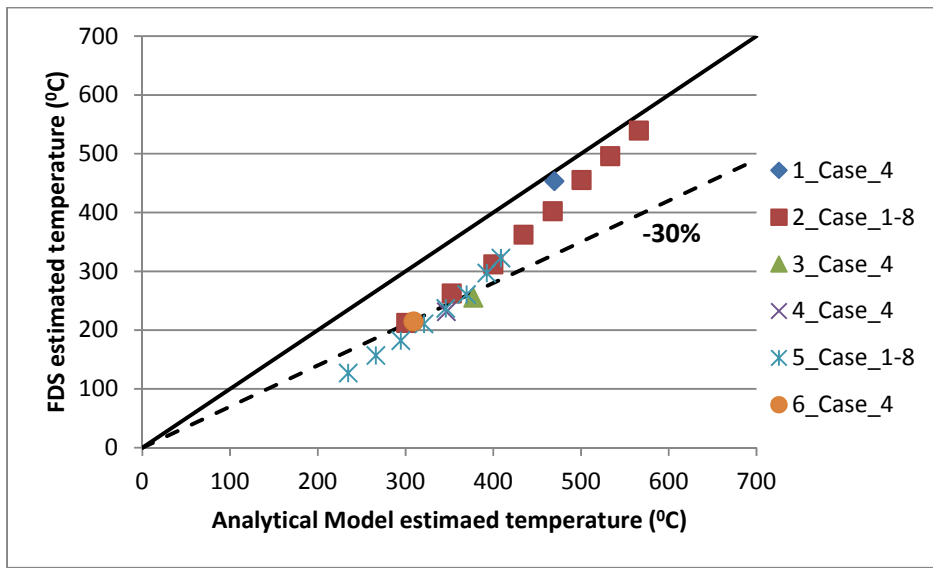


Figure 4-26 Hot layer temperature estimated by FDS and Analytical model for constant HRR

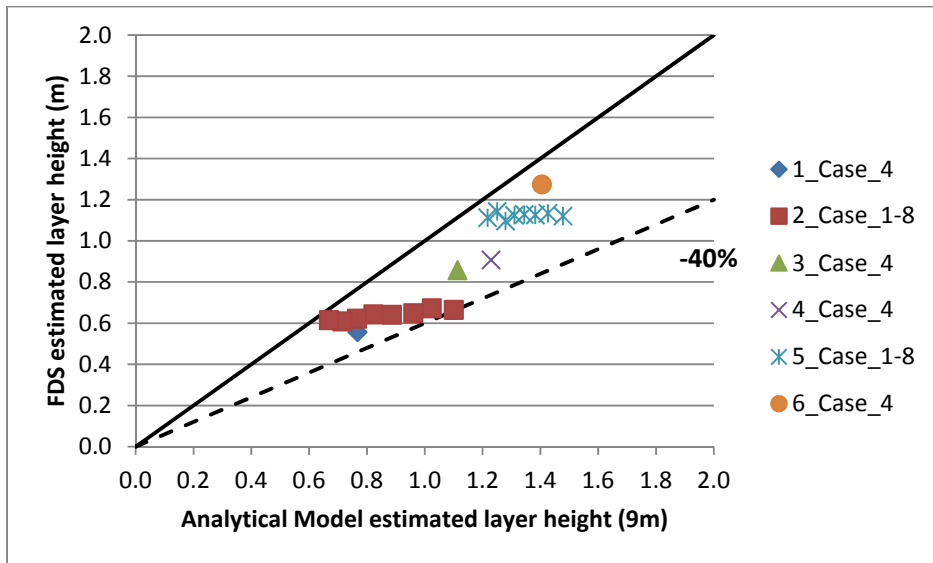


Figure 4-27 Smoke layer height estimated by FDS and Analytical model for constant HRR

In case of linearly increasing HRR, the hot layer temperature is again underpredicted but this time the difference between results is bigger. On the other hand, for smoke layer height the difference becomes negligible with higher HRR. The comparison between the two models is shown in Figure 4-28 and Figure 4-29.

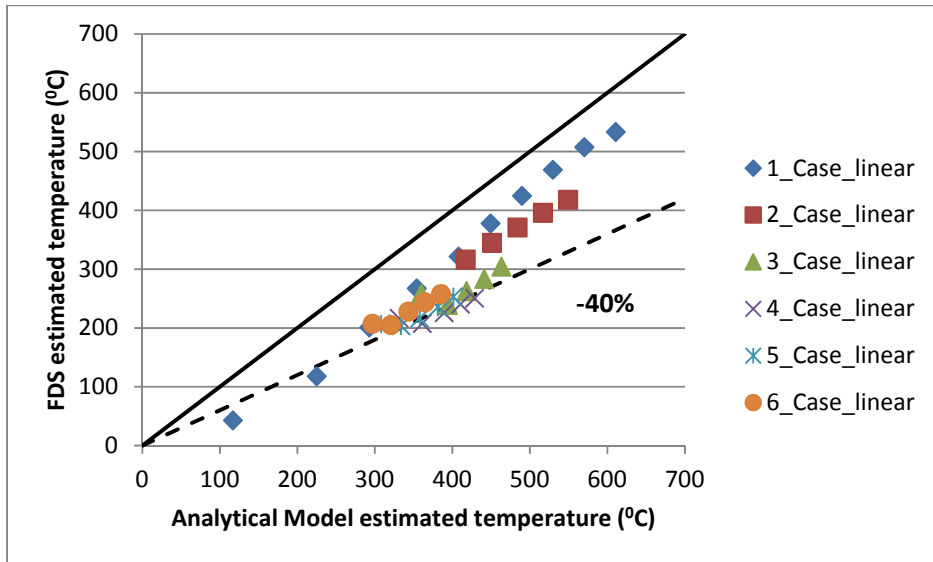


Figure 4-28 Hot layer temperature estimated by FDS and Analytical model for linearly increasing HRR

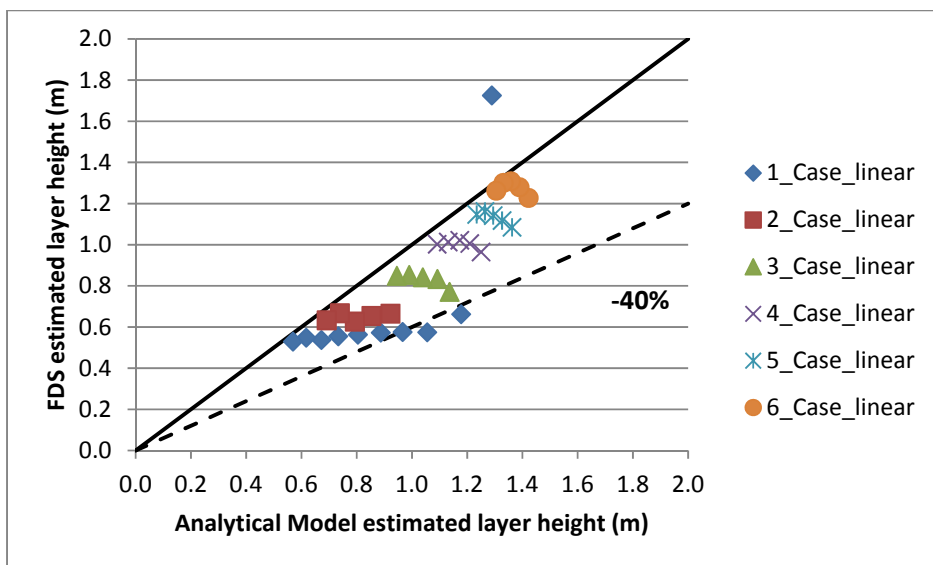


Figure 4-29 Smoke layer height estimated by FDS and Analytical model for linearly increasing HRR

4.4.2 Between CFAST and the Analytical model

Since both models are based on a simple conservation equations, the results are comparable. The upper layer temperature is slightly underpredicted by CFAST, whereas the layer height is overpredicted compared to the analytical model, which makes sense. Lower temperature estimated by CFAST means less smoke accumulation and thus the smoke layer height decreases.

With the increasing HRR, the difference with the upper layer temperature prediction decreases. Overall, the results are in good agreement for both constant and linearly increasing HRR. Compared to FDS, in CFAST the effect of increasing HRR on smoke layer height is distinctively observable.

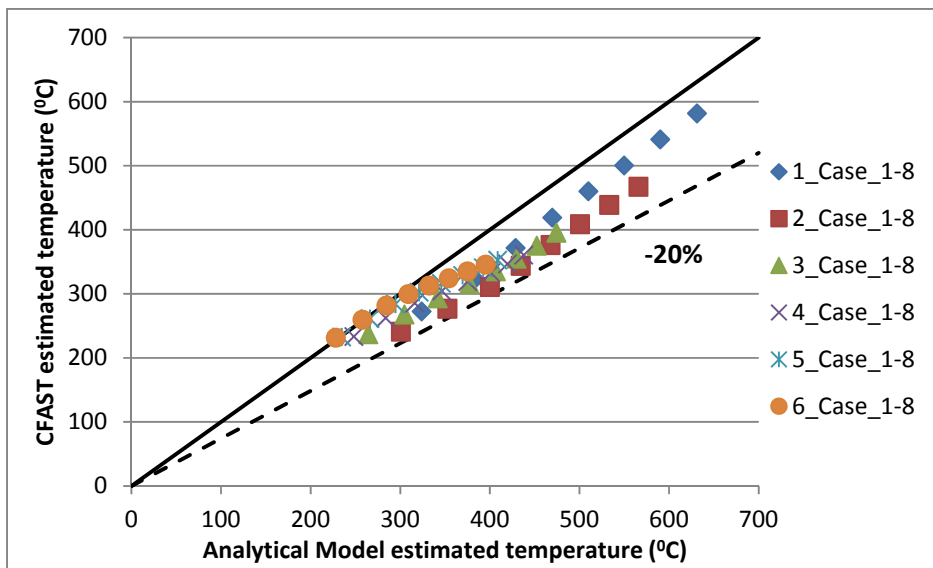


Figure 4-30 Hot layer temperature estimated by CFAST and Analytical model for constant HRR

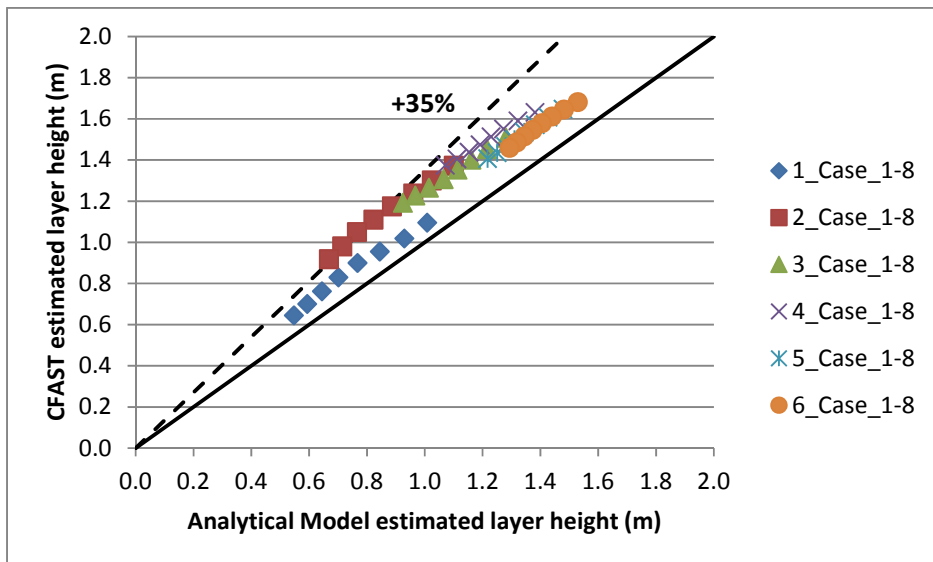


Figure 4-31 Smoke layer height estimated by CFAST and Analytical model for constant HRR

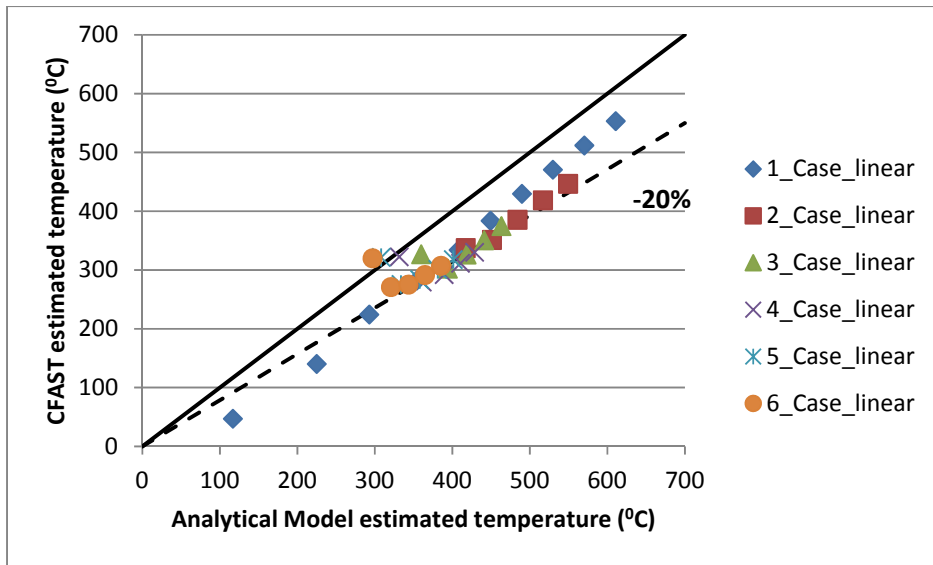


Figure 4-32 Hot layer temperature estimated by CFAST and Analytical model for linearly increasing HRR

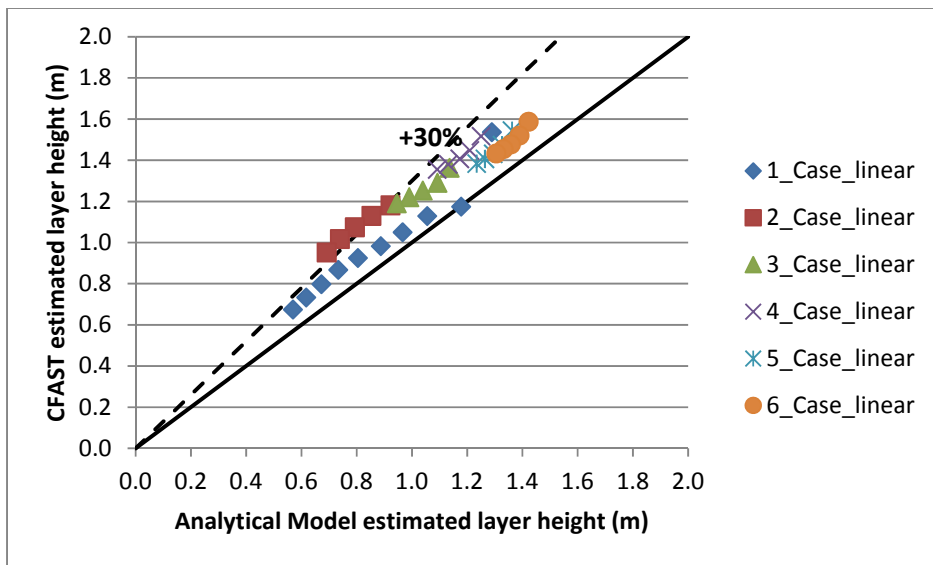


Figure 4-33 Smoke layer height estimated by CFAST and Analytical model for linearly increasing HRR

Since the results predicted by the analytical model are well within the range and comparable with the fire models, the analytical model is used to develop the inverse model. FDS is computationally more expensive; therefore, CFAST results will be used as an input in the inverse model.

4.4.3 Between FDS and CFAST

Comparing the results of the estimated hot layer temperature by FDS and CFAST gives a 40% deviation. FDS solves the problem using large eddy simulation (LES) approach and divides the domain into numerous grid cell sized control volumes compared to only two zones in CFAST. Although this refined resolution may give better results but it increases the computational cost considerably. On the other hand, the simplification done in CFAST can still give comparable results instantaneously. Figure 4-34 and Figure 4-35 demonstrate that both models follow the same trend, i.e. with increasing HRR, upper layer temperature increases. CFAST provides a single value of measurement which was averaged over a specified interval, whereas FDS data is taken as an average from all the sensors located at different positions. The location of the sensors may also affect the averaged data.

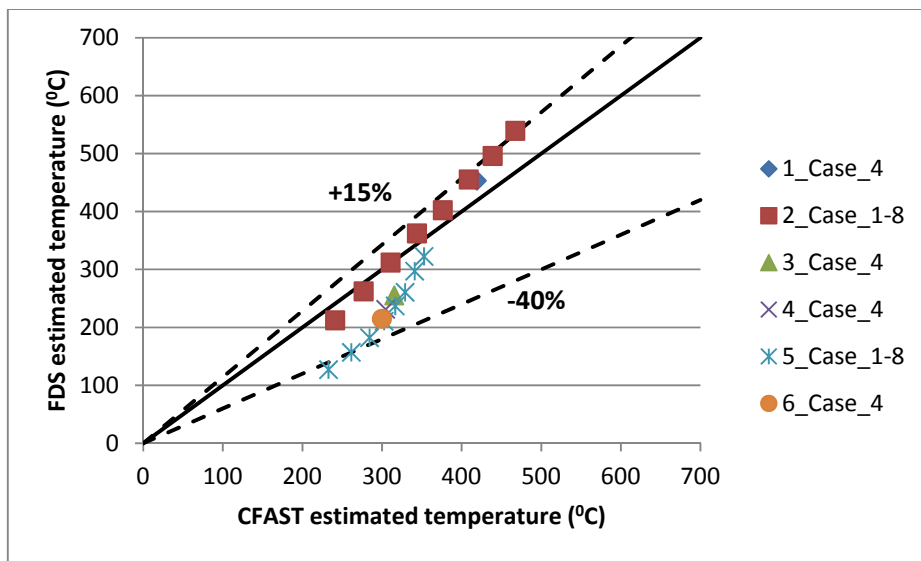


Figure 4-34 Hot layer temperature estimated by FDS and CFAST for constant HRR

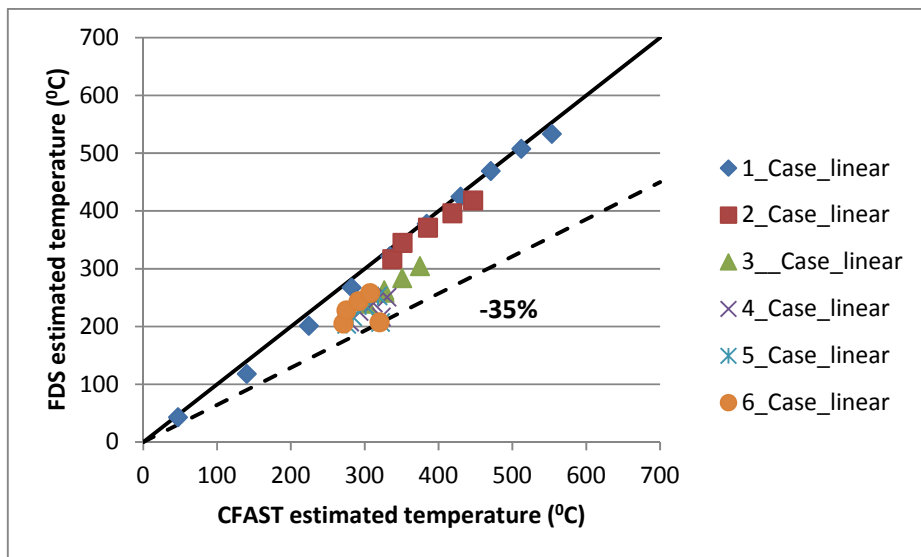


Figure 4-35 Hot layer temperature estimated by FDS and CFAST for linearly increasing HRR

In case of the comparison between the estimated values of smoke layer height by FDS and CFAST, a deviation of 50% is observed. As discussed earlier in section 4.4.1, FDS solves the smoke movement in more details. The evolution of smoke layer height with the increase in HRR is not recognizable. In theory, for a similar ventilation condition the smoke layer should descend with the increase in HRR, whereas the estimation of smoke layer height by FDS is not influenced by increasing HRR.

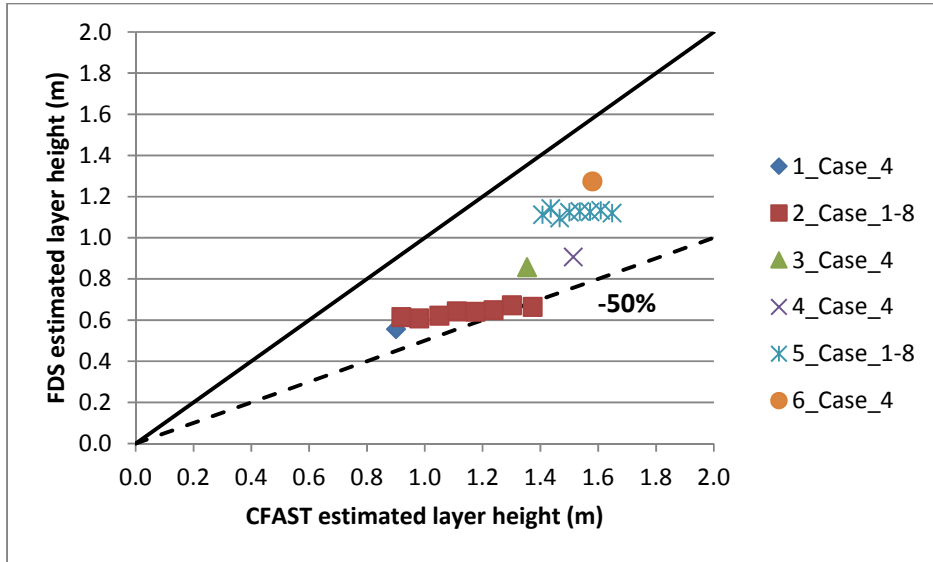


Figure 4-36 Smoke layer height estimated by FDS and CFAST for constant HRR

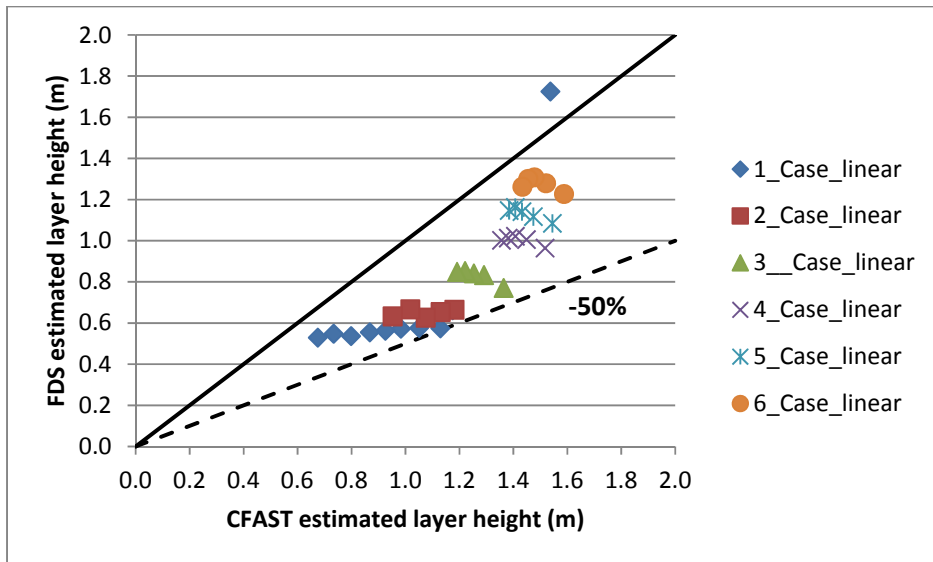


Figure 4-37 Smoke layer height estimated by FDS and CFAST for linearly increasing HRR

5 Inverse Modeling

For the inverse modeling, the same set of equations of energy and mass conservation are used as discussed earlier in development of the forward analytical model. Contrary to the forward analytical model as used by most of the fire models, the inverse model uses the upper layer temperature and smoke layer height as input, and predicts the HRR \dot{Q}_f and change in ventilation factor $A_o \sqrt{H_o}$ which can be due to window breakage. The input parameters are taken from CFAST.

The modeling procedure is discussed below in the sub-section. For calculation purpose MATLAB is used and the detailed code is presented in **Appendix B3**. The output file from CFAST is imported to MATLAB, and the required input parameters are taken directly.

5.1 Description of the procedure

Since there are 2 unknowns, i.e. HRR and the ventilation factor, 2 equations are needed to solve the variables. This can be achieved by using the same energy and mass conservation equations discussed in section 3.3. The input for these equations is taken directly from the output data of CFAST.

Energy conservation:

$$\frac{d}{dt} [\rho_u c_p (T_u - T_a) A (H - h)] = (1 - \lambda_c) \dot{Q}_f - \dot{m}_{out,u} c_p (T_u - T_a) \quad (3-6)$$

Mass conservation:

$$\frac{d}{dt} [\rho_u A (H - h)] = \dot{m}_p + \dot{m}_{in,u} - \dot{m}_{out,u} \quad (3-7)$$

Similar simplifications and assumptions are made as in the analytical model. Only adiabatic configuration is studied, meaning there are no losses to the boundary and surroundings except to the hot upper layer. This results in λ_c being equal to zero. Secondly, the transient terms in both energy and mass conservation equations are neglected. The resulting simplified correlation is:

Energy conservation:

$$\dot{Q}_f = \dot{m}_{out} c_p (T_u - T_a) \quad (3-8)$$

Mass conservation:

$$\dot{m}_{out} = \dot{m}_p \quad (3-9)$$

where \dot{m}_p and \dot{m}_{out} can be obtained from **Equations 3-4 and 3-12**.

$$\dot{m}_p = a \dot{Q}_f \left(\frac{h}{\dot{Q}_f^{2/5}} \right)^n \quad (3-4)$$

$$\dot{m}_{out} = \frac{2}{3} C_d A_o \sqrt{H_o} \rho_a \sqrt{2g \frac{T_a}{T_u} \left(1 - \frac{T_a}{T_u} \right)} \left(1 - \frac{h}{H_D} \right)^{3/2} \quad (3-12)$$

using \dot{m}_p in the energy conservation since $\dot{m}_{out} = \dot{m}_p$

$$\begin{aligned}\dot{Q}_f &= a \dot{Q}_f \left(\frac{h}{\dot{Q}_f^{2/5}} \right)^n c_p (T_u - T_a) \\ \dot{Q}_f^{2n/5} &= a h^n c_p (T_u - T_a) \\ \dot{Q}_f &= \left(a h^n c_p (T_u - T_a) \right)^{5/2n}\end{aligned}\quad (5-1)$$

or simplified as

$$\dot{Q}_f = C_4^{5/2n} \quad (5-2)$$

where,

$$C_4 = a h^n c_p (T_u - T_a)$$

now using value of \dot{Q}_f from **Equation 5-2** in mass conservation **Equation 3-9**

$$\begin{aligned}\frac{2}{3} C_d A_o \sqrt{H_o} \rho_a \sqrt{2g \frac{T_a}{T_u} \left(1 - \frac{T_a}{T_u}\right) \left(1 - \frac{h}{H_D}\right)^{3/2}} &= a h^n \dot{Q}_f^{(1-2n/5)} \\ A_o \sqrt{H_o} C_5 &= a h^n \dot{Q}_f^{(1-2n/5)}\end{aligned}\quad (5-3)$$

which can be simplified as

$$A_o \sqrt{H_o} = \frac{a h^n \dot{Q}_f^{(1-2n/5)}}{C_5} \quad (5-4)$$

where,

$$C_5 = \frac{2}{3} C_d \rho_a \sqrt{2g \frac{T_a}{T_u} \left(1 - \frac{T_a}{T_u}\right) \left(1 - \frac{h}{H_D}\right)^{3/2}}$$

The HRR can be calculated using **Equation 5-2**, and the ventilation factor $A_o \sqrt{H_o}$ using **Equation 5-4**.

5.2 Results and Discussions

Hot layer temperature and smoke layer height from CFAST are provided as an input to the inverse model developed above. Detailed results of scenarios with constant HRR are provided in **Appendix A5**, and for scenarios with linearly increasing HRR, the results are presented in **Appendix A6**.

For the inverse modeling, the mass flow rate of plume is given by the McCaffrey's plume correlation which gives 3 separate equations depending on the location in the flame/plume region. The criterion to determine which region and correlation can be applied is given by the ratio $\frac{h}{Q_f^{2/5}}$. For every scenario or step (in case of linear HRR), the predicted HRR and input smoke layer height is used to determine the appropriate McCaffrey's. The comparison of the of HRR and ventilation factor predicted by the inverse model and the actual values is provided and discussed below.

Figure 5-1 shows the spread of predicted HRR for scenarios with constant HRR. Although the prediction of HRR follows the expected trend i.e. increasing, the prediction of HRR becomes better with the increasing reference HRR. On the other hand, with the increasing reference ventilation factor, the predicted HRR increases compared to the reference. The scatter is provided on the figure. The use of the appropriate McCaffrey's correlations depends on the combination of the HRR and the ventilation factor. For a small HRR, the intermittent flame region correlation is used which shifts to the continuous flame region with the increasing HRR. On the other hand, with the increasing ventilation factor, the continuous flame region equation is not valid anymore, and thus the intermittent flame region correlation is used.

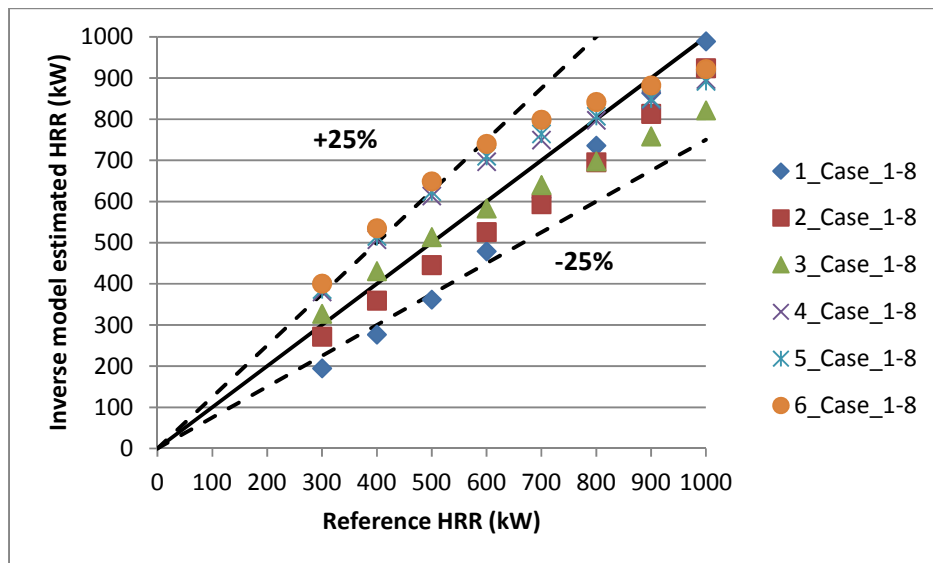


Figure 5-1 Inverse model estimation of HRR for constant HRR scenarios using McCaffrey's correlations

Using the inverse model, although the change in ventilation factor can be detected, it is quite overpredicted compared to the predicted HRR as shown in Figure 5-2. The prediction of the ventilation factor, along with other input parameters, depends on the predicted HRR. Any error in the HRR will result in deflection in ventilation factor.

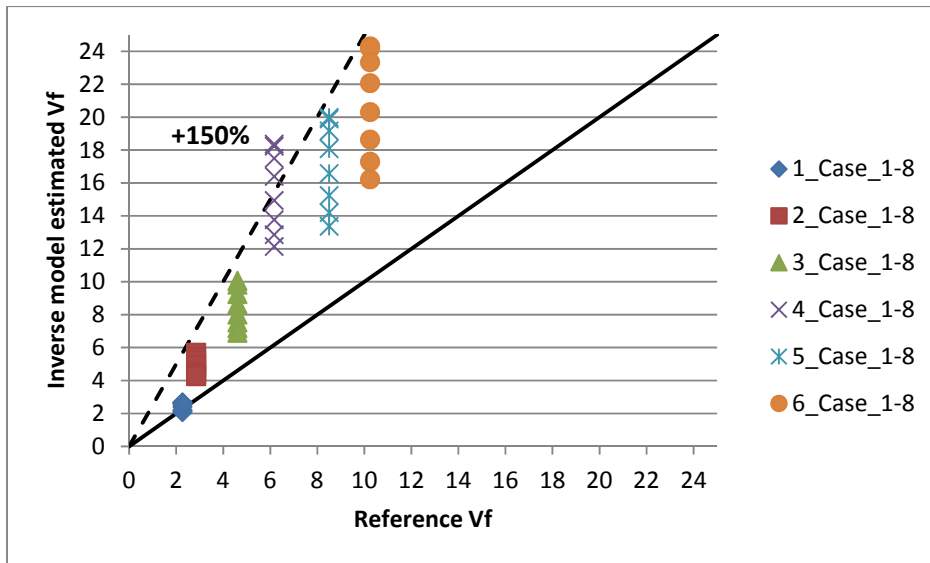


Figure 5-2 Inverse model estimation of ventilation factor for constant HRR scenarios using McCaffrey's correlations

The above-mentioned results are based on the use of the $\frac{h}{\dot{Q}_f^{2/5}}$ ratio for determining the correct McCaffrey correlation. The criterion for choosing the correlation is only dependant on the HRR and the smoke layer height. If for simplicity, only the continuous flame region equation is used, the prediction of ventilation factor is not too overpredicted as shown in Figure 5-3. The use of the continuous flame region equation results in underpredicted HRR as shown in Figure 5-4. Using the same assimilated upper layer temperature and height in the continuous flame region compared to the intermittent region gives lower HRR, which is obvious because the temperature in the continuous region is usually quite high compared to the intermittent and plume region.

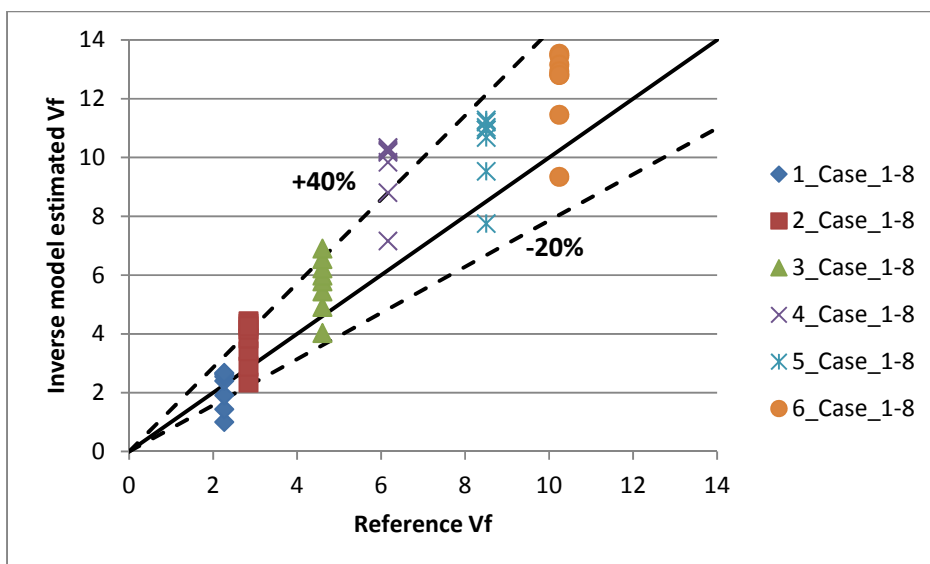


Figure 5-3 Inverse model estimation of ventilation factor for constant HRR scenarios using only continuous flame region

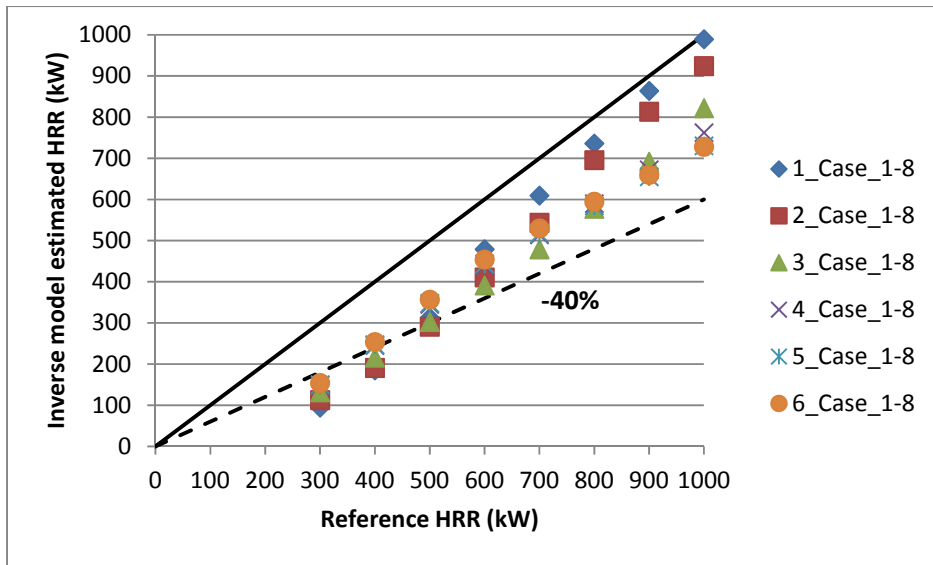


Figure 5-4 Inverse model estimation of HRR for constant HRR scenarios using only continuous flame region

Comparisons of the prediction of HRR and the ventilation factor for the scenarios with linearly increasing HRR are provided in Figure 5-5 and Figure 5-6. The HRR is underpredicted by the inverse model while the ventilation factor is overpredicted. Scenario 1_Case_linear starts from the beginning since it represents the scenarios where only one vent in form of a door is present. For other scenarios where the vents are activated after 150s, the prediction for the first 150 seconds is similar to 1_Case_linear.

The inverse model is able to detect the changes in the HRR and the ventilation conditions depending on the upper layer temperature and smoke layer height. Although the HRR is underpredicted, it still follows the general trend and gives the idea of increase. In this case, the reference HRR curve starts from 0; therefore, in the beginning the mass flow rate of plume is calculated by the plume region correlation.

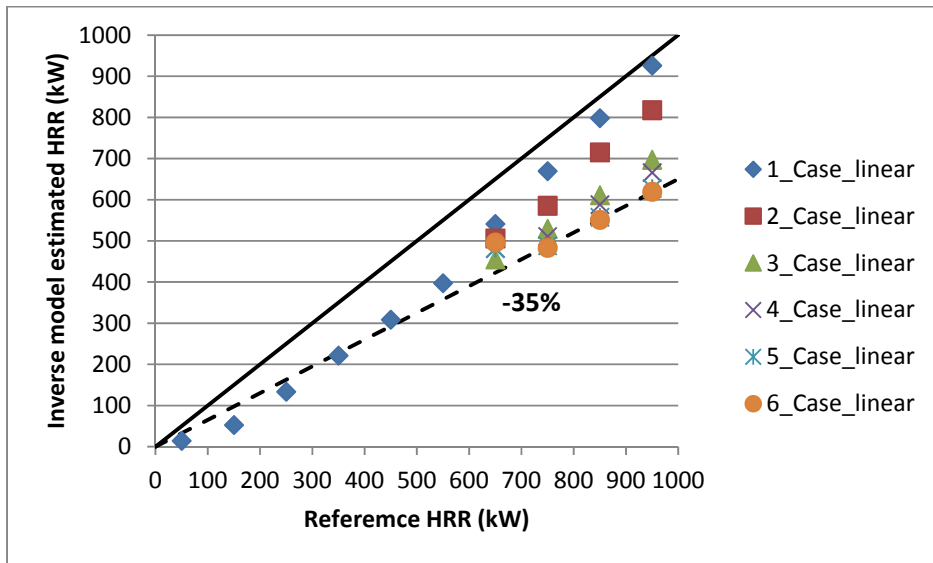


Figure 5-5 Inverse model estimation of HRR for linear HRR scenarios using McCaffrey's correlations

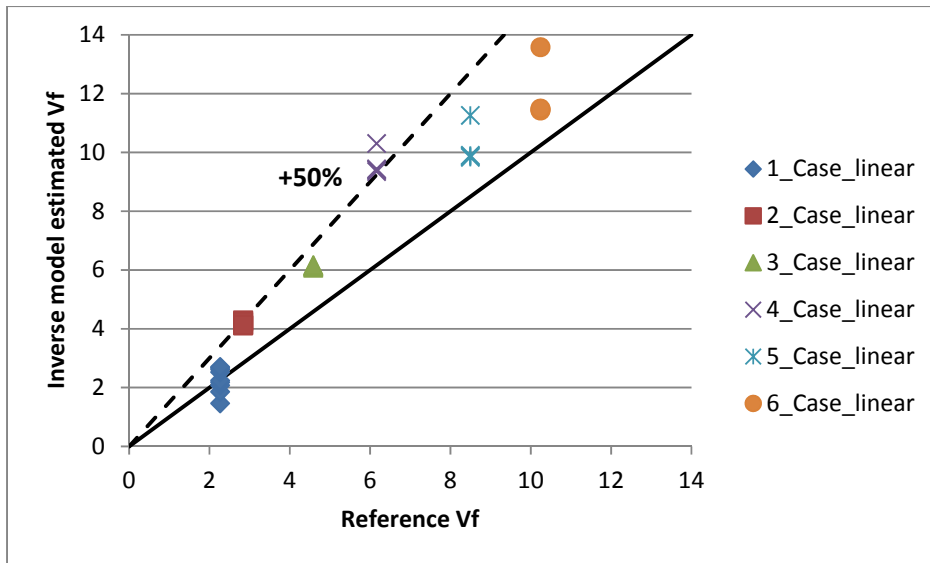


Figure 5-6 Inverse model estimation of ventilation factor for linear HRR scenarios using McCaffrey's correlations

The inverse model is successful in interpreting the change in the ventilation conditions with the time. At the instant when the vent(s) are activated, hot smoke escapes the compartment while ambient air enters. This also results in lowering the hot upper layer temperature. The decrease in temperature is not that abrupt as compared to the decrease in smoke layer height. This sudden decrease in the smoke layer height introduces fluctuation in the results as shown for scenarios 3_Case_linear in Figure 5-7.

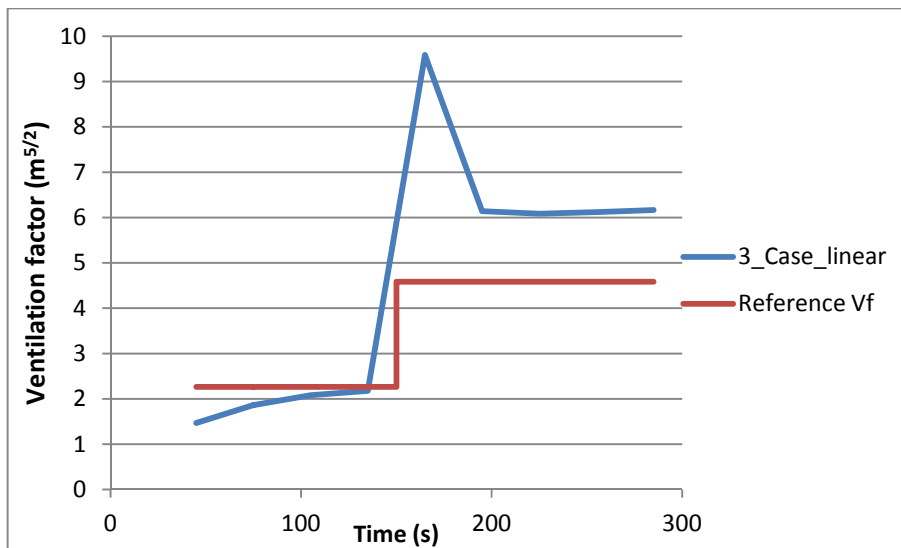


Figure 5-7 Ventilation factor estimation for 3_Case_linear

This is due to the fact that the correlation used for calculating HRR using the Equation 5-2 depends on the smoke layer height which affects the HRR prediction by a factor $h^{5/2}$. Similarly, this sudden change in smoke layer height will also affect the ventilation factor since it also depends on Q and h as per Equation

5-4. To minimize this effect, either a filter mechanism can be developed or sufficient time is provided to achieve a steady state after the activation of the vent.

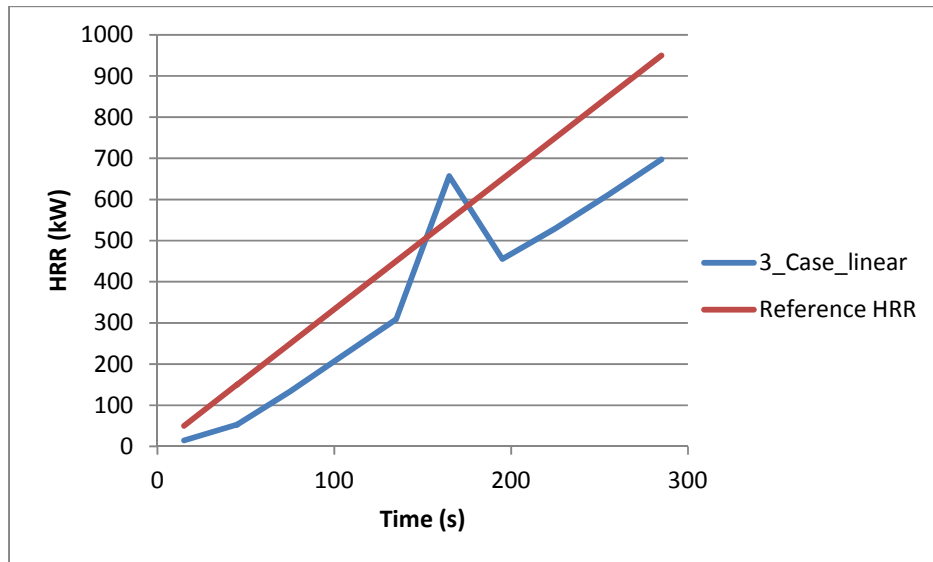


Figure 5-8 HRR estimation for 3_Case_linear

Although the results have some fluctuations and errors, the model is able to detect the changes in the ventilation condition along with providing a reasonable approximation of the HRR. The divergence can be decreased by improving the input mechanism. A set of conditions can be applied to check the percentage error and compare the results and adjust the prediction accordingly.

Additionally, improvements can be made by incorporating the neutral layer height X_N for calculating mass flow out of the compartment instead of the smoke layer height. The change in the neutral layer height is not as abrupt as for smoke layer height. Furthermore, including the transient terms in both energy and mass conservation equations also helps to reduce the error.

6 Conclusion

A numerical model was developed to estimate the heat release rate and detect changes in ventilation conditions in the case of an enclosure (ISO room) fire. FDS and CFAST were used as fire models. At first, the results of the forward analytical model were compared with the fire models, and they are in good agreement especially with CFAST with a maximum deviation of 20-35%. The heat release rate and ventilation factor were used as an input to estimate the upper layer temperature and smoke layer height. The purpose of this step was to be able to develop a mathematical model which uses similar basic conservation equations and still gives reasonable results instantaneously, compared to the fire model.

At the second stage, an inverse model was developed using the same energy and mass conservation correlations. Although the inverse model is able to detect changes in the ventilation conditions as well as the evolution of fire based on the smoke layer height and upper layer temperature, the results differ from the reference values by 40% in case of HRR and in a range of 50-150% in case of ventilation factor.

This error in the estimation may be the result of simplifications and assumptions during the development of the mathematical model. One simplification is based on the assumption that the transient terms can be neglected in the conservation equations since this makes calculations computationally expensive. Similarly, the use of smoke layer height instead of neutral layer height for the calculation of mass flow rate out of the compartment introduces error. Most importantly, the effective height of the opening(s) is not known in advance, and as a simplification it is replaced by the height of the door which also adds to the error.

This methodology can be coupled with a forecasting model which uses the results from the inverse model to predict the properties and evolution of the fire. The idea would be to provide this information with a positive lead time, i.e. before the stage occurs. The forecast model usually takes the current situation into account and predicts the fire development which will follow the same trend. In practice, long-term prediction is not possible since the evolution of fire depends on many parameters such as the ventilation conditions or even the amount of fuel. Thus, the ideal model should compare the predicted curve with actual data and adjust the evolution accordingly.

For future studies, it is recommended to develop a system which can compare the estimated values with the reference values in case of deviation and adjust the forecast accordingly.

7 Acknowledgement

My deepest and sincerest gratitude to my supervisor Dr. Tarek Beji for his continuous guidance throughout the thesis and his availability at all times. I would also like to thank Prof. Bart Merci for his valuable feedback and for giving me a chance to work on this project. A special thanks to all the faculty members of IMFSE who provided valuable insights and assistance during the Masters.

Finally, I would like to thank my family for their unconditional support, especially my father for his unfailing support and encouragement and my mother for the many ways in which she has enriched my life. Last but not least, special thanks to Liselotte Van Vlem for her continuous support and her generous help by proofreading this dissertation.

References

- [1] Cowlard A., Jahn W., Abecassis-Empis C., et al. (2010). Sensor Assisted Fire Fighting. *Fire Technology*; 46: 719-741, DOI:10.1007/s10694-008-0069-1
- [2] Jahn W. (2010). Inverse Modelling to Forecast Enclosure Fire Dynamics. PhD thesis, The University of Edinburgh, UK. <http://hdl.handle.net/1842/3418>
- [3] Jahn W., Rein G. and Torero J. L. (2010). Forecasting Fire Growth Using an Inverse Zone Modeling Approach. *Fire Safety Journal*; 46: 81-88. DOI:10.1016/j.firesaf.2010.10.001
- [4] Davis W. D. and Forney G. P. (2001). A Sensor-Driven Fire Model Version 1.1. National Institute of Standards and Technology. Building and Fire Research Laboratory, Gaithersburg, MD, NISTIR 6705, <http://fire.nist.gov/bfrlpubs/fire01/PDF/fo1002.pdf>
- [5] Richards R., Munk B. and Plumb O. (1997). Fire Detection, Location and Heat Release Rate Trough Inverse Problem Solution. Part I: Theory. *Fire Safety Journal*; 28(4). DOI:10.1016/S0379-7112(97)00005-2
- [6] Neviackas A. W. (2007). Inverse Fire Modeling to Estimate the Heat Release Rate of Compartment Fires. Master's thesis, University of Maryland, College Park, <http://hdl.handle.net/1903/7290>
- [7] Overholt K. J. and Ezekoye O. A. (2012). Characterizing Heat Release Rates Using an Inverse Fire Modeling Technique. *Fire Technology*; 48(4): 893-909, DOI: 10.1007/s10694-011-0250-9
- [8] Beji T., Verstockt S., Van de Walle R., Merci B. (2012). Prediction of Smoke Filling in Large Volumes by Means of Data Assimilation-Based Numerical Simulations. *Journal of Fire Science*; 30: 300-317 DOI: 10.1177/0734904112437845
- [9] Beji T., Verstockt S., Van de Walle R., Merci B. (2012). On the Use of Real-Time Video to Forecast Fire Growth in Enclosures. *Fire Technology*, DOI: 10.1007/s10694-012-0262-0
- [10] Beji T., Verstockt S., Van de Walle R., Merci B. (2013). Experimental and Numerical Study of Furniture Fires in an ISO-Room for Use in a Fire Forecasting Framework. *Journal of Fire Sciences*, DOI: 10.1177/0734904113479774
- [11] ISO 9705:1993. Fire Tests - Full Scale Room Tests for Surface Products. International Standard
- [12] Drysdale D. (2011). *An Introduction to Fire Dynamics*. 3rd ed. New York: Wiley & Sons. ISBN:0-470-31903-8.
- [13] Karlsson B. and Quintiere J. (2000). *Enclosure Fire Dynamics*. CRC Press
- [14] McGrattan K., McDermott R., Hostikka S. and Floyd F. (2010). *Fire Dynamics Simulator (Version 5) User's Guide*. NIST Special Publication 1019-5. Gaithersburg, MD, USA: National Institute of Standards and Technology

[15] Pope S. B. (2004). Ten Questions Concerning the Large-Eddy Simulation of Turbulent Flows. *New Journal of Physics*; 6(35)

[16] Peacock R. D., Jones W. W., Reneke P. A. and Forney G. P. (2005). CFAST – Consolidated Model of Fire Growth and Smoke Transport (Version 6): User’s Guide. Special Publication 1041, National Institute of Standards and Technology, Gaithersburg, Maryland

[17] Jones W. W., Peacock R. D., Forney G. P. and Reneke P. A. (2008). CFAST – Consolidated Model of Fire Growth and Smoke Transport (Version 6): Technical Reference Guide. Special Publication 1026, National Institute of Standards and Technology, Gaithersburg, Maryland

[18] McCaffrey B. J. (1983). Momentum Implications for Buoyant Diffusion Flames. *Combustion and Flame*, 52:149

[19] Heskestad G. (1984). Engineering Relations for Fire Plumes. *Fire Safety Journal*; 7:25–32

Appendix A1

Comparison of McCaffrey's Plume Correlations

In the table below a comparison between the results and implementation of different McCaffrey's plume correlation is shown for the Forward Analytical Model. The model check for the ratio $\frac{h}{\dot{Q}_f^{2/5}}$ and apply the appropriate correlation.

Scenarios	Ventilation factor	Heat release rate (kW)	Continuous Flame region		Intermittent Flame region		Plume region		Correct result	
			T _u (°C)	h (m)	T _u (°C)	h (m)	T _u (°C)	h (m)	T _u (°C)	h (m)
1_Case_1	2.26	300.00	342.56	1.05	323.78	1.01	449.36	1.20	323.78	1.01
1_Case_2	2.26	400.00	386.64	0.94	383.25	0.93	580.17	1.17	383.25	0.93
1_Case_3	2.26	500.00	428.64	0.84	440.81	0.86	713.36	1.15	428.64	0.84
1_Case_4	2.26	600.00	469.56	0.77	496.81	0.81	848.73	1.12	469.56	0.77
1_Case_5	2.26	700.00	509.85	0.70	552.46	0.76	988.77	1.10	509.85	0.70
1_Case_6	2.26	800.00	549.71	0.64	608.47	0.72	1131.92	1.08	549.71	0.64
1_Case_7	2.26	900.00	590.03	0.59	664.35	0.68	1277.46	1.06	590.03	0.59
1_Case_8	2.26	1000.00	631.09	0.55	720.30	0.65	1429.59	1.04	631.09	0.55
2_Case_1	2.84	300.00	325.69	1.15	300.60	1.10	407.42	1.27	300.60	1.10
2_Case_2	2.84	400.00	364.08	1.05	352.49	1.02	521.86	1.24	352.49	1.02
2_Case_3	2.84	500.00	399.92	0.96	401.65	0.96	637.69	1.22	399.92	0.96
2_Case_4	2.84	600.00	434.32	0.89	448.94	0.91	754.18	1.20	434.32	0.89
2_Case_5	2.84	700.00	467.63	0.82	495.57	0.86	873.38	1.17	467.63	0.82
2_Case_6	2.84	800.00	500.52	0.77	541.79	0.82	995.53	1.15	500.52	0.77
2_Case_7	2.84	900.00	533.16	0.71	587.87	0.79	1118.88	1.14	533.16	0.71
2_Case_8	2.84	1000.00	565.74	0.67	633.51	0.75	1244.74	1.12	565.74	0.67
3_Case_1	4.58	300.00	299.62	1.35	264.31	1.28	340.74	1.40	264.31	1.28
3_Case_2	4.58	400.00	329.95	1.26	304.61	1.22	431.03	1.38	304.61	1.22
3_Case_3	4.58	500.00	357.23	1.19	341.69	1.16	520.43	1.36	341.69	1.16
3_Case_4	4.58	600.00	382.48	1.12	377.19	1.11	609.29	1.34	377.19	1.11
3_Case_5	4.58	700.00	406.60	1.07	410.89	1.07	698.52	1.33	406.60	1.07
3_Case_6	4.58	800.00	429.68	1.01	444.02	1.03	789.39	1.31	429.68	1.01
3_Case_7	4.58	900.00	452.21	0.97	476.24	1.00	879.83	1.29	452.21	0.97
3_Case_8	4.58	1000.00	474.19	0.92	507.82	0.97	970.73	1.28	474.19	0.92
4_Case_1	6.16	300.00	288.29	1.45	248.18	1.38	310.95	1.48	248.18	1.38
4_Case_2	6.16	400.00	315.22	1.37	283.59	1.32	390.36	1.46	283.59	1.32

4_Case_3	6.16	500.00	339.04	1.31	316.07	1.27	469.06	1.44	316.07	1.27
4_Case_4	6.16	600.00	360.98	1.25	346.41	1.23	546.64	1.42	346.41	1.23
4_Case_5	6.16	700.00	381.51	1.20	375.22	1.19	623.92	1.41	375.22	1.19
4_Case_6	6.16	800.00	400.95	1.15	403.14	1.16	701.01	1.40	400.95	1.15
4_Case_7	6.16	900.00	419.55	1.11	429.91	1.13	777.93	1.38	419.55	1.11
4_Case_8	6.16	1000.00	437.78	1.07	456.15	1.10	855.78	1.37	437.78	1.07
5_Case_1	8.49	300.00	278.80	1.54	234.52	1.48	285.19	1.55	234.52	1.48
5_Case_2	8.49	400.00	302.93	1.48	266.06	1.43	356.36	1.53	266.06	1.43
5_Case_3	8.49	500.00	324.05	1.42	294.57	1.38	425.33	1.52	294.57	1.38
5_Case_4	8.49	600.00	343.21	1.37	320.92	1.34	493.63	1.51	320.92	1.34
5_Case_5	8.49	700.00	361.05	1.33	345.77	1.31	561.15	1.49	345.77	1.31
5_Case_6	8.49	800.00	377.65	1.29	369.50	1.28	628.02	1.48	369.50	1.28
5_Case_7	8.49	900.00	393.59	1.25	392.48	1.25	695.13	1.47	392.48	1.25
5_Case_8	8.49	1000.00	408.63	1.22	414.49	1.22	761.75	1.46	408.63	1.22
6_Case_1	10.24	300.00	274.26	1.59	228.01	1.53	272.69	1.59	228.01	1.53
6_Case_2	10.24	400.00	297.14	1.53	257.74	1.48	339.57	1.58	257.74	1.48
6_Case_3	10.24	500.00	317.02	1.48	284.50	1.44	404.92	1.56	284.50	1.44
6_Case_4	10.24	600.00	334.98	1.44	309.02	1.41	468.48	1.55	309.02	1.41
6_Case_5	10.24	700.00	351.56	1.40	332.15	1.37	531.54	1.54	332.15	1.37
6_Case_6	10.24	800.00	366.96	1.36	354.10	1.34	593.78	1.53	354.10	1.34
6_Case_7	10.24	900.00	381.48	1.33	374.97	1.32	656.02	1.52	374.97	1.32
6_Case_8	10.24	1000.00	395.53	1.29	395.30	1.29	717.59	1.51	395.30	1.29

Appendix A2

Effect of Opening Height

Table below shows a comparison between the results obtained by using different opening heights for the Forward Analytical Model.

Scenarios	Vf	Q	Using door height		Using effective height	
			T _u (°C)	h (m)	T _u (°C)	h (m)
1_Case_1	2.26	300.00	323.78	1.01	323.78	1.01
1_Case_2	2.26	400.00	383.25	0.93	383.25	0.93
1_Case_3	2.26	500.00	428.64	0.84	428.64	0.84
1_Case_4	2.26	600.00	469.56	0.77	469.56	0.77
1_Case_5	2.26	700.00	509.85	0.70	509.85	0.70
1_Case_6	2.26	800.00	549.71	0.64	549.71	0.64
1_Case_7	2.26	900.00	590.03	0.59	590.03	0.59
1_Case_8	2.26	1000.00	631.09	0.55	631.09	0.55
2_Case_1	2.84	300.00	300.60	1.10	342.45	0.94
2_Case_2	2.84	400.00	352.49	1.02	400.02	0.88
2_Case_3	2.84	500.00	399.92	0.96	436.81	0.82
2_Case_4	2.84	600.00	434.32	0.89	472.91	0.76
2_Case_5	2.84	700.00	467.63	0.82	507.88	0.71
2_Case_6	2.84	800.00	500.52	0.77	542.40	0.66
2_Case_7	2.84	900.00	533.16	0.71	576.35	0.62
2_Case_8	2.84	1000.00	565.74	0.67	610.59	0.58
3_Case_1	4.58	300.00	264.31	1.28	297.84	1.11
3_Case_2	4.58	400.00	304.61	1.22	342.48	1.06
3_Case_3	4.58	500.00	341.69	1.16	383.82	1.01
3_Case_4	4.58	600.00	377.19	1.11	414.53	0.97
3_Case_5	4.58	700.00	406.60	1.07	439.98	0.92
3_Case_6	4.58	800.00	429.68	1.01	464.19	0.88
3_Case_7	4.58	900.00	452.21	0.97	487.75	0.84
3_Case_8	4.58	1000.00	474.19	0.92	510.71	0.81
4_Case_1	6.16	300.00	248.18	1.38	298.53	1.11
4_Case_2	6.16	400.00	283.59	1.32	340.56	1.07
4_Case_3	6.16	500.00	316.07	1.27	378.68	1.03
4_Case_4	6.16	600.00	346.41	1.23	408.20	0.99
4_Case_5	6.16	700.00	375.22	1.19	430.72	0.96

4_Case_6	6.16	800.00	400.95	1.15	452.08	0.92
4_Case_7	6.16	900.00	419.55	1.11	472.42	0.89
4_Case_8	6.16	1000.00	437.78	1.07	492.09	0.86
5_Case_1	8.49	300.00	234.52	1.48	247.13	1.39
5_Case_2	8.49	400.00	266.06	1.43	280.20	1.34
5_Case_3	8.49	500.00	294.57	1.38	310.06	1.30
5_Case_4	8.49	600.00	320.92	1.34	337.72	1.27
5_Case_5	8.49	700.00	345.77	1.31	363.95	1.23
5_Case_6	8.49	800.00	369.50	1.28	388.68	1.21
5_Case_7	8.49	900.00	392.48	1.25	407.27	1.17
5_Case_8	8.49	1000.00	408.63	1.22	422.87	1.14
6_Case_1	10.24	300.00	228.01	1.53	242.19	1.42
6_Case_2	10.24	400.00	257.74	1.48	273.67	1.38
6_Case_3	10.24	500.00	284.50	1.44	301.81	1.34
6_Case_4	10.24	600.00	309.02	1.41	327.80	1.31
6_Case_5	10.24	700.00	332.15	1.37	352.23	1.28
6_Case_6	10.24	800.00	354.10	1.34	375.31	1.26
6_Case_7	10.24	900.00	374.97	1.32	397.42	1.23
6_Case_8	10.24	1000.00	395.30	1.29	411.18	1.20

Appendix A3

Comparison between FDS, CFAST and Forward Analytical Model for Constant HRR Scenarios

Scenarios	Ventilation Factor	HRR (kW)	FDS		CFAST		Forward Analytical Model	
			T _u (°C)	h (m)	T _u (°C)	h (m)	T _u (°C)	h (m)
1_Case_1	2.26	300.00			272.59	1.10	323.78	1.01
1_Case_2	2.26	400.00			323.24	1.02	383.25	0.93
1_Case_3	2.26	500.00			371.74	0.96	428.64	0.84
1_Case_4	2.26	600.00	453.39	0.56	419.07	0.90	469.56	0.77
1_Case_5	2.26	700.00			460.15	0.83	509.85	0.70
1_Case_6	2.26	800.00			500.50	0.76	549.71	0.64
1_Case_7	2.26	900.00			541.11	0.70	590.03	0.59
1_Case_8	2.26	1000.00			581.78	0.65	631.09	0.55
2_Case_1	2.84	300.00	212.33	0.66	241.00	1.37	300.60	1.10
2_Case_2	2.84	400.00	262.35	0.67	276.81	1.30	352.49	1.02
2_Case_3	2.84	500.00	311.97	0.65	310.70	1.24	399.92	0.96
2_Case_4	2.84	600.00	362.39	0.64	343.77	1.18	434.32	0.89
2_Case_5	2.84	700.00	402.35	0.64	376.26	1.11	467.63	0.82
2_Case_6	2.84	800.00	455.46	0.62	408.86	1.05	500.52	0.77
2_Case_7	2.84	900.00	496.03	0.61	438.85	0.98	533.16	0.71
2_Case_8	2.84	1000.00	539.45	0.62	467.33	0.92	565.74	0.67
3_Case_1	4.58	300.00			237.00	1.51	264.31	1.28
3_Case_2	4.58	400.00			267.84	1.45	304.61	1.22
3_Case_3	4.58	500.00			293.03	1.40	341.69	1.16
3_Case_4	4.58	600.00	255.19	0.86	315.27	1.35	377.19	1.11
3_Case_5	4.58	700.00			335.31	1.31	406.60	1.07
3_Case_6	4.58	800.00			355.15	1.27	429.68	1.01
3_Case_7	4.58	900.00			375.27	1.23	452.21	0.97
3_Case_8	4.58	1000.00			395.61	1.19	474.19	0.92
4_Case_1	6.16	300.00			233.41	1.63	248.18	1.38
4_Case_2	6.16	400.00			262.47	1.59	283.59	1.32
4_Case_3	6.16	500.00			285.67	1.55	316.07	1.27
4_Case_4	6.16	600.00	231.23	0.91	304.53	1.51	346.41	1.23
4_Case_5	6.16	700.00			319.16	1.47	375.22	1.19
4_Case_6	6.16	800.00			333.04	1.44	400.95	1.15

4_Case_7	6.16	900.00			346.79	1.41	419.55	1.11
4_Case_8	6.16	1000.00			360.52	1.37	437.78	1.07
5_Case_1	8.49	300.00	127.03	1.12	232.72	1.65	234.52	1.48
5_Case_2	8.49	400.00	156.92	1.13	261.42	1.61	266.06	1.43
5_Case_3	8.49	500.00	182.21	1.13	284.22	1.57	294.57	1.38
5_Case_4	8.49	600.00	210.72	1.13	302.66	1.54	320.92	1.34
5_Case_5	8.49	700.00	237.04	1.12	316.55	1.50	345.77	1.31
5_Case_6	8.49	800.00	260.66	1.10	328.91	1.47	369.50	1.28
5_Case_7	8.49	900.00	297.15	1.14	340.93	1.44	392.48	1.25
5_Case_8	8.49	1000.00	322.60	1.11	352.74	1.41	408.63	1.22
6_Case_1	10.24	300.00			231.58	1.68	228.01	1.53
6_Case_2	10.24	400.00			259.69	1.65	257.74	1.48
6_Case_3	10.24	500.00			281.91	1.61	284.50	1.44
6_Case_4	10.24	600.00	214.91	1.27	299.75	1.58	309.02	1.41
6_Case_5	10.24	700.00			313.07	1.55	332.15	1.37
6_Case_6	10.24	800.00			324.37	1.52	354.10	1.34
6_Case_7	10.24	900.00			335.12	1.49	374.97	1.32
6_Case_8	10.24	1000.00			345.61	1.46	395.30	1.29

Appendix A4

Comparison between FDS, CFAST and Forward Analytical Model for linearly increasing HRR Scenarios

Time	HRR (kW)	Ventilation Factor	FDS		CFAST		Forward Analytical Model	
			T _u (°C)	h (m)	T _u (°C)	h (m)	T _u (°C)	h (m)
1_Case_linear								
15.00	50.00	2.26	42.93	1.73	47.06	1.54	116.71	1.29
45.00	150.00	2.26	117.92	0.66	140.24	1.17	224.92	1.18
75.00	250.00	2.26	201.13	0.57	224.27	1.13	292.76	1.06
105.00	350.00	2.26	267.33	0.58	282.16	1.05	353.97	0.97
135.00	450.00	2.26	321.68	0.57	334.14	0.98	407.94	0.89
165.00	550.00	2.26	377.82	0.56	383.77	0.93	449.19	0.80
195.00	650.00	2.26	424.85	0.56	429.65	0.87	489.68	0.73
225.00	750.00	2.26	469.12	0.54	470.66	0.80	529.60	0.67
255.00	850.00	2.26	507.66	0.55	511.91	0.73	570.21	0.62
285.00	950.00	2.26	533.41	0.53	553.36	0.67	610.70	0.57
2_Case_linear								
15.00	50.00	2.26	42.78	1.72	47.06	1.54	116.71	1.29
45.00	150.00	2.26	117.07	0.65	140.24	1.17	224.92	1.18
75.00	250.00	2.26	199.09	0.60	224.27	1.13	292.76	1.06
105.00	350.00	2.26	265.29	0.59	282.16	1.05	353.97	0.97
135.00	450.00	2.26	322.69	0.55	334.14	0.98	407.94	0.89
165.00	550.00	2.84	316.51	0.67	337.29	1.18	417.18	0.92
195.00	650.00	2.84	344.76	0.65	351.17	1.13	451.06	0.85
225.00	750.00	2.84	371.05	0.63	385.55	1.07	484.02	0.79
255.00	850.00	2.84	396.04	0.67	418.65	1.02	516.79	0.74
285.00	950.00	2.84	418.10	0.63	446.69	0.95	549.20	0.69
3_Case_linear								
15.00	50.00	2.26	42.56	1.73	47.06	1.54	116.71	1.29
45.00	150.00	2.26	118.15	0.66	140.24	1.17	224.92	1.18
75.00	250.00	2.26	199.22	0.59	224.27	1.13	292.76	1.06
105.00	350.00	2.26	264.87	0.57	282.16	1.05	353.97	0.97
135.00	450.00	2.26	324.98	0.56	334.14	0.98	407.94	0.89
165.00	550.00	4.58	258.38	0.77	326.88	1.36	359.69	1.14
195.00	650.00	4.58	239.50	0.83	302.36	1.29	394.16	1.09
225.00	750.00	4.58	262.86	0.84	326.42	1.25	418.21	1.04
255.00	850.00	4.58	283.64	0.85	350.67	1.22	441.02	0.99
285.00	950.00	4.58	304.48	0.85	374.74	1.19	463.27	0.95

4_Case_linear								
15.00	50.00	2.26	42.51	1.73	47.06	1.54	116.71	1.29
45.00	150.00	2.26	117.24	0.65	140.24	1.17	224.92	1.18
75.00	250.00	2.26	198.75	0.60	224.27	1.13	292.76	1.06
105.00	350.00	2.26	265.09	0.59	282.16	1.05	353.97	0.97
135.00	450.00	2.26	324.26	0.57	334.14	0.98	407.94	0.89
165.00	550.00	6.16	216.46	0.96	322.50	1.52	331.41	1.25
195.00	650.00	6.16	207.63	1.01	279.54	1.45	361.10	1.21
225.00	750.00	6.16	225.90	1.02	292.27	1.41	389.32	1.17
255.00	850.00	6.16	240.56	1.01	311.57	1.38	410.45	1.13
285.00	950.00	6.16	250.69	1.00	330.15	1.36	428.65	1.09
5_Case_linear								
15.00	50.00	2.26	42.61	1.73	47.06	1.54	116.71	1.29
45.00	150.00	2.26	119.24	0.66	140.24	1.17	224.92	1.18
75.00	250.00	2.26	199.70	0.60	224.27	1.13	292.76	1.06
105.00	350.00	2.26	270.69	0.58	282.16	1.05	353.97	0.97
135.00	450.00	2.26	325.03	0.57	334.14	0.98	407.94	0.89
165.00	550.00	8.49	206.95	1.08	321.45	1.54	308.04	1.36
195.00	650.00	8.49	203.75	1.12	275.52	1.47	333.62	1.33
225.00	750.00	8.49	216.70	1.14	283.65	1.43	357.79	1.29
255.00	850.00	8.49	235.64	1.16	301.12	1.41	381.14	1.26
285.00	950.00	8.49	253.07	1.15	317.87	1.38	401.14	1.23
6_Case_linear								
15.00	50.00	2.26	42.92	1.74	47.06	1.54	116.71	1.29
45.00	150.00	2.26	118.57	0.67	140.24	1.17	224.92	1.18
75.00	250.00	2.26	197.18	0.60	224.27	1.13	292.76	1.06
105.00	350.00	2.26	265.94	0.57	282.16	1.05	353.97	0.97
135.00	450.00	2.26	325.86	0.58	334.14	0.98	407.94	0.89
165.00	550.00	10.24	207.30	1.23	319.97	1.59	296.97	1.42
195.00	650.00	10.24	205.08	1.28	271.07	1.52	320.67	1.39
225.00	750.00	10.24	227.99	1.31	275.23	1.48	343.29	1.36
255.00	850.00	10.24	243.77	1.30	291.57	1.45	364.58	1.33
285.00	950.00	10.24	257.79	1.26	307.18	1.43	385.29	1.31

Appendix A5

Inverse Modeling estimation of HRR and Ventilation Factor for constant HRR scenarios

Scenarios	Reference Ventilation factor	Reference HRR (kW)	Inverse HRR (kW)			Inverse Ventilation factor		
			Continuous Flame Region	Intermittent Flame Region	Corrected	Continuous Flame Region	Intermittent Flame Region	Corrected
1_Case_1	2.26	300.00	94.29	194.71	194.71	1.01	2.08	2.08
1_Case_2	2.26	400.00	184.76	276.78	276.78	1.44	2.16	2.16
1_Case_3	2.26	500.00	312.73	361.89	361.89	1.91	2.22	2.22
1_Case_4	2.26	600.00	479.09		479.09	2.41		2.41
1_Case_5	2.26	700.00	609.55		609.55	2.55		2.55
1_Case_6	2.26	800.00	735.98		735.98	2.62		2.62
1_Case_7	2.26	900.00	863.76		863.76	2.66		2.66
1_Case_8	2.26	1000.00	989.30		989.30	2.68		2.68
2_Case_1	2.84	300.00	112.43	271.94	271.94	2.35	5.69	5.69
2_Case_2	2.84	400.00	190.72	359.29	359.29	2.90	5.46	5.46
2_Case_3	2.84	500.00	290.76	445.63	445.63	3.42	5.24	5.24
2_Case_4	2.84	600.00	410.62	525.99	525.99	3.85	4.93	4.93
2_Case_5	2.84	700.00	543.47	593.71	593.71	4.15	4.54	4.54
2_Case_6	2.84	800.00	695.58		695.58	4.44		4.44
2_Case_7	2.84	900.00	813.32		813.32	4.35		4.35
2_Case_8	2.84	1000.00	924.10		924.10	4.27		4.27
3_Case_1	4.58	300.00	131.33	327.34	327.34	4.03	10.06	10.06
3_Case_2	4.58	400.00	215.84	430.90	430.90	4.92	9.83	9.83
3_Case_3	4.58	500.00	302.48	513.77	513.77	5.45	9.26	9.26
3_Case_4	4.58	600.00	391.12	583.24	583.24	5.79	8.64	8.64
3_Case_5	4.58	700.00	478.74	640.15	640.15	5.99	8.01	8.01
3_Case_6	4.58	800.00	577.35	697.61	697.61	6.24	7.53	7.53
3_Case_7	4.58	900.00	691.62	758.50	758.50	6.55	7.18	7.18
3_Case_8	4.58	1000.00	821.83	821.66	821.66	6.91	6.91	6.91
4_Case_1	6.16	300.00	148.46	380.49	380.49	7.17	18.37	18.37
4_Case_2	6.16	400.00	245.07	507.50	507.50	8.81	18.24	18.24
4_Case_3	6.16	500.00	345.19	613.63	613.63	9.84	17.50	17.50
4_Case_4	6.16	600.00	439.66	696.89	696.89	10.35	16.40	16.40
4_Case_5	6.16	700.00	514.05	749.48	749.48	10.25	14.94	14.94
4_Case_6	6.16	800.00	589.75	797.62	797.62	10.18	13.77	13.77

4_Case_7	6.16	900.00	672.16	846.54	846.54	10.21	12.86	12.86
4_Case_8	6.16	1000.00	762.30	896.71	896.71	10.32	12.14	12.14
5_Case_1	8.49	300.00	149.92	386.33	386.33	7.76	19.99	19.99
5_Case_2	8.49	400.00	247.14	515.52	515.52	9.54	19.89	19.89
5_Case_3	8.49	500.00	347.92	624.14	624.14	10.69	19.17	19.17
5_Case_4	8.49	600.00	443.22	710.32	710.32	11.28	18.08	18.08
5_Case_5	8.49	700.00	516.92	764.50	764.50	11.21	16.58	16.58
5_Case_6	8.49	800.00	584.31	807.54	807.54	11.03	15.25	15.25
5_Case_7	8.49	900.00	655.08	849.87	849.87	10.95	14.20	14.20
5_Case_8	8.49	1000.00	730.28	892.34	892.34	10.95	13.38	13.38
6_Case_1	10.24	300.00	154.08	400.64	400.64	9.35	24.31	24.31
6_Case_2	10.24	400.00	253.55	535.27	535.27	11.46	24.19	24.19
6_Case_3	10.24	500.00	356.54	649.07	649.07	12.82	23.34	23.34
6_Case_4	10.24	600.00	453.95	740.17	740.17	13.54	22.07	22.07
6_Case_5	10.24	700.00	529.64	798.88	798.88	13.47	20.31	20.31
6_Case_6	10.24	800.00	594.62	842.10	842.10	13.16	18.64	18.64
6_Case_7	10.24	900.00	659.83	882.23	882.23	12.94	17.30	17.30
6_Case_8	10.24	1000.00	728.03	922.01	922.01	12.81	16.23	16.23

Appendix A6

Inverse Modeling estimation of HRR and Ventilation Factor for linearly increasing HRR scenarios

Time	Reference Ventilation factor	Reference HRR (kW)	Inverse HRR (kW)				Inverse Ventilation factor			
			Continuous Flame Region	Intermittent Flame Region	Plume Region	Corrected	Continuous Flame Region	Intermittent Flame Region	Plume Region	Corrected
1_Case_linear										
15	2.26	50	0.01	1.11	14.46	14.46	0.01	0.53	6.93	6.93
45	2.26	150	5.14	34.38	52.84	52.84	0.14	0.95	1.47	1.47
75	2.26	250	48.40	133.74		133.74	0.67	1.86		1.86
105	2.26	350	121.55	221.62		221.62	1.14	2.08		2.08
135	2.26	450	228.91	308.73		308.73	1.61	2.18		2.18
165	2.26	550	376.32	397.46		397.46	2.12	2.24		2.24
195	2.26	650	541.44			541.44	2.53			2.53
225	2.26	750	669.81			669.81	2.62			2.62
255	2.26	850	798.59			798.59	2.68			2.68
285	2.26	950	926.30			926.30	2.70			2.70
2_Case_linear										
15	2.26	50	0.01	1.11	14.46	14.46	0.01	0.53	6.93	6.93
45	2.26	150	5.14	34.38	52.84	52.84	0.14	0.95	1.47	1.47
75	2.26	250	48.40	133.74		133.74	0.67	1.86		1.86
105	2.26	350	121.55	221.62		221.62	1.14	2.08		2.08
135	2.26	450	228.91	308.73		308.73	1.61	2.18		2.18
165	2.84	550	378.99	502.70		502.70	3.67	4.86		4.86
195	2.84	650	409.85	506.20		506.20	3.47	4.29		4.29
225	2.84	750	559.03	585.66		585.66	3.93	4.12		4.12
255	2.84	850	715.41			715.41	4.24			4.24
285	2.84	950	817.96			817.96	4.13			4.13

3_Case_linear										
15	2.26	50	0.01	1.11	14.46	14.46	0.01	0.53	6.93	6.93
45	2.26	150	5.14	34.38	52.84	52.84	0.14	0.95	1.47	1.47
75	2.26	250	48.40	133.74		133.74	0.67	1.86		1.86
105	2.26	350	121.55	221.62		221.62	1.14	2.08		2.08
135	2.26	450	228.91	308.73		308.73	1.61	2.18		2.18
165	4.58	550	468.33	656.73		656.73	6.84	9.58		9.58
195	4.58	650	282.60	455.28		455.28	3.81	6.14		6.14
225	4.58	750	376.58	529.39		529.39	4.33	6.08		6.08
255	4.58	850	493.78	611.40		611.40	4.94	6.12		6.12
285	4.58	950	633.06	697.23		697.23	5.60	6.17		6.17
4_Case_linear										
15	2.26	50	0.01	1.11	14.46	14.46	0.01	0.53	6.93	6.93
45	2.26	150	5.14	34.38	52.84	52.84	0.14	0.95	1.47	1.47
75	2.26	250	48.40	133.74		133.74	0.67	1.86		1.86
105	2.26	350	121.55	221.62		221.62	1.14	2.08		2.08
135	2.26	450	228.91	308.73		308.73	1.61	2.18		2.18
165	6.16	550	573.79	824.15		824.15	12.85	18.46		18.46
195	6.16	650	259.71	481.50		481.50	5.56	10.31		10.31
225	6.16	750	298.56	511.07		511.07	5.46	9.35		9.35
255	6.16	850	385.24	588.32		588.32	6.16	9.41		9.41
285	6.16	950	483.55	666.20		666.20	6.85	9.44		9.44
5_Case_linear										
15	2.26	50	0.01	1.11	14.46	14.46	0.01	0.53	6.93	6.93
45	2.26	150	5.14	34.38	52.84	52.84	0.14	0.95	1.47	1.47
75	2.26	250	48.40	133.74		133.74	0.67	1.86		1.86
105	2.26	350	121.55	221.62		221.62	1.14	2.08		2.08
135	2.26	450	228.91	308.73		308.73	1.61	2.18		2.18
165	8.49	550	590.49	853.06		853.06	14.47	20.90		20.90
195	8.49	650	253.29	481.98		481.98	5.92	11.26		11.26

225	8.49	750	270.38	488.34		488.34	5.45	9.84		9.84
255	8.49	850	343.71	557.80		557.80	6.08	9.87		9.87
285	8.49	950	425.91	627.67		627.67	6.72	9.90		9.90
6_Case_linear										
15	2.26	50	0.01	1.11	14.46	14.46	0.01	0.53	6.93	6.93
45	2.26	150	5.14	34.38	52.84	52.84	0.14	0.95	1.47	1.47
75	2.26	250	48.40	133.74		133.74	0.67	1.86		1.86
105	2.26	350	121.55	221.62		221.62	1.14	2.08		2.08
135	2.26	450	228.91	308.73		308.73	1.61	2.18		2.18
165	10.24	550	619.13	901.77		901.77	17.70	25.78		25.78
195	10.24	650	253.38	496.48		496.48	6.93	13.58		13.58
225	10.24	750	253.55	483.41		483.41	5.99	11.43		11.43
255	10.24	850	320.74	551.39		551.39	6.67	11.46		11.46
285	10.24	950	395.62	619.65		619.65	7.34	11.49		11.49

Appendix B1

FDS Script File for Constant HRR Scenario

ABSAR AHMAD, IMFSE THESIS,

Methane Fire IS Room 9705, 10cm grid with 0.5x domain and adiabatic

ISO ROOM DIMENTION : 3.6,2.4,2.4

Domain : 6,4,3.2

10cm the grid distance

600KW fire with Vf=6.16

&HEAD CHID='4_Case_4', TITLE='600kW_Vf6.16'/

_____ MESH DISCRPTION _____

&MESH IJK=60,40,32 XB=-1.2,4.8,-0.4,3.6,0.0,3.2 /

_____ TIME _____

&TIME T_END=120. /

&DUMP NFRAMES=120. /

_____ MISC CONFIG _____

&MISC RADIATION=.TRUE.,TMPA=20./

&RADI NUMBER_RADIATION_ANGLES= 300./

&RADI RADIATIVE_FRACTION=0.33/

_____ FUEL PROPERTIES _____

&REAC ID='METHANE'

SOOT_YIELD=0.015

HEAT_OF_COMBUSTION=50000,

C=1.

H=4.

IDEAL= .TRUE. /

MATERIAL PROPERTIES

&SURF ID='Wall'

ADIABATIC=.TRUE. /

FIRE SOURCE

HRR:

&SURF ID='FIRE', HRRPUA=1666.67 / 600KW

Location of the burner (0.6mx0.6m):

&OBST SURF_ID='INERT',XB=1.5,2.1,0.9,1.5,0.0,0.0, COLOR='RED' /

&VENT XB=1.5,2.1,0.9,1.5,0.0,0.0, SURF_ID='FIRE',COLOR='RED'/

GEOMETRY of the ROOM

&OBST SURF_ID='Wall' XB=0.0,3.6,-0.2,0.0,0.0,2.4, COLOR='KHAKI', TRANSPARENCY=0.0 / 'SideWall'

&OBST SURF_ID='Wall' XB=0.0,3.6,2.4,2.6,0.0,2.4, RGB= 200,200,200 / 'Sidewall'

&OBST SURF_ID='Wall' XB=-0.2,0.0,-0.2,2.6,0,2.4, RGB= 200,200,200 / 'backwall'

&OBST SURF_ID='Wall' XB=3.6,3.8,-0.2,2.6,0,2.4, RGB= 200,200,200 / 'frontwall'

&OBST SURF_ID='Wall' XB=-1.2,4.8,-0.3,2.7,0.0,0.0, COLOR='KHAKI' / 'floor'

&OBST SURF_ID='Wall' XB=-0.2,3.8,-0.2,2.6,2.4,2.6, COLOR='KHAKI', TRANSPARENCY=0.2/ 'roof'

OPENINGS

Door:

&HOLE XB=3.59,3.81,0.8,1.6,0.0,2.0 / Door

Window_1:

&DEVC XYZ=0.0,1.2,1.6, ID='timer', QUANTITY='TIME', SETPOINT=60., INITIAL_STATE= .FALSE. / Controls the opening of the window at given time

&HOLE XB=-0.21,0.01,0.5,1.9,0.6,2.0, DEVC_ID='timer', COLOR='GRAY'/ Window

Window_2:

&HOLE XB=1.2,2.4,2.39,2.61,0.8,2.0, DEVC_ID='timer', COLOR='GRAY'/ Window

Boundary around window for Mout

Window_1:

&OBST SURF_ID='INERT', XB=-0.3,-0.2,0.4,2.0,0.5,2.1, COLOR='BRICK' /

&HOLE XB=-0.31,-0.2,0.5,1.9,0.6,2.0 /

Window_2:

&OBST SURF_ID='INERT', XB=1.1,2.5,2.6,2.7,0.7,2.1, COLOR='BRICK' /

&HOLE XB=1.2,2.4,2.6,2.71,0.8,2.0 /

VENTS

&VENT MB='XMAX',SURF_ID='OPEN'/ 'FRONT'

&VENT MB='XMIN',SURF_ID='OPEN'/ 'BACK'

&VENT MB='YMAX',SURF_ID='OPEN'/ 'SIDES'

&VENT MB='YMIN',SURF_ID='OPEN'/ 'SIDES'

&VENT MB='ZMAX',SURF_ID='OPEN'/ 'CEILING'

UPPER LAYER TEMPERATURE

&DEVC XB=0.6,0.6,0.4,0.4,0.0,2.4, QUANTITY='UPPER TEMPERATURE', ID='Temp1' /

&DEVC XB=0.6,0.6,1.2,1.2,0.0,2.4, QUANTITY='UPPER TEMPERATURE', ID='Temp2' /

&DEVC XB=0.6,0.6,2.0,2.0,0.0,2.4, QUANTITY='UPPER TEMPERATURE', ID='Temp3' /

&DEVC XB=1.8,1.8,0.4,0.4,0.0,2.4, QUANTITY='UPPER TEMPERATURE', ID='Temp4' /

&DEVC XB=1.8,1.8,2.0,2.0,0.0,2.4, QUANTITY='UPPER TEMPERATURE', ID='Temp5' /

&DEVC XB=3.0,3.0,0.4,0.4,0.0,2.4, QUANTITY='UPPER TEMPERATURE', ID='Temp6' /

&DEVC XB=3.0,3.0,1.2,1.2,0.0,2.4, QUANTITY='UPPER TEMPERATURE', ID='Temp7' /

&DEVC XB=3.0,3.0,2.0,2.0,0.0,2.4, QUANTITY='UPPER TEMPERATURE', ID='Temp8' /

HEIGHT OF INTERFACE

&DEVC XB=0.6,0.6,0.4,0.4,0.0,2.4, QUANTITY='LAYER HEIGHT', ID='HGL1' /

&DEVC XB=0.6,0.6,1.2,1.2,0.0,2.4, QUANTITY='LAYER HEIGHT', ID='HGL2' /

&DEVC XB=0.6,0.6,2.0,2.0,0.0,2.4, QUANTITY='LAYER HEIGHT', ID='HGL3' /

&DEVC XB=1.8,1.8,0.4,0.4,0.0,2.4, QUANTITY='LAYER HEIGHT', ID='HGL4' /

&DEVC XB=1.8,1.8,2.0,2.0,0.0,2.4, QUANTITY='LAYER HEIGHT', ID='HGL5' /

&DEVC XB=3.0,3.0,0.4,0.4,0.0,2.4, QUANTITY='LAYER HEIGHT', ID='HGL6' /

&DEVC XB=3.0,3.0,1.2,1.2,0.0,2.4, QUANTITY='LAYER HEIGHT', ID='HGL7' /

&DEVC XB=3.0,3.0,2.0,2.0,0.0,2.4, QUANTITY='LAYER HEIGHT', ID='HGL8' /

MASS FLOW RATE IN THE COMPARTMENT

Door:

&DEVC XB=3.6,3.6,0.8,1.6,0.0,2.0, QUANTITY= 'MASS FLOW +' , ID='Mp_door_out' / at the door

&DEVC XB=3.8,3.8,0.8,1.6,0.0,2.0, QUANTITY= 'MASS FLOW -' , ID='Mp_door_in' / at the door

Window_1:

&DEVC XB=-0.3,-0.3,0.5,1.9,0.6,2.0, QUANTITY= 'MASS FLOW +' , ID='Mp_win1_out' / at the window

&DEVC XB=-0.3,-0.3,0.5,1.9,0.6,2.0, QUANTITY= 'MASS FLOW -' , ID='Mp_win1_in' / at the window

Window_2:

&DEVC XB=1.2,2.4,2.7,2.7,0.8,2.0, QUANTITY= 'MASS FLOW +' , ID='Mp_win2_out' / at the window

&DEVC XB=1.2,2.4,2.7,2.7,0.8,2.0, QUANTITY= 'MASS FLOW -' , ID='Mp_win2_in' / at the window

SLICE OUTPUT

Temperature:

&SLCF PBX=1.8, QUANTITY='TEMPERATURE' /

&SLCF PBY=1.2, QUANTITY='TEMPERATURE' /

&SLCF PBZ=2.0, QUANTITY='TEMPERATURE' /

Velocity:

&SLCF PBY=1.2, QUANTITY='VELOCITY', VECTOR=.TRUE. /

End of script

&TAIL /

Appendix B2

MATLAB Script File for Forward Analytical Model

```
%Code for the forward analytical model, using the HRR and Ventilation  
%factor as an input and gives upper layer temperature and height as output.  
%McCaffrey's correlation conditioning is used.
```

```
clear  
clc
```

```
% Ask user for input file  
[filename,path] = uigetfile ('*.xlsx','Select the input file','D:\');
```

```
Data = xlsread(fullfile(path,filename));  
rows = length(Data(:,1));
```

```
% Get input for constants from the user using gui  
% Title  
title='Enter values for calculation';  
% Fields with the questions  
prompt={'Enter Ambient Temperature in Celcius:', 'Enter flow coefficient  
Cd:', 'Enter door Height:'};  
% lines per answer  
num_lines = 1;  
% Default values of the constants  
def = {'20', '0.7', '2.0'};  
% Store input  
answer=inputdlg(prompt,title,num_lines,def);  
ta = str2double(answer{1}); % Ambient temperature in degree celcius  
Cd = str2double(answer{2}); % Flow coefficient  
Ho = str2double(answer{3}); % Height of the door
```

```
Ventilation_factor=Data(:,1);  
HRR=Data(:,2);
```

```
Ta=ta+273.15;  
Roh_amb=(353/Ta);  
g=9.81;
```

```
Hu=zeros(rows,1);  
Hu_1=zeros(rows,1);  
Hu_2=zeros(rows,1);  
Hu_3=zeros(rows,1);  
Tu=zeros(rows,1);  
Tu_1=zeros(rows,1);  
Tu_2=zeros(rows,1);  
Tu_3=zeros(rows,1);
```

```
for i=1:rows
```

```
    Vf=Ventilation_factor(i);  
    Q=HRR(i);
```

```
    % For the Continuous flame region
```

```

a=0.011;
n=0.566;

C1=((2/3)*Cd*Vf*Roh_amb);
C2=((Q^((2*n)/5))/a);
C3=((Q^(1-((2*n)/5)))*a);

j=1;

for h=0.001:0.001:Ho

    A(j)=abs((C1*sqrt(2*g*(Ta/((C2/(h^n))+Ta))*(1-
(Ta/((C2/(h^n))+Ta))))*((1-(h/Ho))^(3/2)))-(C3*(h^n)));

    [r,c]=find(A==min((min(A))));

    j=j+1;

end

Hu_1(i)= 0.001+(c*0.001);
Tu_1(i)=(C2/(Hu_1(i)^n))+ta;

if ((Hu_1(i)/(Q^(2/5))) >0) && ((Hu_1(i)/(Q^(2/5))) < 0.08)
    Hu(i)=Hu_1(i);
    Tu(i)=Tu_1(i);

else
    % For the Intermittent flame region
    a=0.026;
    n=0.909;

    C1=((2/3)*Cd*Vf*Roh_amb);
    C2=((Q^((2*n)/5))/a);
    C3=((Q^(1-((2*n)/5)))*a);

    j=1;

    for h=0.001:0.001:Ho

        A(j)=abs((C1*sqrt(2*g*(Ta/((C2/(h^n))+Ta))*(1-
(Ta/((C2/(h^n))+Ta))))*((1-(h/Ho))^(3/2)))-(C3*(h^n)));

        [r,c]=find(A==min((min(A))));

        j=j+1;

    end

    Hu_2(i)= 0.001+(c*0.001);
    Tu_2(i)=(C2/(Hu_2(i)^n))+ta;

    if ((Hu_2(i)/(Q^(2/5))) >0.08) && ((Hu_2(i)/(Q^(2/5))) < 0.2)

```



```

    Hu(i)=Hu_2(i);
    Tu(i)=Tu_2(i);

else
    % For the Plume region
    a=0.124;
    n=1.895;

    C1=((2/3)*Cd*Vf*Roh_amb);
    C2=((Q^((2*n)/5))/a);
    C3=((Q^(1-((2*n)/5)))*a);

    j=1;

    for h=0.001:0.001:Ho

        A(j)=abs((C1*sqrt(2*g*(Ta/((C2/(h^n))+Ta))*(1-
(Ta/((C2/(h^n))+Ta))))*((1-(h/Ho))^(3/2)))-(C3*(h^n)));

        [r,c]=find(A==min((min(A))));

        j=j+1;

    end

    Hu_3(i)= 0.001+(c*0.001);
    Tu_3(i)=(C2/(Hu_3(i)^n))+ta;

    if ((Hu_3(i)/(Q^(2/5))) >0.2)
        Hu(i)=Hu_3(i);
        Tu(i)=Tu_3(i);

    else
        Hu(i)=0;
        Tu(i)=0;
    end
end
end
end

% Output data stored in excel
% Ask the user to name the output file
[filename path] = uinputfile('D:\*.xls','Save As');
% Column header for excel file
col_header = {'Upper layer temperature','Upper layer Height'};
% Define the sheet where data should be saved
Sheet=1;
% Write the column header
xlswrite(fullfile(path,filename),col_header,Sheet,'A1');
% Output Corrected upper layer temperature
xlswrite(fullfile(path,filename),Tu,Sheet,'A2');
% Output Corrected upper layer height
xlswrite(fullfile(path,filename),Hu,Sheet,'B2');

```

Appendix B3

MATLAB Script File for Inverse Model

```
%Code for the inverse analytical model, using the upper layer temperature and
height as an input and gives HRR and Ventilation factor as output.
%McCaffrey's correlation conditioning is used.

clear
clc
% Ask user for input csv file (CFAST_n.csv)
[filename,path] = uigetfile ('*.xlsx','Select the CFAST file','D:\TEST');
Data = xlsread(fullfile(path,filename));
rows = length(Data(:,1));

% Get input for constants from the user using gui
% Title
title='Enter values for calculation';
% Fields with the questions
prompt={'Enter Ambient Temperature in Celcius:', 'Enter flow coefficient
Cd:', 'Enter door Height:'};
% lines per answer
num_lines = 1;
% Default values of the constants
def = {'20', '0.7', '2.0'};
% Store input
answer=inputdlg(prompt,title,num_lines,def);
ta = str2double(answer{1}); % Ambient temperature in degree celcius
Cd = str2double(answer{2}); % Flow coefficient
H = str2double(answer{3}); % Height of the door

Tu_avg=(Data(:,1)+273.15);
h_avg=Data(:,2);

Ta=ta+273.15;
cp=1.0;
Rho_amb=(353/Ta);
g=9.81;

Q=zeros(rows,1);
Q_1=zeros(rows,1);
Q_2=zeros(rows,1);
Q_3=zeros(rows,1);
Vf=zeros(rows,1);
Vf_1=zeros(rows,1);
Vf_2=zeros(rows,1);
Vf_3=zeros(rows,1);

for i=1:rows

    Tu=Tu_avg(i);
    h=h_avg(i);

    % For the Continuous flame region
    a=0.011;
```

```

n=0.566;

C4=(a*(h^n)*cp*(Tu-Ta));
C5= ((2/3)*Cd*Rho_amb*(sqrt(2*g*(Ta/Tu)*(1-(Ta/Tu))))*((1-(h/H))^(3/2)));

Q_1(i) = (C4^(5/(2*n)));
Vf_1(i)= ((a*(h^n)*(Q_1(i)^(1-((2*n)/5))))/C5);

if ((h/(Q_1(i)^(2/5))) >0) && ((h/(Q_1(i)^(2/5))) < 0.08)
    Q(i)=Q_1(i);
    Vf(i)=Vf_1(i);

else
    % For the Intermittent flame region
    a=0.026;
    n=0.909;

    C4=(a*(h^n)*cp*(Tu-Ta));
    C5= ((2/3)*Cd*Rho_amb*(sqrt(2*g*(Ta/Tu)*(1-(Ta/Tu))))*((1-
(h/H))^(3/2)));

    Q_2(i) = (C4^(5/(2*n)));
    Vf_2(i)= ((a*(h^n)*(Q_2(i)^(1-((2*n)/5))))/C5);

    if ((h/(Q_2(i)^(2/5))) >0.08) && ((h/(Q_2(i)^(2/5))) < 0.2)
        Q(i)=Q_2(i);
        Vf(i)=Vf_2(i);

    else
        % For the Plume region
        a=0.124;
        n=1.895;

        C4=(a*(h^n)*cp*(Tu-Ta));
        C5= ((2/3)*Cd*Rho_amb*(sqrt(2*g*(Ta/Tu)*(1-(Ta/Tu))))*((1-
(h/H))^(3/2)));

        Q_3(i) = (C4^(5/(2*n)));
        Vf_3(i)= ((a*(h^n)*(Q_3(i)^(1-((2*n)/5))))/C5);

        if ((h/(Q_3(i)^(2/5))) >0.2)
            Q(i)=Q_3(i);
            Vf(i)=Vf_3(i);

        else
            Q(i)=0;
            Vf(i)=0;
        end
    end
end
end
end

% Output data stored in excel

```

```
% Ask the user to name the output file
[filename path] = uiputfile('D:\*.xls','Save As');
% Column header for excel file
col_header = {'Inverse HRR','Inverse Vf'};
% Define the sheet where data should be saved
Sheet=1;
% Write the column header
xlswrite(fullfile(path,filename),col_header,Sheet,'A1');
% Output Corrected upper layer temperature
xlswrite(fullfile(path,filename),Q,Sheet,'A2');
% Output Corrected upper layer height
xlswrite(fullfile(path,filename),Vf,Sheet,'B2');
```